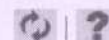


Document

Discussion



[Return To Library](#) > [Records](#) > [ERID-92000 through ERID-92999](#) > ERID-092033 1)WELL R-26 COMPLETION REPORT

Document Number: 04192006-AGGY-HBBM  
Created By: Aurelia A. Martinez  
Date Created: 04/19/2006 08:57:33 AM  
File name: Target-ERID #.pdf  
Version: 1.0  
Document Type: RPF Record  
Document State: Released  
Description: SUBMITTED BY CARRIE COOK, KLEINFELDER INC

**Document Details:**

**Title:** ERID-092033 1)WELL R-26 COMPLETION REPORT  
**ERID Number.StartPage:** ERID-092033  
**Office of Record:** ENV-ECR  
**Date Received:** 04/18/2006  
**Official Use Only:** N  
**Page Count:** 141  
**Record Type:** Report  
**Document Date:** 01/25/2005  
**To:(Addressees - Organization)** N/A  
*(separate multiple values with semicolons)*  
**From:(Senders - Organization)** MARK EVERETT  
*(separate multiple values with semicolons)*  
**Other Document Number(s):** PKG-1691, PROJECT NO. 37151  
*(separate multiple values with semicolons)*  
**TA:** N/A  
*(separate multiple values with semicolons)*  
**PRS Number(s):** N/A  
*(separate multiple values with semicolons)*  
**Record Box Number:**

\* Denotes Fields that are mandatory.

To download this file, right mouse click on the file and select 'Save to Disk' or 'Save Target as'

[Target-ERID #.pdf](#) <-- This link points to this version.

To check-out and/or edit this file, select Edit Document or Check Out Document from the Document menu above.



File Cabinet: [Records](#)



Binder Category: [ERID-90000 through ERID-99999](#)



Binder: [ERID-92000 through ERID-92999](#)

## RRES-R Records Package Transmittal Form

Page 1 of 4

### Section I — Records Transmitter Information: (Completed by Records Transmitter.)

Name: Carrie Cook Package transmittal date: 4/13/06 TA: \_\_\_\_\_  
 Organization: Kleinfelder, Inc. Electronic file(s) transmitted? ☐ Yes ☒ NA OU: \_\_\_\_\_  
 Z number: 207220 Phone: (505) 344-7373 Privileged record? ☐ Yes ☒ No Project: DOE Deep Wells Program

This record package transmittal (check one)

☒ is an addition to a previous package. (Include number: 1691)

PRS(s): \_\_\_\_\_

Is a reconciliation report requested? ☒ Yes ☐ No

☐ is a new package.

Records package number: 1691

(RPF use only)

Records package title: \_\_\_\_\_

### Record Package Table of Contents

File Folder Name	Record Title or Subject (Limited to 255 characters)	Doc. Date	Author/Originator	Page Count	ER ID #
47151.1.2 - ALB03WP001	Kleinfelder Drilling Plan for Characterization Wells R-2, R-4, R-11 and R-26	11/7/03	Mark Everett	44	09-2023
37151.1.3 - ALB03HS004	Site Specific Health & Safety Plan Characterization Well R-26	12/12/03	Paul Fensterer	16	09-2024
47151.8.12 - ALB03FB001	R-26 Field Notebook	8/25/06	Steffanie Metzger	80	09-2025

### Section II (Completed by RPF personnel only.)

Name: Aurelia Metzger (Print Name) 4-18-06 (Date)

QP-4.4, R2

**Los Alamos National Laboratory**  
**RRES-Remediation Services Project**

# RRES-R Records Package Transmittal Continuation Form

Page 2 of 4

**Section I** (Completed by record transmitter.)

Enter the previous record package number, 1691, or the new records package title: \_\_\_\_\_

## Record Package Table of Contents

File Folder Name	Record Title or Subject (Limited to 255 characters.)	Doc. Date	Author/Originator	Page Count	ER ID # (RPF Use Only)
37151.13.12 - ALB03FB001	R-26 Field Notebook	9/18/03	Paula Schuh	81	092026
37151.13.12 - ALB04FB001	R-26 Field Notebook	2/11/04	Stephen Woodall	44	092027
37151.13.12 - ALB04FB002	R-26 Field Notebook	4/6/04	Catherine Goetz	8	092029
37151.12.12 - ALB04FB003	R-26 Field Notebook	6/16/04	Mathew Cramer	70	092030
37151.13.12 - ALB04FR003	R-26 Field Notebook	6/28/04	Stephen Woodall	19	092031
37151.17.12 - ALB04FB004	R-26 Field Notebook	9/20/04	Cember Hardison	70	092032
37151.13.12 - ALB04RP001	Well R-26 Completion Report	1/25/05	Mark Everett	141	092033

QP-4.4, R2

**Los Alamos National Laboratory**  
**RRES-Remediation Services Project**

## RRES-R Records Package Transmittal Continuation Form

Page 3 of 4

**Section I** (Completed by record transmitter.)

Enter the previous record package number, 1691, or the new records package title: \_\_\_\_\_

### Record Package Table of Contents

File Folder Name	Record Title or Subject (Limited to 255 characters.)	Doc. Date	Author/Originator	Page Count	ER ID # (RPF Use Only)
37151.13.12 - ALB04RP002	R-26 Addendum to the R-26 Completion Report	11/29/04	Carol Craiglow	14	092035
Druatek	R-26 Waste Determination for Drill Cuttings from Hydrogeologic Work Plan	11/17/04	Thomas Benson	5	092037
37151.13.12 - ALB04TD001	R-26 Information Management Forms - Coring	3/10/06	Benjamin Trujillo	8	092039
37151.13.12 - ALB04TD002	R-26 Information Management Forms - Drill & Install	3/10/06	Benjamin Trujillo	28	092041
37151.13.12 - ALB04TD003	R-26 Daily Field Reports	3/10/06	Benjamin Trujillo	114	092042
37151.13.12 - ALB04TD004	R-26 Sample Collection Records	3/10/06	Benjamin Trujillo	83	092043
QSR-2006-10	Quality Surveillance Report QSR-2006-10	2/20/06	Benjamin Trujillo	1	092044

QP-4.4, R2

**Los Alamos National Laboratory  
RRES-Remediation Services Project**

## RRES-R Records Package Transmittal Continuation Form

Page 4 of 4

**Section I** (Completed by record transmitter.)

Enter the previous record package number, 1691, or the new records package title: \_\_\_\_\_

### Record Package Table of Contents

File Folder Name	Record Title or Subject (Limited to 255 characters.)	Doc. Date	Author/Originator	Page Count	ER ID # (RPF Use Only)
QIR 2005-14	Quality Improvement Report 2005-14	10/5/05	Benjamin Trujillo	7	092045
QIR-2005-20	Quality Improvement Report 2005-20	10/10/05	Benjamin Trujillo	8	092046
QIR-2006-7	Quality Improvement Report 2006-7	2/20/06	Benjamin Trujillo	13	092047

QP-4.4, R2

Los Alamos National Laboratory  
RRES-Remediation Services Project

**FINAL  
WELL R-26 COMPLETION REPORT  
LOS ALAMOS NATIONAL LABORATORY  
LOS ALAMOS, NEW MEXICO  
PROJECT NO. 37151  
Revision No. 1**

Prepared for:

The United States Department of Energy and the  
National Nuclear Security Administration through the  
United States Army Corps of Engineers  
Sacramento District



Prepared by:

**KF KLEINFELDER**  
8300 Jefferson NE, Suite B  
Albuquerque, New Mexico 87113

January 25, 2005

## TABLE OF CONTENTS

LIST OF ACRONYMS AND ABBREVIATIONS .....	iii
ABSTRACT .....	v
1.0 INTRODUCTION .....	1
2.0 PRELIMINARY ACTIVITIES .....	1
2.1 Administrative Preparation .....	1
2.2 Site Preparation .....	1
3.0 SUMMARY OF DRILLING ACTIVITIES .....	3
3.1 Phase I Drilling Activities .....	4
3.2 Phase II Drilling Activities .....	7
4.0 SAMPLING AND ANALYSIS OF DRILL CUTTINGS AND GROUNDWATER .....	9
4.1 Sampling of Drill Cuttings and Core .....	9
4.2 Sampling of Groundwater .....	9
5.0 BOREHOLE GEOPHYSICS .....	10
5.1 KA-Supported Geophysical Logging .....	10
5.2 Schlumberger Geophysical Logging .....	11
6.0 LITHOLOGY AND HYDROGEOLOGY .....	12
6.1 Stratigraphy and Lithologic Logging .....	13
6.2 Groundwater Occurrence and Characteristics .....	14
7.0 WELL DESIGN AND CONSTRUCTION .....	16
7.1 Well Design .....	16
7.2 Well Construction .....	16
7.2.1 Steel Installation .....	18
7.2.2 Annular Fill Placement .....	18
7.3 Piezometer Construction .....	19
8.0 WELL DEVELOPMENT AND HYDROLOGIC TESTING .....	19
8.1 Well Development .....	21
8.2 Hydrologic Testing .....	24
8.3 Dedicated Sampling System Installation .....	24
8.4 Wellhead Completion .....	24
8.5 Geodetic Survey .....	24
8.6 Site Restoration .....	25
9.0 DEVIATIONS FROM THE R-26 SAP .....	26
10.0 ACKNOWLEDGEMENTS .....	26
11.0 REFERENCES .....	26

## TABLE OF CONTENTS (continued)

### APPENDIXES

A	Borehole Videos (DVDs included)
B	Schlumberger Geophysical Report and Montages (CD included)
C	Groundwater Analytical Results
D	Lithology Log
E	Aquifer Testing Report and Aquifer Test Data
F	Westbay Installation Report
G	NMED Discharge Approval and Discharge Media Analytical Results
H	Activities Planned for Well R-26 Compared with Work Performed

### LIST OF FIGURES

1.0-1	Site Location Map, Well R-26 Location
3.0-1	Well Summary Data Sheet for Well R-26
7.2-1	Schematic Diagram of Well R-26
7.3-1	Schematic Diagram of Corehole Piezometers of Well R-26
8.1-1	Effects of Pump Development of the Upper Screen on Water Quality Parameters at Well R-26
8.1-2	Effects of Pump Development of the Lower Screen on Water Quality Parameters at Well R-26

### LIST OF TABLES

3.0-1	Operations Chronology for Well R-26
3.2-1	Introduced and Recovered Drilling Fluids
5.1-1	Borehole and Well Logging Surveys Conducted in R-26
7.1-1	Summary of Well Screen Information for Well R-26
7.2-1	Annular Fill Materials Used in Well R-26
8.1-1	Development and Testing of Well R-26
8.5-1	Geodetic Data for Well R-26

**LIST OF ACRONYMS AND ABBREVIATIONS**

ASTM	American Society for Testing and Materials
bgs	below ground surface
DOE	United States Department of Energy
DTH	down-the-hole
DTW	depth to water
DVD	digital video disc
EES	Earth and Environmental Sciences
ELAN	Elemental Analysis
EnviroWorks	EnviroWorks, Inc.
ft	feet
g	grams
gal.	gallon
g/cc	grams per cubic centimeter
GEL	General Engineering Laboratories
hr	hour
HSA	hollow-stem auger
ID	inner diameter
in.	inches
KA	Kleinfelder, Inc.
KBr	potassium bromide
LANL	Los Alamos National Laboratory
MDL	Method Detection Limit
mil	1/1000 of an inch
MP	multiport
NAD	North American Datum
NGS	natural gamma spectroscopy
NMED	New Mexico Environment Department
NOI	Notice of Intent
NTU	nephelometric turbidity unit
OD	outer diameter

psi	pounds per square inch
PVC	polyvinyl chloride
Qbog	Guaje Pumice Bed
Qbt	Tsirege Member of Bandelier Tuff
R-26	Well R-26
SAP	Sampling and Analysis Plan
TA	technical area
TD	total depth
TLD	triple detector lithodensity
TOC	total organic carbon
$\mu\text{S}/\text{cm}$	microsiemens per centimeter
WDC	WDC Exploration & Wells, Inc.

## ABSTRACT

Well R-26 was installed at Los Alamos National Laboratory (LANL) for LANL's Groundwater Protection Program as part of the "Hydrogeologic Workplan" (LANL 1998). The Department of Energy (DOE) contracted and directed the installation of Well R-26. The purpose of the well is (1) to characterize intermediate-depth perched groundwater penetrated by existing wells R-25 and SHB-3, and (2) to provide background water chemistry for perched and regional groundwater upgradient of LANL activities in the Technical Area (TA)-16 vicinity. Well R-26 is located on the downthrown block of the Pajarito fault system; data from this well will be used to evaluate the influence of the Pajarito fault system on the regional aquifer piezometric surface and to provide information on the role of faults in recharge.

The well was drilled in two phases. Phase I consisted of collecting continuous core from the surface to a depth of 250 feet (ft) below ground surface (bgs). Core will be used to characterize anion profiles in the vadose zone. In Phase II drilling, a borehole was advanced to a total depth (TD) of 1,490.5 bgs into the regional aquifer and installing a well. The well was sampled to determine water quality, and hydrologic testing was conducted to evaluate aquifer parameters.

The R-26 borehole was drilled using fluid-assisted air-rotary and mud-rotary drilling methods. The 5-inch outer diameter stainless-steel well was installed on October 18, 2003, to a TD of 1,479 ft bgs with two screened intervals; the upper screened interval was set within the intermediate-depth perched groundwater, and the lower screened interval was set in the regional aquifer. A Westbay multi-port sampling system was installed on July 16, 2004 for long-term monitoring of water levels and collection of groundwater samples. The stratigraphy encountered during borehole drilling included, in descending order, alluvium, ash-flow tuffs of the Tshirege Member of the Bandelier Tuff, Cerro Toledo interval, ash-flow tuffs of the Otowi Member of the Bandelier Tuff, the Guaje Pumice Bed of the Otowi Member, and Puye Formation sediments.

Samples of drill cuttings were collected at regular intervals for stratigraphic, petrographic, and geochemical analysis. A perched water zone was encountered in the R-26 corehole at 240 ft bgs in the Tshirege Member of the Bandelier Tuff. A groundwater sample was collected at 240 ft bgs and was submitted for analysis. Groundwater saturation was first noted while drilling at 650 ft bgs. A groundwater screening sample was collected at 604 ft bgs and was submitted for analysis. Groundwater samples were collected from the completed well's upper screen at 651.8 to 669.9 ft bgs and from the lower screen at 1,421.8 to 1,445 ft bgs. All samples were analyzed for organic, inorganic, and radiochemical compounds.

## 1.0 INTRODUCTION

This completion report summarizes the drilling, well construction, well development, and related activities conducted from August 27, 2003 to July 18, 2004 to characterize Well R-26 (R-26). R-26 was drilled and installed for Los Alamos National Laboratory's (LANL's) Groundwater Protection Program as part of the "Hydrogeologic Workplan" (LANL 1998). Characterization and sampling activities were conducted in accordance with the SAP (Sampling and Analysis Plan) for Drilling and Testing Characterization Wells R-2, R-4, R-11, and R-26 (LANL 2003). R-26 is located in Cañon de Valle, just east of State Highway 4 and upgradient of LANL activities at Technical Area (TA)-16. The locations of R-26 and adjacent wells are shown in Figure 1.0-1. An electronic copy of this report and appendixes is included on the CD on the inside back cover.

R-26 was funded and directed by the U.S. Department of Energy (DOE). Kleinfelder, Inc. (KA), under contract to the United States Army Corps of Engineers (USACE), was responsible for executing the drilling, installation, testing, and sampling activities with technical assistance from LANL.

The information presented in this report was compiled from field reports and activity summaries generated by KA, LANL, and subcontractor personnel, such as Schlumberger, who provided geophysical logging services and data interpretation. Results of these activities are discussed briefly and shown in tables and figures contained in this report.

R-26 is designed to provide water quality and water level monitoring data from the regional aquifer. R-26 will provide hydrologic and water-quality data for regional groundwater upgradient of potential contaminant sources in TA-16. Data from R-26 and other hydrogeologic data will provide a basis for evaluating the need for groundwater monitoring and will form the technical basis for the design of a groundwater monitoring system. Water quality, geochemical, hydrologic, and geologic information obtained from R-26 will augment knowledge of regional subsurface characteristics and will serve as a monitoring well upgradient of potential release sites.

## 2.0 PRELIMINARY ACTIVITIES

Preliminary activities at R-26 included administrative and site preparation.

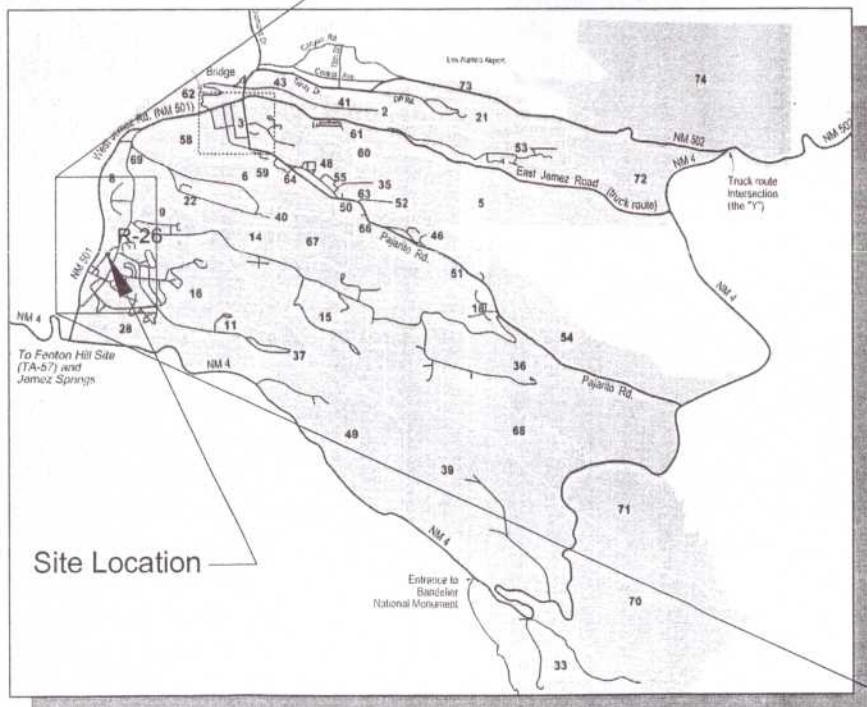
### 2.1 Administrative Preparation

On July 11, 2003, KA received contractual authorization, in the form of a notice to proceed, to start administrative preparation tasks. As part of this preparation, KA developed a Project Management Plan (KA 2003a), a Contractor's Quality Management Plan (KA 2003b), a Site-Specific Health and Safety Plan (KA 2003c), a traffic control plan, and a Drilling Plan (KA 2003d) for the work at Well R-26. The host facility signed a Facility-Tenant Agreement to provide access and security controls for site preparation, drilling and well installation activities. Necessary permits and access agreements were obtained before beginning fieldwork.

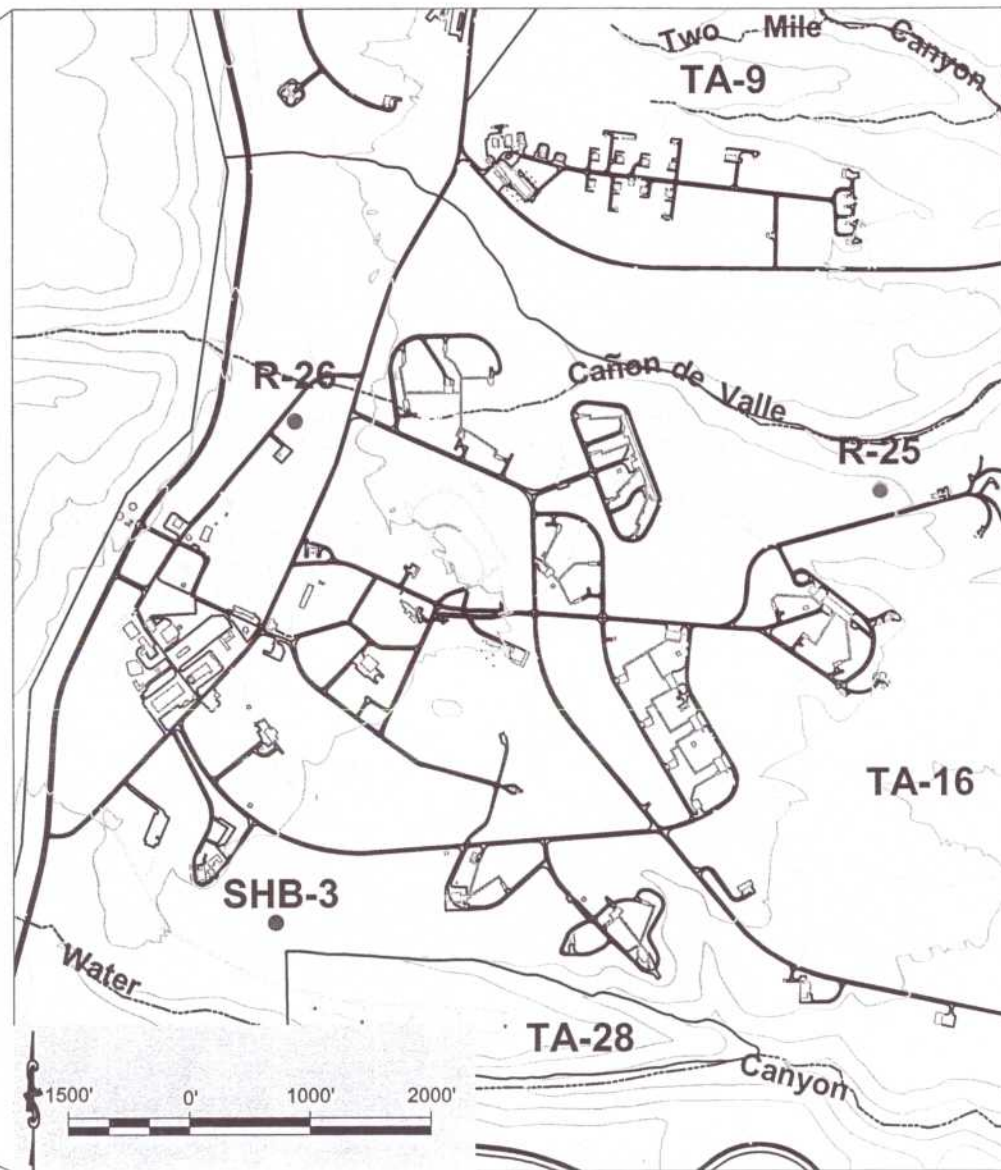
### 2.2 Site Preparation

EnviroWorks, Inc. (EnviroWorks) was subcontracted by KA to prepare the site. Activities included site clearing, access road improvement, construction of the drill pad, and construction of a lined borehole-cuttings containment area. Site preparation was begun on August 27, 2003 and was completed on September 16, 2003.

Los Alamos



Los Alamos National Laboratory Boundary



● Observation Well

● R-26 Characterization Well

● Existing R Characterization Wells



**KLEINFELDER**

Drawn By: C. Landon

Date: April 2004

Project No.: 37151

Filename: FIGURE 1.0-1

Scale: 1" = 2000'

Revision: 0

**SITE LOCATION MAP**  
Well R-26 Location  
LANL Well Program  
Los Alamos National Laboratory  
Los Alamos, New Mexico

FIGURE

**1.0-1**

Note: R-26 Well Identification Modified from  
Proposed R Characterization Well Location Map  
Provided by Los Alamos National Laboratory

The site was initially cleared of vegetation. The drilling pad was then developed by grading an area with a front-end loader. A primary layer of base-course gravel was distributed over the drill pad area. To store Well R-26 drilling fluids and borehole cuttings, a 30-foot (ft) -wide by 60-ft-long by 7-ft-deep borehole-cuttings containment pit was excavated along the eastern drill pad boundary. A secondary containment area was lined with 6-mil (1/1000 of an inch) polyethylene and surrounded by straw bales to accommodate a 21,000-gallon (gal.) tanker trailer used for storing development water and drilling fluids pumped from the borehole-cuttings containment area. Drill pad construction was completed with an additional graded layer of base-course gravel. Safety barriers and signs were installed around the borehole-cuttings containment area and at the site entrance. Office and supply trailers, generators, and safety lighting equipment were moved to the site during subsequent mobilization of drilling equipment. Base course was also placed on the access road, as necessary. Equipment necessary for the completion of the drilling project was situated at the work site to provide a safe, secure work site. Orientation and placement of the equipment was dependent on borehole location and physical constraints at the drill site.

Potable water for drilling at Well R-26 was pumped from a hydrant adjacent to the fire station located off West Jemez Road and delivered to the site through a fire hose.

### 3.0 SUMMARY OF DRILLING ACTIVITIES

Drilling activities at Well R-26 were completed in two phases during September and October 2003. Phase I drilling was performed by KA using a StrataStar SS15 drill rig equipped with a 2-ft-long split spoon used to collect 2.0-in.-diameter samples, a 5-ft-long core barrel used to collect 3.0-in.-diameter continuous core samples, and an HQ sampler to collect 2.4-in.-diameter core samples. Phase II drilling was performed in an offset borehole by WDC Exploration and Wells, Inc. (WDC) using a Dresser T70W drill rig equipped with conventional circulation drilling rods, tricone bits, down-the-hole (DTH) hammer bits, and support equipment. Drilling fluid mixing and circulation equipment included a mixing tank and pump assembly, an auxiliary pump, a shaker unit to remove solids from the discharged drilling fluids, and a generator to power the mixing unit.

The goal of Phase I drilling was to collect continuous rock core samples for geologic characterization and to determine moisture, anion, stable isotope, radionuclide, metals, and tritium distributions in the upper section of the borehole. Planned total depth (TD) for Phase I was 250 ft bgs, or approximately 250 ft into the Tshirege Member of the Bandelier Tuff. Groundwater samples were to be collected from significant perched zones, if encountered.

Drilling of the borehole for Phase II was performed using air-rotary, fluid-assisted air-rotary, and mud-rotary drilling techniques using open-hole and casing-advance methods, as appropriate for changing geologic and drilling conditions. Various additives were mixed with municipal water to improve borehole stability, to minimize fluid loss, and to facilitate cuttings removal from the borehole. Air-rotary drilling was assisted with water at shallow depths to suppress dust emissions and, at greater depths, with a foam mixture that consisted of municipal water mixed with QUIK-FOAM<sup>®</sup> (surfactant) and EZ-MUD<sup>®</sup> (polymer). Mud-rotary drilling fluids were comprised of a mixture of water, bentonite, soda ash, and Pac-L polyanionic cellulose.

Primary Phase II drilling objectives were (1) to collect cuttings of encountered geologic formations; (2) to collect water samples from perched and regional groundwater zones; (3) to

complete a borehole for geophysical logging; and (4) to install a well with two screened intervals, one in the intermediate perched zone, if present, and one in the regional aquifer. The planned TD for Phase II drilling was approximately 1,414 ft bgs, roughly 100 ft below the predicted regional water table.

Coring and deep drilling activities were conducted from September 8 through October 17, 2003. Phase I drilling was completed in one shift per day from September 8 through September 12, 2003. Phase II drilling activities were performed generally in one shift per day from September 18 through October 14, 2003. Two shifts per day began on October 14 and continued through October 21, 2003, during well construction. A drill shift nominally represents a 12-hour (hr) period spent on the project by the drill crew, two site geologists, and onsite support equipment. Drilling and well construction work was conducted under a 7-days-per-week schedule.

Figure 3.0-1 summarizes well data and graphically depicts groundwater and geologic conditions encountered in R-26. Sections 3.1 and 3.2 discuss Phase I and Phase II drilling activities, respectively, for R-26.

A tabular chronology of drilling and other onsite activities is presented as Table 3.0-1.

### 3.1 Phase I Drilling Activities

On September 8, 2003, KA mobilized a StrataStar SS15 hollow-stem auger (HSA) drill rig and support equipment to the R-26 site and began Phase I core drilling. The corehole drilling was initiated with an 8-in. nominal outer diameter (OD) HSA using a DTH hammer with a split-spoon sampler. At 19 ft bgs, KA switched to the continuous sampler system to achieve optimal core recovery. This proved ineffective, and drilling and sampling with the split-spoon sampler was resumed at 25 ft bgs. Split-spoon sampling proved to be difficult from 25 ft to 31 ft bgs.

At 31 ft bgs, KA switched to an air-assisted drilling method using a conventional 3-in. OD core barrel attached to an HQ drill rod. Dust suppression equipment was installed. Coring from 31 ft to 55 ft bgs yielded poor recovery. On September 10, 2003, KA reverted to split-spoon sampling and advanced the hole from 55 ft to 65 ft bgs with limited recovery. Coring with the conventional core barrel was resumed at 65 ft bgs for drilling in the strongly welded tuff. At 70 ft bgs, the drillers replaced the conventional core barrel with a Geobarrel<sup>®</sup> and cored continuously to 145 ft bgs, where the Geobarrel<sup>®</sup> core bit was replaced due to excessive wear. Equipped with a new coring bit, the drillers returned to conventional core barrel techniques and advanced the core hole from 145 ft bgs to the planned TD of 250 ft bgs.

On September 15, 2003, the drillers tripped out the drill stem, and video, natural gamma, and resistivity logs were run in the corehole. The video log (Appendix A) revealed possible perched zones of saturation from 150 to 180 ft bgs and 230 to 250 ft bgs. Depth to groundwater was measured at 242 ft bgs in the corehole. A groundwater screening sample was collected from the open corehole at 240 bgs on September 18, 2003, and was submitted for analysis. Two piezometers were installed with screened intervals in the potential zones of saturation. Further discussion on the piezometer installation is in Section 7.3.

Location: Mesa South of Cañon de Valle  
(on down thrown side of Pajarito Fault) TA-16

Description: Brass Marker  
Northing: 1764721.12  
Easting: 1610267.33  
Elevation: 7641.69

Description: Well Casing  
Northing: 1764721.35  
Easting: 1610269.56  
Elevation: 7643.33

Coring:  
(0' - 31') Auger  
(31' - 55') HQ Coring  
(55' - 65') Auger  
(65' - 250') HQ Coring

Drilling:  
(0' - 77') 13-3/8" Air Rotary Casing Hammer  
(77' - 140') 12-1/4" Tri-Cone, Air-rotary  
(140' - 205') Air-rotary with water  
(205' - 1005') Fluid-assisted (AWQE) air rotary  
(1005' - 1490.5') Mud-rotary 8.5" Tri-Cone

Reaming:  
(77' - 1005') 14" Roller Reamed - unsuccessful  
(1005' - 1490') 10" Reamed - partial success

#### Data Collection:

- Hydrologic Properties:
  - Constant discharge pumping test: 2/11/04 - 2/27/04
  - Cores/Cuttings submitted for geochemical and contaminant characterization: 13
  - Ground Water Samples Submitted
    - Perched Ground Water - 9/18/03 (240') - corehole
    - Deep Ground Water -
    - Screening Samples: 9/22/03 (604')
    - Well Samples: 11/14/03 (1430')
    - 11/16/03 (860')
- Geologic Properties:
  - Cuttings submitted for mineralogy, petrography, and chemistry: 7

#### Borehole Logs:

- Lithologic: 0' - 1490.5'
- Video (LANL tool): 0' - 717'
- Caliper Logging: 0 - 1475'
- Schlumberger logs:
  - Compensated Neutron Log:
    - 9/28/03: Open Hole: 70'-865'
    - 10/14/03: Cased: 500'-1005'; Open Hole: 1005'-1481'
  - Triple Litho-Density:
    - 9/28/03: Open Hole: 70'-865'
    - 10/14/03: Cased: 500'-1005'; Open Hole: 1005'-1481'
  - Array Induction Imager:
    - 9/28/03: Open Hole: 70'-879'
    - 10/14/03: Cased: 500'-1005'; Open Hole: 1005'-1476'
  - Elemental Capture Sonde:
    - 9/28/03: Open Hole: 70'-981'
    - 10/14/03: Cased: 500'-1005'; Open Hole: 1005'-1477'
  - Natural GR Spectroscopy:
    - 9/28/03: Open Hole: 70'-979'
    - 10/14/03: Cased: 500'-1005'; Open Hole: 1005'-1460'
  - Combination Magnetic Resonance:
    - 9/28/03: Open Hole: 70'-967'
    - 10/14/03: Cased: none; Open Hole: 1005'-1464'
  - Fullbore Formation Micro Imager:
    - 9/28/03: Open Hole: 450'-985'
    - 10/14/03: Cased: none; Open Hole: 1005'-1483'

#### Corehole Logs:

- Lithologic: 0' - 250'
- Video (LANL tool): 0' - 241'
- Gamma Ray (LANL Tool): 0'-245'
- Array Induction (LANL Tool): 0'-245'

Core Drilling Completed: 9/8/03-9/12/03

Rotary Drilling Completed: 9/18/03-10/17/03

Contract Geophysics: 9/28/03 and 10/14/03-10/15/03

Well Installation: 10/17/03-10/21/03

Well Developed: 10/29/03-11/16/03

- Casing:
  - 4.46" ID / 5.0" OD A304 Stainless Steel casing with external couplings
- Number of Screens:
  - Two (2) 4.46" ID wire wrapped stainless steel with external couplings.
  - Screen #1 (Upper): 5.53" OD Pipe based 0.010 slot
  - Screen #2 (Lower): 5.27" OD Rod based 0.020 slot
- Screen Intervals:
  - Screen #1 (Upper): 651.8' - 669.9'
  - Screen #2 (Lower): 1421.8' - 1445'

Well Development performed by airlifting, swabbing, bailing, and pumping.

Total Volume Purged: 41,069 gallons

#### Corehole Temporary Piezometer Completions

- Casing - 1" OD Sched. 40 PVC threaded
- Number of Screens - One (1) 1" OD Sched. 40 PVC 0.010 slotted in each piezometer
- Screen Interval -
- Piezometer 1 - 230'-250'
- Piezometer 2 - 150'-180'

Geologic contacts for R-26

were determined from core samples, cuttings, borehole video, and geophysical logs.

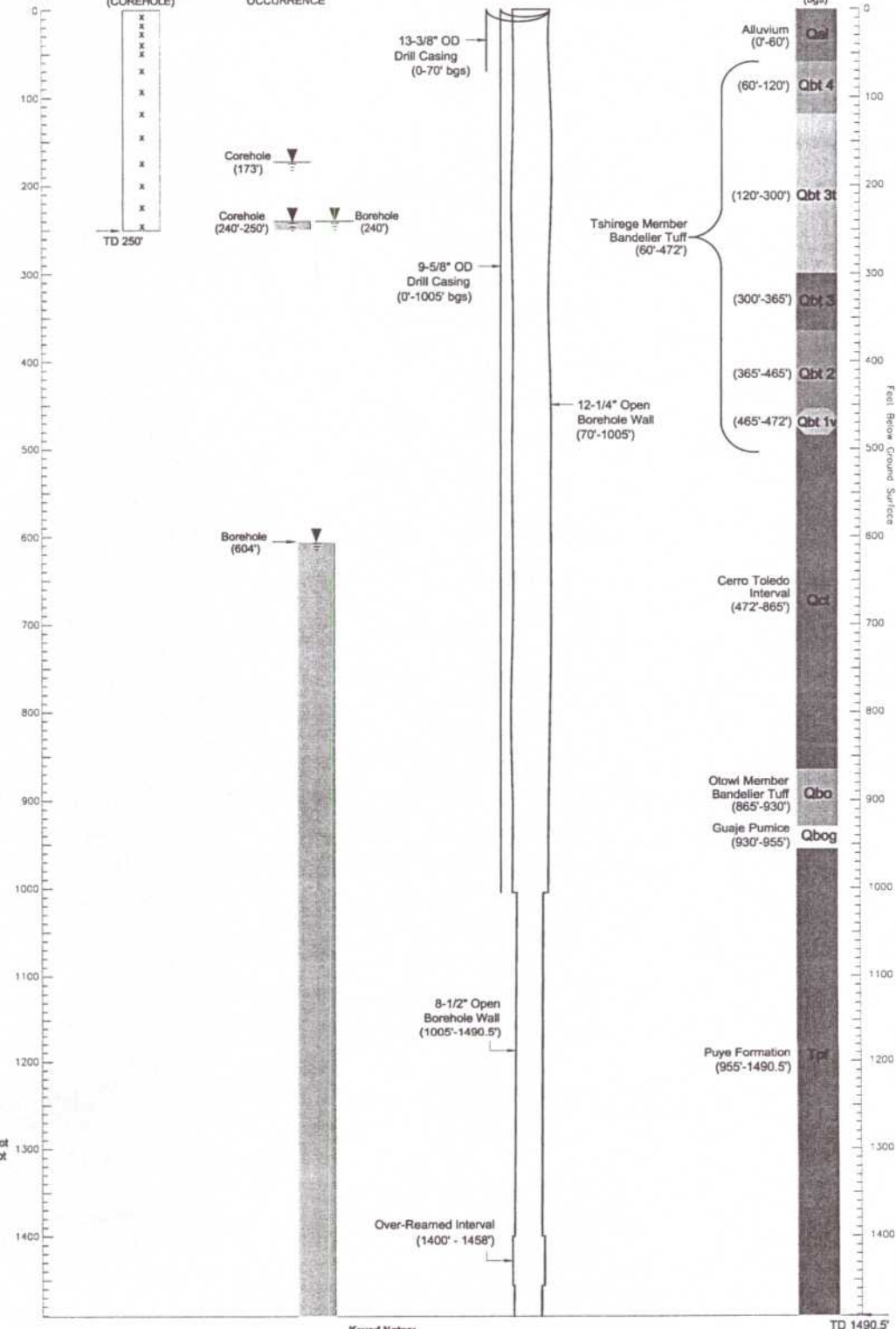
BOREHOLE (bgs)

CONTAMINANT CHAR. SAMPLES (x) (COREHOLE)

BOREHOLE/COREHOLE GROUNDWATER OCCURRENCE

R-26 CONFIG. AT TD (BOREHOLE)

STRATIGRAPHY ENCOUNTERED (bgs)



#### Keyed Notes:

- Coordinates - NM State Plane Grid Central Zone (North America) Datum - 1983 (NAD83); expressed in feet.
- Elevations - National Geodetic Vertical Datum (NGVD29); expressed in feet above mean sea level.
- All depths are below ground surface (bgs).
- Drill casing removed prior to well installation.
- Borehole reamed across Screen #2 Interval (1421.8'-1445').
- Water level measurement in shallow piezometer was 172.97'; the deep piezometer was dry when sounded on 11-25-03.
- Post-development composite groundwater level measurement recorded on 9-21-03.

TD 1490.5'



KLEINFELDER

Drawn By: C. Landon

Date: January 2005

Project No.: 37151

Filename: Figure 3.0-1.dwg

Scale: not-to-scale

Revision: 4

WELL SUMMARY DATA SHEET  
Well R-26  
Los Alamos National Laboratory  
Los Alamos, New Mexico

FIGURE

3.0-1

TABLE 3.0-1. OPERATIONS CHRONOLOGY GRAPH FOR WELL R-26

TASK DESCRIPTIONS	DATE													
	August-03	Sep-03	Oct-03	Nov-03	Dec-03	Jan-04	Feb-04	Mar-04	Apr-04	May-04	Jun-04	Jul-04		
<b>SITE PREPARATION ACTIVITIES</b>	8/27	9/16												
<b>COREHOLE DRILLING AND SAMPLING</b>		9/8												
Mobilization		9/8												
Continuous Coring		9/8	9/12											
LANL Video & Geophysics			9/15											
Plug & Abandon Corehole														
<b>BOREHOLE DRILLING AND SAMPLING</b>		9/17	10/17											
Mobilization		9/17												
Air Rotary		9/18												
Fluid Assisted Air Rotary		9/19												
Mud Rotary			9/20	10/17										
Groundwater Screening Sampling		9/18, 9/21-22												
<b>BOREHOLE GEOPHYSICS</b>		9/22	10/16											
Schlumberger Logging			9/28	10/14-15										
LANL Video		9/15	9/22											
LANL Geophysics				10/16	10/17									
<b>WELL DESIGN AND CONSTRUCTION</b>			10/17-21											
<b>WELL DEVELOPMENT</b>				10/18		11/17								
<b>GROUNDWATER WELL SAMPLING</b>					11/14	11/16								
<b>HYDROLOGIC TESTING</b>							2/16	2/27	3/6					
<b>SITE RESTORATION</b>									4/4-8				7/16-18	
<b>WESTBAY INSTALLATION</b>														

NOTES:

Shaded area indicates no activity

### 3.2 Phase II Drilling Activities

On September 17, 2003, WDC mobilized a Dresser T70W drill rig, compressor and, support equipment to the site for Phase II drilling. The Phase II borehole was located 91 ft northeast of the corehole. On September 18, 2003, the WDC drill crew advanced 13 $\frac{3}{8}$ -in. OD drill casing to 65 ft bgs with a 12 $\frac{1}{4}$ -in. tricone drill bit. The borehole was drilled ahead of the drill casing to 77 ft bgs.

On September 19, 2003, WDC drove the 13 $\frac{3}{8}$ -in. conductor casing to 70 ft bgs, then advanced the borehole with the 12 $\frac{1}{4}$ -in. tricone drill bit and air-rotary methods from 77 ft bgs to 140 ft bgs. The drillers switched to a 12 $\frac{1}{4}$ -in. DTH hammer bit with air only and drilled open-hole to 147 ft bgs. The borehole was checked for the presence of groundwater at the end of the shift and at the start of work on September 20, 2003; none was present. Open-hole air-rotary drilling resumed at 147 ft bgs, and water was used for dust suppression.

On September 20, 2003, at approximately 205 ft bgs, drilling fluids consisting of QUIK-FOAM<sup>®</sup> and EZ-MUD<sup>®</sup> and potable water were used to facilitate cuttings removal and borehole stabilization. Table 3.2-1 shows the total amount of drilling fluids introduced and recovered from the borehole during Phase II drilling activities. The borehole was advanced through the Tshirege Member of the Bandelier Tuff and into volcanoclastic sediments and pumice beds of the Cerro Toledo interval to 565 ft bgs.

**Table 3.2-1**  
**Introduced and Recovered Drilling Fluids**

Material	Unit	Amount
QUIK-FOAM <sup>®</sup>	Gallon	31
EZ-MUD <sup>®</sup>	Gallon	3.25
Potable Water	Gallon	23,690
Drilling Mud <sup>1</sup>	Gallon	95,500
Recovered Fluids <sup>2</sup>	Gallon	53,856

<sup>1</sup> Drilling Mud is a mixture of water, bentonite, soda ash and Pac-L polyanionic cellulose

<sup>2</sup> Recovered fluids represents approximate fluids recovered during drilling based on pit dimensions. Fluids removed during well development are included in Table 8.1-1.

On September 21, 2003 a measured depth-to-water (DTW) indicated that the borehole was dry. Drilling resumed open hole using air and a mixture of potable water, EZ-MUD<sup>®</sup> and QUIK-FOAM<sup>®</sup>. At 650 ft bgs, observations of the drilling discharge indicated the potential presence of groundwater. The borehole was advanced to 720 ft bgs, where drilling was halted and all tools were tripped out of the borehole. DTW measurements indicated groundwater stabilized after approximately one hour at 604.3 ft bgs. A groundwater screening sample was collected for chemical analysis with a stainless-steel bailer, and the site was secured for the day.

At the beginning of the shift on September 22, 2003, the DTW was measured at 604.2 ft bgs. A second groundwater sample was then collected for chemical analysis with a stainless-steel bailer and the video camera was deployed in the open borehole to document subsurface conditions.

Fluid-assisted drilling resumed open-hole from 720 ft bgs to 900 ft bgs in Cerro Toledo sediments and the Otowi Member of the Bandelier Tuff using a 12¼-in. mill-tooth tricone bit. On the morning of September 23, 2003, the DTW was measured at 611.7 ft bgs. The drillers advanced the borehole from 900 ft through the Guaje Pumice Bed and into the clastic sediments of the Puye Formation to 1,000 ft bgs using a 12¼-in. tricone button bit with fluid-assisted air-rotary drilling methods. At 1,000 ft bgs, WDC elected to switch to the mud-rotary drilling method because of increased borehole sidewall instability.

On September 24 and 25, 2003, WDC mobilized a shaker table and other equipment to prepare for mud-rotary drilling. The New Mexico Environment Department (NMED) approved all mud-drilling additives. On September 25, 2003, three 1,500-gal. batches of drilling mud were mixed and pumped into the borehole. A single batch of drilling mud consisted of 1500-gal. of water, 12 to 22 bags of Aqua-Gel powdered bentonite, 8 quarts of Pac-L (Drispack) and 10 pounds of soda ash. Drilling mud-batch mixing continued through September 26 and 27, 2003. By the end of the shift on September 27, 42,000 gal. of drilling mud had been pumped into the borehole. The calculated capacity of the borehole was 5,932 gal. The top of the mud was last measured at 170 ft bgs, indicating that substantial fluid loss was occurring from the borehole. A total of 7 bags of N-Seal (lost circulation material) had been added to the last five batches of the day to attempt to mitigate the fluid loss from the borehole.

On September 28, 2003, Schlumberger arrived onsite and ran geophysical logging tools described in Section 5.0.

On September 29, 2003, WDC attempted to run 11¾-in. threaded drill casing into the borehole to prevent further fluid loss problems in the borehole. An imperfection in the borehole prevented the 11¾-in. drill casing from being lowered past 131.5 ft bgs. The imperfection was possibly either a slight deviation in the alignment of the borehole or a rock ledge. The borehole was subsequently reamed to 160 ft bgs with a 12½-in. tricone bit in an attempt to remove the imperfection; however, the 11¾-in. casing could not be lowered or pushed past 135 ft bgs when installation was reattempted. On September 30 and October 1, 2003, WDC reamed the entire borehole from ground surface to 1,005 ft bgs with an 8-in. tricone drill bit and an 8-in. roller-reamer bit positioned above the drill bit. The roller-reamer bit was capable of expanding to a maximum effective diameter of 14-in. However, drill rig pump pressures were not sufficient to achieve the maximum reaming diameter. Water and QUIK FOAM® were used to ream the borehole. On October 2, 2003, DTW was measured at 606 ft bgs and the 11¾-in. drill casing was tripped in for a third time to approximately 135 ft bgs, where it once again encountered the imperfection that prevented further advancement of the casing.

A decision was made to install smaller-diameter drill casing that would theoretically bypass the obstruction. On October 3 and 4, 2003, the 9⅝-in. drill casing was installed to a final depth of 1000 ft bgs. At 0830 on the morning of October 4, 2003, the drill crew began days off. On October 10, 2003, drilling operations resumed. WDC mixed and pumped three 1,500-gal. batches of drilling mud into the cased borehole. The batches consisted of water, 10 bags of bentonite, 10 bags of soda ash, and 6 quarts of Pac-L polyanionic cellulose. At approximately 980 ft bgs, while reaming the 9⅝-in. drill casing with the 8½-in. tricone button bit, the drill casing slipped down 5 to 1,005 ft bgs. On the following day, WDC reamed cuttings from the casing and drilled open-hole from 1,005 to 1,145 ft bgs in the Puye fanglomerate using the 8½-in. tricone button bit and mud-rotary techniques.

On the morning of October 11, 2003, the borehole was reamed and drilling resumed. Drilling continued open-hole using the same equipment and methods until October 14, 2003, when the borehole had been advanced to 1,485 ft bgs. Schlumberger mobilized borehole geophysical logging equipment to the site the same day and gathered borehole geophysical data, which are described in Section 5.0. On October 15, 2003, WDC set up to ream the borehole with a 4½-in. tricone pilot bit with a 2½-in. side reamer using mud-rotary methods. The crew worked through the night, and on October 16, 2003, had reamed the borehole to 1,485 ft bgs, still within the Puye Fanglomerate, and had over-drilled an additional 5 ft to 1,490.5 ft bgs, the TD of the borehole. The LANL geophysics trailer was mobilized to the site to run the borehole caliper to verify that the borehole diameter was sufficient to build a monitoring well with the required 2-in. annulus. Caliper data indicated that the borehole diameter was 8.5-in. within the vicinity of the planned well-screen interval, too small to provide the required 2-in. annulus for a 5-in.-diameter well screen (caliper log on compact disk [CD], inside back cover). WDC subsequently reamed the borehole again from 1,400 to 1,475 ft bgs with the 14-in. hydraulic roller-reamer and 4.5-in. tricone pilot bit. After the borehole had been reamed to 1,485 ft bgs, caliper data indicated that the borehole measured at least 9.3-in. in diameter throughout the planned lower screened interval of the monitoring well (caliper log on CD, inside back cover). Phase II drilling was completed on October 17, 2003, and well construction preparations commenced.

## 4.0 SAMPLING AND ANALYSIS OF DRILL CUTTINGS AND GROUNDWATER

### 4.1 Sampling of Drill Cuttings and Core

During drilling operations at R-26, drill cuttings were collected according to the LANL-prepared Sampling and Analysis Plan (LANL 2003). As drilling conditions permitted, an ample quantity of borehole material was collected from the discharge line at 5-ft intervals. A portion of the cuttings was sieved (at >#10 and >#35 mesh, or >#35 and >#60 for finer-grained samples) and placed in chip-tray bins along with an unsieved portion. These chip trays were studied to determine lithologic characteristics and were used to prepare the lithologic logs. The remaining cuttings were sealed in Ziploc® bags and set in core boxes for curation. Seven samples were removed by LANL for mineralogic, petrographic, and geochemical analyses. No cuttings samples were submitted for contaminant characterization analysis.

Core samples were collected from R-26 and analyzed for cations, anions, metals, and radionuclides for characterization purposes. Thirteen samples of core were collected from the vadose (unsaturated) zone during drilling from 5 ft to 250 ft bgs. Approximately 500 grams (g) to 1,000 g of core samples were placed in appropriate sample jars and protective plastic bags before being delivered to Earth and Environmental Sciences (EES)-6, Coastal Science Laboratories, Inc., and General Engineering Laboratories (GEL) for laboratory analysis. Analytical results will be included in future investigation reports for Cañon de Valle.

### 4.2 Sampling of Groundwater

During Phase I drilling operations at R-26, perched groundwater was encountered at 240 ft bgs, and a groundwater screening sample was collected on September 18, 2003, from the corehole for analysis. Groundwater samples have not been collected from the temporary piezometers.

During Phase II drilling operations, groundwater was first encountered at 650 ft bgs on September 21, 2003. After the borehole was advanced to 720 ft bgs, the water table was

measured at 604 ft bgs. At this stage, the drill system was removed from the borehole, and a groundwater screening sample was collected using a wireline bailer. On the morning of September 22, 2003, the DTW was measured at 604 ft bgs, and a second groundwater screening sample was collected from the open borehole. Because the second sample contained less suspended sediment, it was submitted for analysis and the first sample was disposed of.

Although the regional water table was predicted to occur at 1,314 ft bgs, neither the drillers nor the onsite geologists were able to distinguish between the increased flow detected from the drilling discharge line at approximately 600 ft bgs and groundwater in the regional aquifer. Geophysical log interpretation suggests that full saturation does not occur until the Puye Formation is encountered at 955 ft bgs (see Section 5.2 and Appendix B, Schlumberger's Geophysical Report and Montages, for further discussion). During well development activities, two groundwater samples were collected from the completed well R-26 on November 14 and 16, 2003. With a packer isolating the two screened intervals, these samples were collected from 1,430 ft and 660 ft bgs, respectively, and were submitted for analysis.

Further discussion of the groundwater sampling and analytical results are presented in Appendix C.

## **5.0 BOREHOLE GEOPHYSICS**

Using LANL-owned and subcontractor-owned tools, KA and Schlumberger performed borehole geophysics logging operations at R-26.

### **5.1 KA-Supported Geophysical Logging**

On September 15, 2003, video, natural gamma, and resistivity logging were performed in the R-26 corehole using downhole tools provided by LANL. The logs were used to look for perched water and to aid in lithologic contact identification. On September 22, 2003, video logging was performed in borehole R-26 using downhole tools provided by LANL. On October 16, 2003, caliper logging was performed in the borehole to determine whether the borehole diameter was sufficient for well screen installation. On October 17, 2003, after the borehole was reamed, caliper logging was rerun to confirm that the borehole was of sufficient diameter.

Table 5.1-1 summarizes the video and geophysical well logs conducted in R-26. The video logs of the open borehole were digitized onto the two digital videodiscs (DVDs) that are included as Appendix A. The gamma, resistivity, and caliper logs are included on the CD included on the back inside cover of this report.

**Table 5.1-1**  
**Borehole and Well Logging Surveys Conducted in R-26**

Operator	Date	Method	Cased Footage (ft bgs)	Open-hole Interval (ft bgs)	Remarks
KA/LANL	September 15, 2003	Video	0-65	65-241	Corehole video to identify accumulated water
KA/LANL	September 15, 2003	Gamma and Resistivity Log	0-65	65-245	Corehole logging
KA/LANL	September 22, 2003	Video	0-70	70-717	Open-borehole video
Schlumberger	September 28, 2003	Logging suite <sup>a</sup>	0-70	70-985 <sup>b</sup>	Schlumberger borehole logging conducted on open hole before installing casing
Schlumberger	October 14 and October 15, 2003	Logging suite <sup>a</sup>	0-1005	1005-1477 <sup>b</sup>	Schlumberger borehole logging conducted to TD before well installation
KA/LANL	October 16, 2003	Caliper Log	0-1005	977-1459	Borehole logging to determine diameter before well installation
KA/LANL	October 17, 2003	Caliper Log	0-1005	1374-1474	Borehole logging to determine diameter before well installation

<sup>a</sup> Schlumberger suite of borehole logging surveys included triple detector litho-density, array induction tool, epithermal compensated neutron tool, elemental capture spectrometry, full-bore formation microimager, combinable magnetic resonance tool, natural gamma spectrometry, caliper gamma ray, spontaneous potential, and platform express.

<sup>b</sup> Variable effective depths, see Appendix A.

## 5.2 Schlumberger Geophysical Logging

The primary purpose of the Schlumberger logging was to characterize the conditions in the hydrogeologic units penetrated by the R-26 borehole, with emphasis on gathering moisture distribution data, identifying possible perched water zones, measuring capacity for flow (porosity and moisture), and obtaining lithologic/stratigraphic data. Secondary objectives included evaluating borehole geometry and determining the degree of drilling fluid invasion along the borehole wall.

Schlumberger personnel conducted geophysical logging in the R-26 borehole on September 28 and again on October 14 and 15, 2003. During the initial geophysical logging, a 13 $\frac{3}{8}$ -in. OD drill casing extended from the ground surface to 70 ft bgs, and the remainder of the borehole was open to 985 ft bgs. During the second run of geophysical logging, a 13 $\frac{3}{8}$ -in. OD drill casing extended from the ground surface to 70 ft bgs, and a 9 $\frac{5}{8}$ -in. OD steel drive casing extended from the surface to 1,005 ft bgs; the remainder of the hole was open to 1,485 ft bgs.

Schlumberger personnel ran a suite of geophysical logging tools in the cased and uncased portions of the borehole. The suite included the following tools:

- Combinable Magnetic Resonance<sup>TM</sup> tool measures the nuclear magnetic resonance response of the formation. It is used to evaluate total and effective water-filled porosity of the formation and to estimate pore-size distribution and in-situ hydraulic conductivity.
- Array Induction Tool, version H<sup>TM</sup>, measures formation electrical resistivity and borehole fluid resistivity, thus evaluating the drilling fluid invasion into the formation, the presence of moist zones away from the borehole wall, and the presence of clay-rich zones.
- Triple Detector Litho-Density<sup>TM</sup> measures formation bulk-density related to porosity, photoelectric effect related to lithology, and borehole diameter using a single-arm caliper.
- Natural Gamma Spectroscopy (NGS<sup>TM</sup>) measures spectral and overall natural gamma-ray activity, including potassium, thorium, and uranium concentrations, thus evaluating geology and lithology.
- Elemental Capture Spectroscopy<sup>TM</sup> measures concentrations of hydrogen, silicon, calcium, sulfur, iron, aluminum, potassium, titanium, chlorinity, and gadolinium to characterize mineralogy, lithology, and water content of the formations.
- Epithermal Compensated Neutron Tool, model G<sup>TM</sup>, measures volumetric water content beyond the casing to evaluate formation moisture content and porosity.
- Full-Bore Formation Micro-Imager (FMI<sup>TM</sup>) measures electrical conductivity images of the borehole wall and the borehole diameter with a two-axis caliper to evaluate geologic bedding and fracturing, including strike and dip of these features, fracture apertures, and rock textures.

Additionally, a calibrated natural gamma tool was used to record gross natural gamma-ray activity with each logging method (except the NGS<sup>TM</sup> run) to correlate depth runs between each of the surveys conducted.

The Schlumberger interpretive logging report and the geophysical logs, compiled as a montage, can be found as Appendix B (compact disc included). Additionally, an abstract of Schlumberger's report is presented in Appendix B on pages B-1 and B-2.

## 6.0 LITHOLOGY AND HYDROGEOLOGY

A preliminary assessment of the hydrogeologic features encountered during drilling operations at R-26 is presented below. Groundwater occurrences are discussed based on drilling evidence, open-hole video logging, and geophysical logging data. LANL EES-6 staff provided preliminary geologic contacts.

## 6.1 Stratigraphy and Lithologic Logging

Rock units and stratigraphic relations, interpreted primarily from visual examination of rock core, sampled drill cuttings, and geophysical data, are briefly discussed in order of younger to older occurrence. These interpretations may be revised upon further analysis of petrographic, geochemical, mineralogical, and geophysical data. A lithology log for the R-26 borehole is provided in Appendix D.

### Alluvium (0 to 60 ft bgs)

Core samples indicated that unconsolidated alluvium was intersected in R-26 from ground surface to approximately 60 ft bgs. This interval is made up of clastic sediments, including tuffaceous silty sands and gravels as well as weathered boulders and blocks of indurated ash flow tuff. The sedimentary constituents are likely derived from the Tshirege Member of the Bandelier Tuff and Tschicoma dacite lavas.

### Bandelier Tuff (60 to 955 ft bgs)

The Bandelier Tuff is locally represented in borehole R-26 in the interval from 60 to 955 ft bgs by the Tshirege (Qbt) and Otowi Members, including the Guaje Pumice Bed at the base of the section. An unusually thick section of the Cerro Toledo interval was identified between the Tshirege and Otowi Members from 472 to 865 ft bgs.

### Ash flows of the Tshirege Member of the Bandelier Tuff (60 to 472 ft bgs)

Rhyolitic ash flows of the Tshirege Member have been divided into four separate cooling units in the general region of the Pajarito Plateau (Broxton and Reneau, 1995). The drilled R-26 section from 60 to 472 ft bgs is interpreted to represent, in descending order, Units 4, 3t, 3, 2, and 1v. Unit 1g, which is normally present at the base of the Tshirege Member, is absent at R-26. The tuff section is locally typified by strong welding that is characteristic of ash flows occurring in the western part of the plateau.

Unit 4 was intersected from 60 to 120 ft bgs. Core and cuttings samples indicate that Unit 4 is comprised of abundant sanidine and quartz phenocrysts, typically making up 20 to 40% of the sample by volume, and up to 30% pumice lapilli enclosed in a matrix of reddish fine vitric ash. Volcanic lithic fragments (i.e., xenoliths) are locally present in abundances of 1 to 2% by volume. Welding is characterized as weak near the top, possibly due to the effects of weathering, but increases significantly toward the base of the interval.

Units 3t and 3 are represented in the R-26 section from 120 to 300 ft, and from 300 to 365 ft bgs, respectively. Cuttings samples from Unit 3t, a unit having chemical properties transitional between Qbt 3 and Qbt 4, are represented by chips of strongly welded tuff that are typically made up of quartz, sanidine, and minor ferromagnesian minerals (possibly pyroxene), as much as 3% small intermediate volcanic xenoliths, and a well-indurated matrix of light to medium gray vitric ash. Unit 3 appears to be a strongly welded crystal-rich tuff with characteristics that are visually similar to those of Unit 3t.

Cuttings from Unit 2, intersected in R-26 from 365 ft to 465 ft bgs, are made up of light brownish gray, indurated, strongly welded tuff. Crystals (commonly as much as 50% by volume) of sanidine, quartz, and ferromagnesian minerals and small (up to 5 millimeters) felsic and

intermediate volcanic lithics (up to 5% by volume) are enclosed in an aphanitic matrix of vitric ash.

Unit 1v occurs from 465 to 472 ft bgs. It is defined by a downward decrease in bulk density toward the base of the Tshirege Member. The contact between the strongly welded tuffs of Unit 2 and the less welded tuffs of Unit 1v is gradational.

#### **Cerro Toledo Interval (472 to 865 ft bgs)**

Volcaniclastic sedimentary and tephra deposits of the Cerro Toledo interval regionally separate the Tshirege and Otowi Members of the Bandelier Tuff. Geophysical logs suggest that the Cerro Toledo interval occurs in borehole R-26 from 472 to 865 ft bgs. This unexpectedly thick interval of tuff and volcaniclastic sediments appears to represent a filled paleo-channel incised into the underlying Otowi Member. Cuttings indicate that this volcaniclastic deposit is locally made up of silty to clayey sands and gravels. Detrital constituents comprised of hornblende-biotite dacite, rhyolite, andesite, indurated welded tuff, pumice fragments, and local vitrophyre are present in varying abundances throughout the interval.

#### **Ash flows of the Otowi Member of the Bandelier Tuff (865 to 930 ft bgs)**

Ash flows of the Otowi Member of the Bandelier Tuff are recognized in the interval from 865 ft to 930 ft bgs. Cuttings show that the Otowi Member is strongly pumiceous and poorly welded. Pumice fragments in chip samples are vitric and white or orange-brown as a result of iron-oxide staining. Volcanic lithic fragments represent xenoliths of dacite, andesite, rhyolite, and vitrophyre. Free quartz and sanidine crystals are generally abundant in the fine-grained fraction of the sieved cuttings samples.

#### **Guaje Pumice Bed of the Otowi Member (930 to 955 ft bgs)**

The Guaje Pumice Bed (Qbog) was encountered in borehole from 930 to 955 ft bgs. Cuttings from this interval indicate the unit is nonwelded and generally pumice-rich. Samples from this unit are typically made up of pumice, quartz, and sanidine crystals, and lithic fragments of intermediate volcanic composition.

#### **Puye Formation (955 to 1490.5 ft bgs)**

Fanglomerates of the Puye Formation were intersected in the R-26 interval from 955 ft to the borehole TD at 1490.5 ft bgs. The FMI log (Appendix D) indicates that the Puye Formation largely consists of clast- and matrix-supported conglomerate, with clasts commonly 0.5 to 1.5 ft in diameter. Clasts in these sediments are predominantly made up of detritus, likely derived from volcanic rocks of the Tschicoma Formation, including porphyritic dacite, rhyodacite, rhyolite, andesite, and vitrophyre. Minor occurrences of welded tuff and chert are locally present in the interval.

### **6.2 Groundwater Occurrence and Characteristics**

Perched groundwater saturation zones above the regional aquifer were predicted to occur in R-26 within either the Cerro Toledo interval or the Otowi Member of the Bandelier Tuff, or between 700 and 900 ft bgs. However, during Phase I coring, a shallow zone of perched saturation was first observed at 240 ft bgs within the Tshirege Member of the Bandelier Tuff and before

encountering refusal at 250 ft bgs. A video camera survey of the open corehole indicated that water was emanating from a depth of 150 to 180 ft bgs.

Two temporary piezometers were installed side by side in the corehole to collect possible perched groundwater data from two target intervals: an upper screen from 150 ft to 180 ft bgs (piezometer 2) and a lower screen from 230 ft to 250 ft bgs (piezometer 1). On November 25, 2003, approximately 1 month after the installation of the piezometers, the DTW was measured at 173 ft bgs in piezometer 2; however, no water was present in piezometer 1.

An intermediate perched saturated zone was indicated by a sustained increase in flow from the discharge line during Phase II drilling in the Cerro Toledo interval, at approximately 650 ft bgs. A groundwater level measurement of 604 ft bgs was observed on September 21, 2003, when the depth of the borehole was at 720 ft bgs.

The chemical indicator potassium bromide (KBr) was added to drilling fluids when the borehole had been advanced to 200 ft bgs. Monitoring input and output concentrations showed that KBr concentrations were at fairly consistent levels from 300 to 600 ft bgs. KBr concentrations began to decrease significantly at 650 ft bgs, reflecting dilution of the drilling fluids by formational water entry into the borehole. Due to the presence of significant quantities of groundwater in the borehole, KBr monitoring was suspended when the borehole was advanced to 1005 ft bgs.

The processed geophysical logs indicate high water-filled porosity within the porous, glassy tuff/pumice and volcanoclastic sediment sections in R-26 from 575 to 955 ft bgs. However, the processed logs, by themselves, indicate that most of this interval is not fully saturated with water. A water level between 865 ft and 885 ft bgs made when the bottom screen was isolated during hydrologic testing is consistent with these observations. The total porosity in the glassy tuffs/pumice and volcanoclastic sediments, estimated from the elemental analysis (ELAN) integrated log analysis, ranges from 40% to over 50% of total rock volume, with water saturations of generally 50–80%.

The estimated moveable water content is generally high across this water-rich glassy tuff/pumice and volcanoclastic sediment interval ranging from 5 % to 25% of total rock volume. Although much of the 575 to 955 ft bgs interval may not be fully saturated with water, the high total and moveable water content suggests that, in general, the water is quite mobile. The water in this interval is likely connected to the saturated Puye Formation below.

There is strong evidence from the processed geophysical logs that the bottom of Well R-26, below the Guaje Pumice Bed (955 ft bgs) in the Puye Formation, lies within the regional aquifer. The estimated pore volume water saturation (fraction of the total pore volume containing water) computed from the ELAN analysis is over 85% from 954 ft bgs to the bottom of the log interval at 1484 ft bgs. The estimate is even higher when computed directly from bulk density and ELAN water-filled porosity for a grain density range of 2.45 grams per cubic centimeter (g/cc) to 2.65 g/cc, ranging from 90% to a consistent 100%.

The estimated moveable water generally varies from 7% to 15% of total rock volume across the saturated interval. The hydraulic conductivity estimated from the ELAN integrated log analysis (from the CMR moveable water measurement) generally ranges from 0.1–1 gal./day/ft<sup>2</sup>. However, in the intervals from 1,100 to 1,108 ft bgs and 1,186 ft to 1,200 ft bgs the hydraulic conductivity is estimated to be over 3 gal./day/ft<sup>2</sup>.

## 7.0 WELL DESIGN AND CONSTRUCTION

R-26 was installed as a hydrogeologic characterization and groundwater monitoring well as part of LANL's Groundwater Protection Program and in accordance with the "Hydrogeologic Workplan" (LANL 1998). On October 17, 2003, KA received final construction specifications for R-26 following approval of the design by DOE, LANL, and NMED. Well installation activities were performed from October 17 to 21, 2003. Sections 7.1 and 7.2 describe the main aspects of well design and construction, respectively. Section 7.3 discusses the completion of two piezometers in the corehole.

### 7.1 Well Design

Well design was undertaken jointly by DOE, LANL, and KA, and NMED approved the well design before well construction. Data from geophysical logs, borehole video logs, borehole geologic samples, field water level and water quality measurements, and field observations were analyzed to determine the appropriate intervals to be screened. Two well screen intervals were specified for R-26: (1) an upper screen to monitor groundwater associated with an intermediate zone of perched saturation and (2) a lower screen to monitor potential contaminants in the uppermost productive zone of the regional aquifer. The planned well design assumed a typical two-section, rod-based screen length of approximately 23 ft. However, a two-section, pipe-based screen with a perforated length of 18 ft was used for the upper screened interval. In addition, the blank casing length between the two screened intervals is approximately 4 ft shorter than the design due to the limitations of available casing joint lengths. The planned design and actual constructed screen locations for R-26 are listed in Table 7.1-1.

**Table 7.1-1**  
**Summary of Well Screen Information for Well R-26**

Screen No.	Planned Depth (ft bgs) <sup>a</sup>	Actual Depth (ft bgs) <sup>a</sup>	Geologic/Hydrologic Setting
1	643–666	651.8–669.9	Intermediate perched zone in the Cerro Toledo interval of the Bandelier Tuff
2	1422–1445	1421.8–1445	Regional zone of saturation in the Puye Formation

<sup>a</sup> These intervals represent the perforated area of the screen.

### 7.2 Well Construction

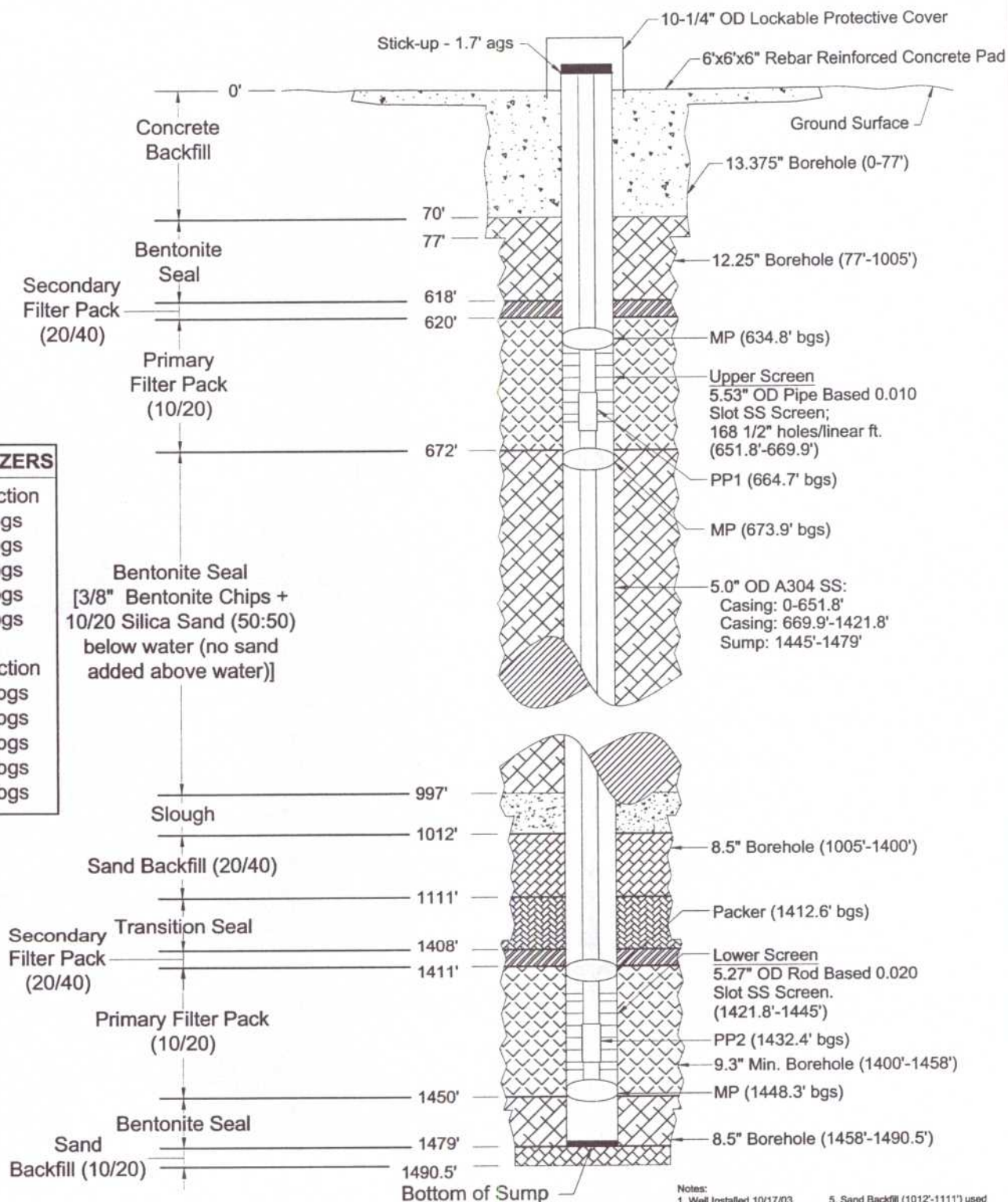
R-26 was constructed of 4.46-in. inner diameter (ID)/5.0-in.-OD, type A304 stainless-steel casing fabricated to American Society for Testing and Materials (ASTM) A312 standards. The upper screen was constructed of two 10-ft joints of wire-wrapped 5.53-in.-OD, pipe-based 0.010-in. slotted well screens. The lower screen was constructed using 5.27-in.-OD, rod-based 0.020-in. slotted screens. Stainless-steel casing was installed below the lower screen to provide a 34-ft-long well sump. Figure 7.2-1 is a schematic as-built diagram of the completed R-26 well.

External couplings, also of type A304 stainless steel fabricated to ASTM A312 standards, were used to connect individual casing and screen joints. Centralizers were installed above and below

# CENTRALIZERS

Upper Section  
347 ft. bgs  
529 ft. bgs  
620 ft. bgs  
659 ft. bgs  
670 ft. bgs

Lower Section  
1086 ft. bgs  
1298 ft. bgs  
1420 ft. bgs  
1432 ft. bgs  
1446 ft. bgs



- Notes:
1. Well installed 10/17/03.
  2. ags - above ground surface.
  3. bgs - below ground surface.
  4. Screen depths are slotted intervals.
  5. Sand Backfill (1012'-1111') used for casing support.
  6. Borehole reamed 1400'-1458'.
  7. Drill Casing removed prior to well installation.
  8. Westbay installed: 7/16/05
  9. MP - Packer / PP - Port



**KLEINFELDER**

Drawn By: C. Landon  
Project No.: 37151  
Scale: not-to-scale

Date: January 2005  
Filename: Figure 7.2-1.dwg  
Revision: 0

**WELL SCHEMATIC DIAGRAM**  
**Well R-26**  
**Los Alamos National Laboratory**  
**Los Alamos, New Mexico**

FIGURE

**7.2-1**

each joint of well screen. In addition, one centralizer was placed approximately 100 ft above each screen interval. Centralizers for R-26 are located at 347 ft, 529 ft, 620 ft, 659 ft, 670 ft, 1,086 ft, 1,298 ft, 1,420 ft, 1,432 ft, and 1,446 ft bgs (Figure 7.2-1).

The casing and screens were factory-cleaned before being shipped and delivered to the site. Additional decontamination of the stainless-steel components was performed onsite using a high-pressure steam cleaner and scrub brushes. Annular fill was placed in casing/borehole annulus through use of a tremie pipe. Well installation occurred on October 17, 2003, and backfilling was completed on October 21, 2003.

### 7.2.1 Steel Installation

R-26 well steel installation consisted of connecting joints of stainless-steel casing and screen sections by means of external threaded couplings. The bottom of the well was set at 1,479 ft bgs. Figure 7.2-1 shows the as-built well configuration and indicates the depths of the various well components as measured from ground surface.

### 7.2.2 Annular Fill Placement

Placement of annular fill consisted of using a 2.5-in. OD steel tremie pipe to deliver various materials to specified backfill intervals. Filter packs across screened intervals consisting of silica sand were generally transported using municipal water and placed in the annulus as a fluid slurry. Bentonite materials were placed between screened intervals to seal the annular space and to isolate the water-bearing zones.

The bottom of the open R-26 borehole was measured at 1,490.5 ft bgs before beginning backfill activities. Well casing and screens were lowered in the hole, and the bottom of the sump was positioned at 1,479 ft bgs. The lower part of the borehole was backfilled with 10/20 silica sand from 1,490.5 ft (TD) to 1,479 ft bgs, and bentonite chips were then tremied in the annulus from the top of the sand to 1,450 ft bgs to create a seal around the well sump. A primary filter pack consisting of 10/20 silica sand was placed across the lower screen in the annular interval from 1,450 to 1,411 ft bgs, and a secondary filter pack of 20/40 silica sand was placed above the screen from 1,411 to 1,408 ft bgs. A swabbing tool was run through the screened interval to settle the primary filter pack before placement of the secondary filter pack. Next, a transition seal was placed above the secondary filter pack in the annular space between 1,408 and 1,111 ft bgs. The transition seal consisted of a 50:50 mixture of 10/20 sand and bentonite chips.

To provide casing support, 20/40 silica sand backfill was placed above the transition seal from 1,111 to 1,012 ft bgs. After placing the transition seal, 15 ft of formation material was sloughed into the annulus. A bentonite seal was installed above the backfill sand from 997 to 672 ft bgs. A primary filter pack consisting of 10/20 silica sand was then tremied across the upper screen interval from 672 to 620 ft bgs, followed by a secondary filter pack of 20/40 silica sand from 620 to 618 ft bgs. A swabbing tool was run through the screened interval to settle the primary filter pack before placement of the secondary filter pack. A final bentonite seal was then placed above the secondary filter pack from 618 to 70 ft bgs. Concrete backfill, consisting of 2,500 pounds per square inch (psi) concrete with 4 percent bentonite, was placed from 70 ft bgs to near the surface. Approximately 16,000 gal. of water were used during well completion. The quantities of annular fill materials used in the completion of R-26 are presented in Table 7.2-1.

**Table 7.2-1**  
**Annular Fill Materials Used in Well R-26**

Function/Material	Amount	Unit <sup>a</sup>	Mix
Backfill: 10/20 sand	10	Bag	—
Seal: ⅜-in. bentonite chips	15.5	Bag	—
Primary filter pack, lower screen: 10/20 sand	15.5	Bag	—
Secondary filter pack, lower screen: 20/40 sand	1	Bag	—
Transition seal: 10/20 sand and bentonite	65 sand/34 bentonite	Bag/5-gal. bucket	50:50
Backfill: 20/40 sand	56	Bag	—
Seal: ⅜-in. bentonite chips	5.875	Bag	—
Primary filter pack, upper screen: 10/20 sand	70	Bag	—
Secondary filter pack, upper screen: 20/40 sand	5	Bag	—
Seal: ⅜-in. bentonite chips	7.75	Supersack	—
Surface seal: concrete backfill	2	Cubic Yards	2,500 psi concrete with 4% bentonite
Potable water	15,978	Gallons	—

<sup>a</sup> Sand bag = 45 lb each, bentonite bag/bucket = 50 lb ea, bentonite supersack = 3,000 lb ea (equivalent to 3 yd<sup>3</sup>)  
Sand bag = 0.5 ft<sup>3</sup> each, bentonite bag/bucket = 0.67 ft<sup>3</sup>, bentonite supersack = 41.4 ft<sup>3</sup>

### 7.3 Piezometer Construction

Two piezometers were installed in the open 8½-in. R-26 corehole to monitor two potential zones of perched saturated water observed during Phase I drilling. Piezometer construction was performed on October 1, 2003. Piezometers 1 and 2 were completed using 1-in. OD, Schedule 40 flush-jointed polyvinyl chloride (PVC) casing and 0.010-in. slotted screen. PZ-1 was screened across the interval from 230 to 250 ft bgs. A filter pack of 10/20 silica sand was tremied across the screened interval from 250 to 225 ft bgs, and a bentonite seal was then placed from 225 to 185 ft bgs. PZ-2 was constructed above the bentonite seal with its screen positioned from 150 to 180 ft bgs and sump from 180 to 185 ft bgs. The PZ-2 filter pack of 10/20 silica sand was installed from 185 to 145 ft bgs, and a bentonite seal was placed from 145 to 60 ft bgs. The annular interval from 60 to 2 ft bgs was backfilled with bentonite, and concrete was poured from 2 ft bgs to ground surface. A total of 14 bags of 10/20 silica sand and 41.5 bags of bentonite chips were used in constructing the two piezometers. Figure 7.3-1 is a schematic as-built diagram of these piezometers.

## 8.0 WELL DEVELOPMENT AND HYDROLOGIC TESTING

Well development activities at R-26 were conducted from October 18, 2003, to November 17, 2003. Well development procedures, described below, included airlifting, well-screen swabbing,

Location: Mesa South of Cañon de Valle  
(on down thrown side of Pajarito Fault) TA-16

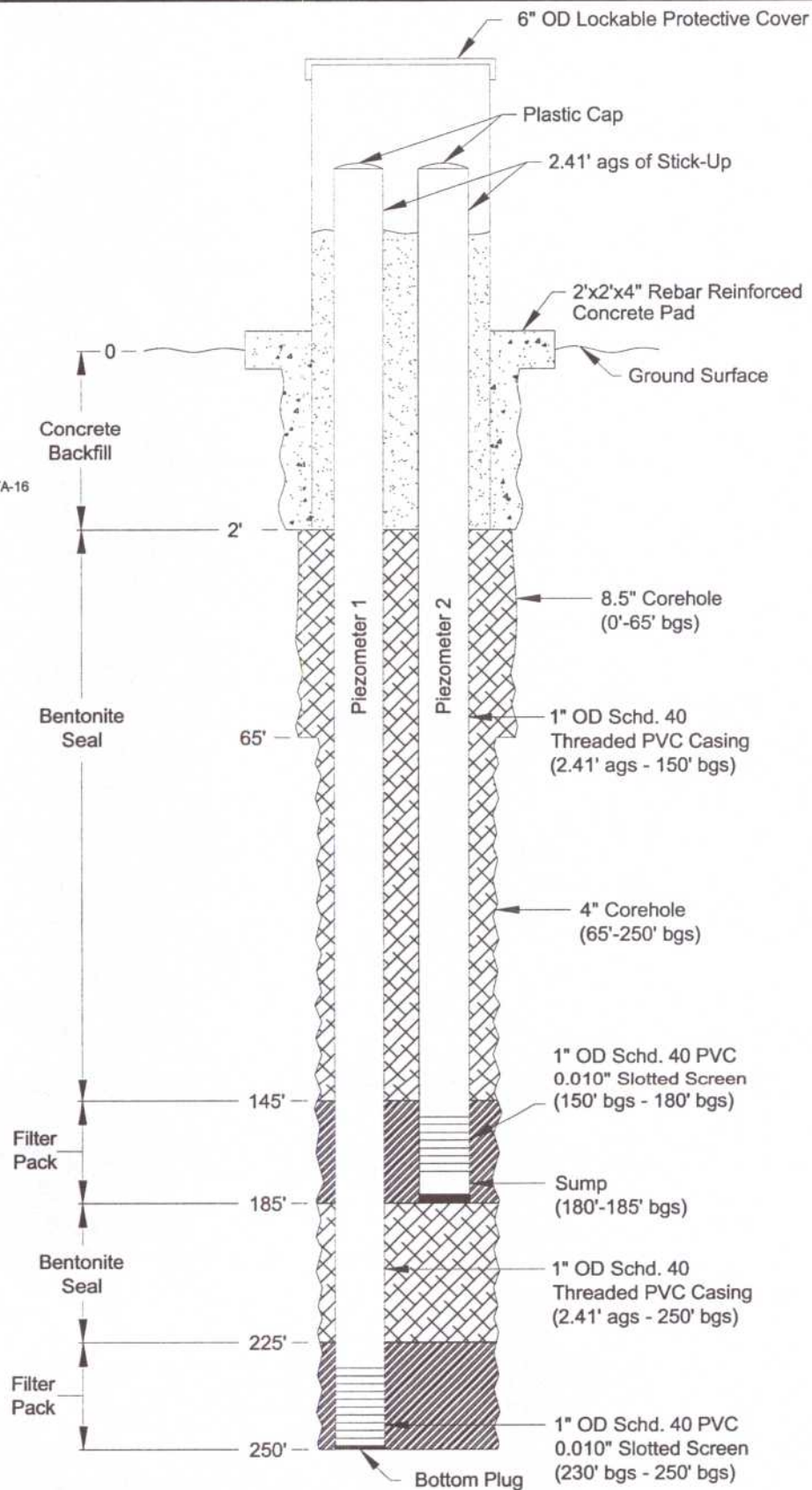
Survey Coordinates / Elevations:  
• Coordinates: NAD83  
• Elevation: NGVD29

Description: Core Hole Piezometer 1  
Northing: 1764660.49  
Easting: 1610201.92  
Elevation Top of Casing: 7641.95'  
Description: Core Hole Piezometer 2  
Northing: 1764660.61  
Easting: 1610201.96  
Elevation Top of Casing: 7641.95'



**Keyed Notes:**

1. Completion Date: 10-01-03
2. bgs: below ground surface
3. ags: above ground surface



**KLEINFELDER**

Drawn By: C. Landon	Date: January 2005
Project No.: 37151	Filename: Figure 7.3-1.dwg
Scale: not-to-scale	Revision: 4

**SCHEMATIC DIAGRAM**  
**Corehole Piezometers Well R-26**  
**Los Alamos National Laboratory**  
**Los Alamos, New Mexico**

FIGURE

**7.3-1**

surging, bailing, and pumping, and also, during well construction, surging was done to encourage settlement of the filter packs. A total of 55,294 gal. of water were removed during well development and hydrologic testing. All produced fluids were stored in lined pits and storage tanks until discharge approval was received from NMED.

Hydrologic testing consisted of two constant rate pumping tests and one falling head test. The tests were conducted from February 16 to February 20, 2004. Results from these tests are in Appendix A of the Addendum to this report (Kleinfelder 2004).

## **8.1 Well Development**

Well development at R-26 was performed in three stages. The initial stage consisted of airlifting to remove excess drilling fluids and to allow for formation water to recharge the well. The second stage consisted of bailing to remove solid materials from the well, followed by swabbing and surging the screened intervals to draw fine sediment from the constructed filter pack. The final stage consisted of lowering a submersible pump into the well and drawing the pump repeatedly across the screened intervals.

The efficiency of well development was monitored by measuring field water-quality parameters (pH, temperature, specific conductance, and turbidity). To monitor progress during each development stage, samples of water were periodically collected and parameter measurements were recorded in the field log book and on field forms. The field log book and forms are on file at KA's Albuquerque office, and copies will be included in the LANL record project file.

The primary objective of well development was to remove suspended sediment from the water until turbidity was less than 5 NTUs for three consecutive samples. Similarly, other measured parameters were required to stabilize before terminating development procedures. In addition, total organic carbon (TOC) samples were collected and analyzed toward the end of development. The target level for TOC was 2 parts per million. Table 8.1-1 presents the final water quality parameter data values measured during the well development process.

Preliminary bailing from the R-26 screened intervals and sump was performed to remove bentonite materials, drilling fluids, and formation sands and fines that had been introduced into the well during drilling and installation. Bailing activities were conducted by WDC using a 5-gal. capacity, 3-in.-diameter by 10-ft-long stainless-steel bailer. Bailing activities continued until water clarity improved. Bailing was followed by swabbing across each screened interval to enhance filter-pack development. A swabbing tool consisting of a 4.25-in.-diameter, 1-in.-thick rubber disc attached to the drill rod was lowered into the well and was drawn repeatedly across the screen interval for approximately one hour. Water turbidity was not measured during the bailing and swabbing process.

**Table 8.1-1**  
**Development and Testing of Well R-26**

Method	Water Removed (gal.)	pH	Temperature (°C)	Specific Conductance (μS/cm) <sup>a</sup>	Turbidity (NTU)
Airlifting	3,872	NM <sup>b</sup>	NM	NM	NM
Bailing/Swabbing Screens	123	7.92	12.7	146	NM
Pumping Upper Screen	5,899	NM	16.8	80	4.87
Pumping Lower Screen	25,210	NM	17.2	80	4.58
Sump	5,965	NM	NM	NM	NM
Hydrologic Testing	14,225	NM	NM	NM	NM
Total	55,294				

<sup>a</sup> Specific conductance is reported in microsiemens per centimeter

<sup>b</sup> NM = Not measured

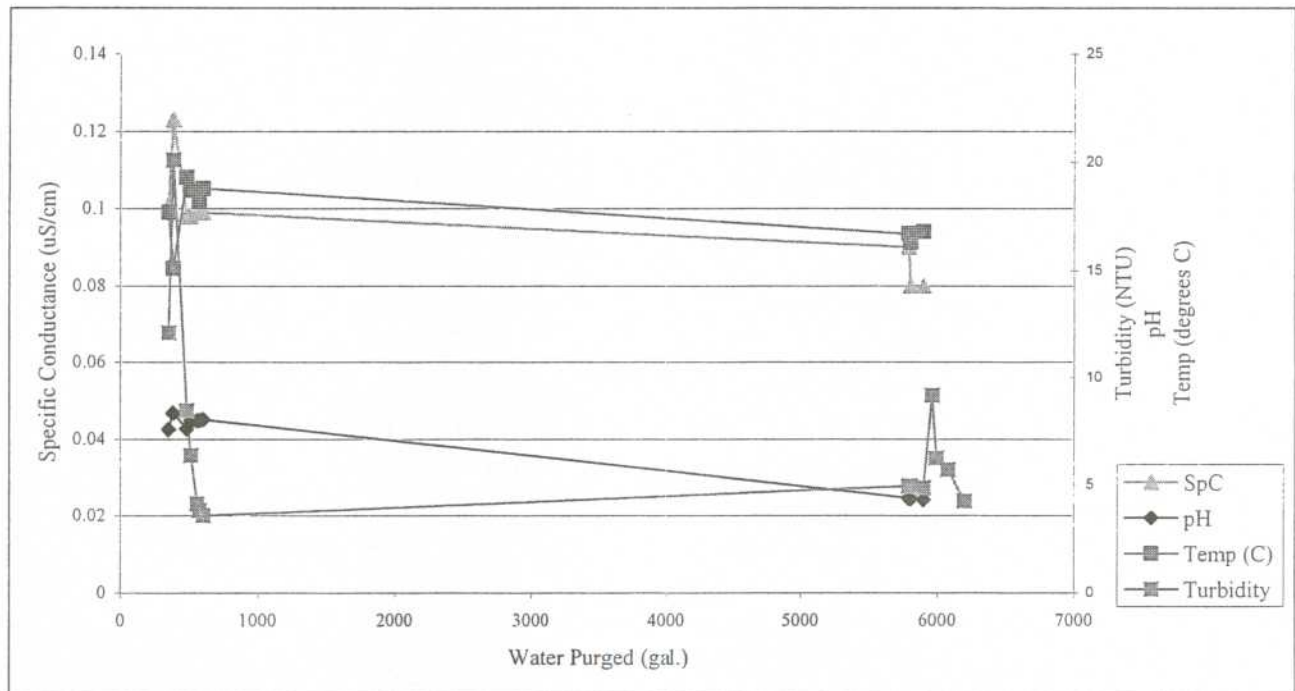
Following swabbing, pump development procedures were applied to the screened intervals (651.8 to 669.9 ft bgs and 1421.8 to 1445 ft bgs) using a 10 horsepower, 4-in. Grundfos submersible pump. The pump intake was lowered to each screened interval and was cycled on at a nominal rate of 6.0 gal. per minute. The pump intake was then drawn across the length of each screened interval to remove remaining fines from the filter pack and adjacent formation. While pumping, water samples were collected for parameter measurements. Once the target water quality parameters were reached (<5 nephelometric turbidity units [NTUs]), the pump was tripped out and the packer, which isolates the screens from one another, was placed above the pump. Initially, the upper screen was pumped with the packer located below the pump. The lower screen and sump were then pumped. Pump development was then completed with additional pumping of the upper screen.

Figure 8.1-1 illustrates the effects of well development in the upper screen on measured field parameters. Figure 8.1-2 illustrates the effects of well development in the lower screen on measured field parameters. R-26 was considered fully developed when the limiting values of acceptability were met. The primary acceptance criterion was that turbidity be less than 5 NTUs.

From July 10 to July 14, 2004, additional well development was conducted at well R-26 prior to the installation of the Westbay Multi-Port (MP) sampling system. A 10 horsepower, 4-in. Grundfos submersible pump was used to pump the well from 1,209 and 1,467 ft bgs prior to sampling. The upper depth was pumped continuously between 10:45 A.M. on July 11, 2004 and 11:57 A.M. on July 13, 2004 and a total of 41,818 gallons (gal.) of water were removed. The lower depth was pumped between 2:40 P.M. and 6:10 P.M. on July 13, 2004, and an additional 3,733 gal. of water were removed.

After the additional well development, a downhole video log was run to observe casing conditions and water clarity prior to the installation of the sampling system. Appendix A, Borehole Video

Logs, contains a DVD of the R-26 borehole video log as well as the corehole video log from the shallow corehole at R-26.



**Figure 8.1-1. Effects of Pump Development of the Upper Screen on Water Quality Parameters at Well R-26**

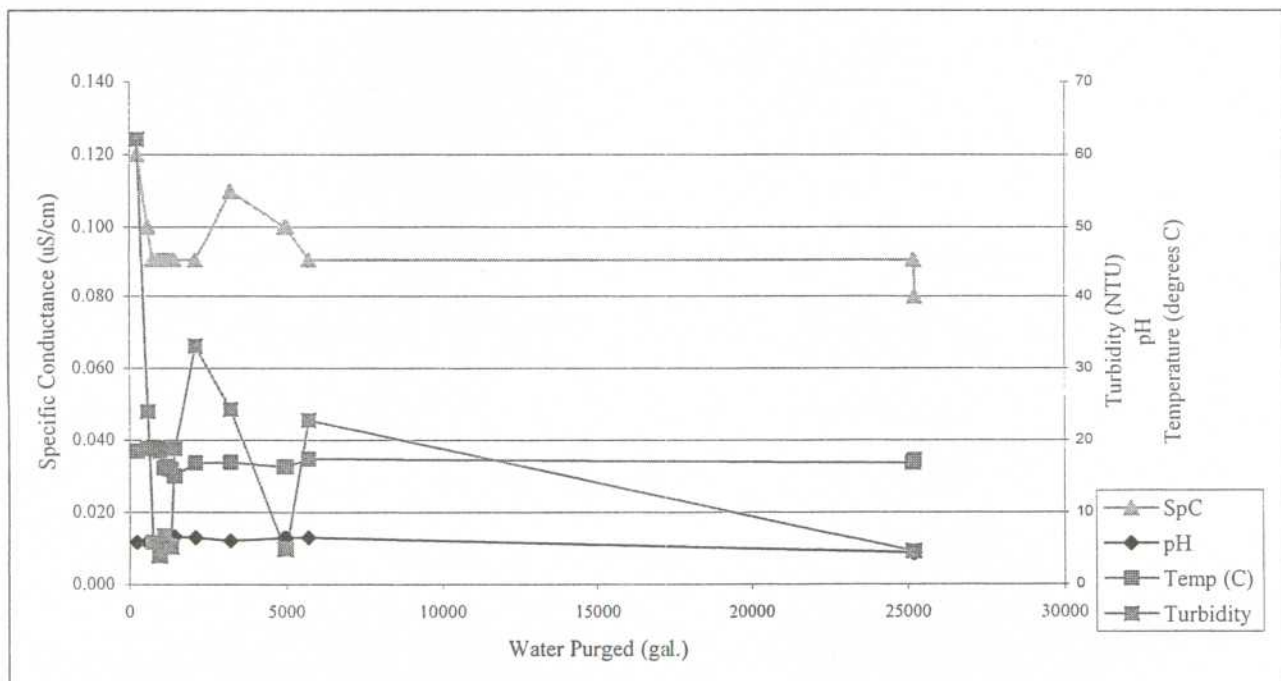


**Figure 8.1-2. Effects of Pump Development of the Lower Screen on Water Quality Parameters at Well R-26**

## **8.2 Hydrologic Testing**

Constant-rate pumping tests and shut-in tests were conducted on the two water-bearing zones in R-26 from February 16, 2004, and March 6, 2004. The purpose of the tests was to determine the hydraulic properties and lateral extent of the two water-bearing zones encountered in R-26. One aquifer test was conducted on the upper intermediate zone, with a screened interval from 651.8 to 669.9 ft bgs, and two tests were conducted on the lower regional zone, screened between 1421.8 to 1445 ft bgs.

The average hydraulic conductivity of the upper zone, in the Cerro Toledo interval, adjacent to the borehole, is approximately 1.7 ft per day. Further from the borehole, average hydraulic conductivities ranged between 2.4 and 3.7 ft per day, depending on the degree of anisotropy. A steep vertical gradient was observed over this interval, suggesting that values in the upper end of the range may be most reliable. The results of the aquifer test on the upper interval indicate that it is limited in areal extent and not well connected to the lower regional aquifer.

The aquifer tests revealed that the lower water-bearing zone, in the Puye Formation fanglomerate, is a much less permeable zone with an average hydraulic conductivity of 0.0022 ft per day, with a lower bound of 0.002 ft per day. The complete report summarizing these tests is included as a compact disc (CD) in Appendix E.

## **8.3 Dedicated Sampling System Installation**

Following final well development activities, a Westbay Instruments, Inc., multi-port sampling system was installed in R-26 to isolate and allow discrete sampling of the two water-bearing zones. Appendix F to this report contains a CD with a PDF file of the complete Installation Report compiled by Westbay Instruments, Inc.

## **8.4 Wellhead Completion**

The surface completion for R-26 involved placing a reinforced (2,500 psi) concrete pad, 6-ft wide by 6-ft long by 6-in. thick on December 19, 2004. A brass survey pin was installed in the northwest corner of the pad. A 10.75-in. steel casing with locking lid protects the well riser. The pad was designed to be slightly elevated, with base course graded up around the pad to allow for drainage. Bollards were installed during site restoration activities.

Some fissures developed in the concrete wellhead surface pad that was installed, necessitating repair and refurbishment of the concrete pad. The refurbishment was completed on October 25, 2004. The specifications for the wellhead pad are the same as those for the previous wellhead.

## **8.5 Geodetic Survey**

The refurbished wellhead pad was resurveyed on October 27, 2004. The brass cap monument in the concrete pad and the top of the stainless-steel well casing were resurveyed; the new coordinates for these features are shown in Table 8.5-1.

**Table 3.5-1**  
**Coordinates for New Wellhead Features at R-26 and Piezometers**

<b>Description</b>	<b>Northing<sup>a</sup></b>	<b>Easting<sup>a</sup></b>	<b>Elevation<sup>b</sup></b>
Brass cap in R-26 Pad	1764721.12	1610267.33	7641.69
Top of stainless-steel casing	1764721.35	1610269.56	7643.33
PZ 1 (185 ft TD)	1764660.49	1610201.92	7641.95 <sup>(c)</sup>
PZ 2 (250 ft TD)	1764660.61	1610201.96	7641.95 <sup>(c)</sup>

<sup>a</sup> Coordinates are NM State Plane Grid, Central Zone, NAD83, determined from LANL monument A1601 with static Global Positioning Satellite observation.

<sup>b</sup> Feet above mean sea level relative to the National Geodetic Vertical Datum of 1929.

## 8.6 Site Restoration

On December 12, 2003, a Notice of Intent (NOI) to discharge drilling and development water from the borehole-cuttings containment area at R-26 was forwarded, via e-mail, to Mr. Curt Frishkorn with the NMED. Approval to discharge drilling and development water was received via e-mail from the NMED on January 14, 2004. A copy of the e-mail received from the NMED is in Appendix G.

Fluids produced during drilling and development were sampled in accordance with the NOI to Discharge, Hydrogeologic Workplan Wells and filed with the NMED. Results of the sampling data were reviewed by the NMED and LANL, and discharge was approved. A copy of the sample analysis is included in Appendix A of the Addendum to this report (Kleinfelder 2004).

Water from the borehole-cuttings containment area has been land-applied in the area of the general drill site using a 2,000-gal. capacity water truck. Silt fencing and straw bales have been left in place to minimize possible sediment impacts from future precipitation.

Site restoration activities included removing the polyethylene liner and borehole cuttings from the borehole-cuttings containment area, removing the containment area berms, and backfilling and grading the containment area. The cuttings were thinly spread onsite after obtaining NMED-approval.

The former drill site was graded, seeded with native vegetation, and mulched. Native vegetation has been re-established with 70% coverage. The Best Management Practices for the site, per the National Pollution Discharge Elimination System permit, included temporary site fencing to minimize silt runoff from the site. DOE filed a Notice of Termination on October 29, 2004 and the temporary site fencing to control silt runoff was removed on November 14, 2004.

## 9.0 DEVIATIONS FROM THE R-26 SAP

Appendix H compares the actual characterization activities that were performed at R-26 with the planned activities described in the "Hydrogeologic Workplan" (LANL 1998, 59599) and the R-26 SAP (LANL 2003, 03-4782). The main deviations from planned activities are summarized below:

- Planned depth – the SAP stated that the approximate depth of the well would be 1414 ft bgs. The completed borehole TD was 1490.5 ft bgs to ensure that the top of the regional aquifer was penetrated.
- Number of core and cuttings samples collected for contaminant analysis – up to 15 samples from the unsaturated zone and two samples each from saturated zones were planned for as specified in the R-26 SAP; 13 were actually collected. Use of drilling fluids precluded the collection of cuttings for contaminant characterization within the zones of saturation.
- Piezometer installation – piezometer installation was not specified in the SAP. Two temporary piezometers were installed in the corehole to monitor perched water conditions. Details about piezometer installation are presented in Section 7.3.
- Drilling methods – The borehole was reamed across the lower screen interval to increase the diameter of the hole.

## 10.0 ACKNOWLEDGEMENTS

D. Schafer of David Schafer and Associates contributed the hydrologic testing section of this report.

E. Tow, P. Schuh, and R. Lawrence of Tetra Tech EM, Inc., Albuquerque, NM, contributed to the preparation of this report.

EnviroWorks, Inc provided site preparation and restoration activities.

Lynn Engineering & Surveying, Inc. provided the final geodetic survey.

N. Clayton of Schlumberger provided processing and interpretation of borehole geophysical data.

P. Longmire of LANL contributed the geochemistry section of this report.

Tetra Tech EM, Inc. provided support for well site geology, sample collection, and hydrologic testing.

WDC Exploration & Wells provided rotary drilling services.

## 11.0 REFERENCES

Broxton, D.E. and S.L. Reneau, 1995. "Stratigraphic Nomenclature of the Bandelier Tuff for the Environmental Restoration Project at Los Alamos National Laboratory," LA-13010-MS, August 1995. (Broxton and Reneau 1995)

Kleinfelder, Inc., 2004. "Addendum to the Final Well R-26 Completion Report, Los Alamos National Laboratory," Los Alamos, New Mexico, November 29, 2004. (Kleinfelder 2004)

Los Alamos National Laboratory, July 2003. "Sampling and Analysis Plan for Drilling and Testing Characterization Wells R-2, R-4, R-11, and R-26," Los Alamos National Laboratory Report LA-UR-03-4782, Los Alamos, New Mexico. (LANL 2003)

Los Alamos National Laboratory, May 1998. "Hydrogeologic Work Plan," Los Alamos, New Mexico. (LANL 1998)

Los Alamos National Laboratory, January 1996. "Groundwater Protection Management Program Plan," Rev. 0.0, Los Alamos, New Mexico. (LANL 1996)

Kleinfelder, Inc., 2003. "Project Management Plan for DOE Monitoring Well Installation at Los Alamos National Laboratory," Los Alamos, New Mexico, October 29, 2003. (Kleinfelder 2003a)

Kleinfelder, Inc., 2003. "Final Contractor Quality Management Plan, Revision 1, DOE Monitoring Well Installation at Los Alamos National Laboratory," Los Alamos, New Mexico, November 24, 2003. (Kleinfelder 2003b)

Kleinfelder, Inc., 2003. "Site Specific Health and Safety Plan, Characterization Well R-26, DOE Monitoring Well Installation at Los Alamos National Laboratory," Los Alamos, New Mexico, September 16, 2003. (Kleinfelder 2003c)

Kleinfelder, Inc., 2003. "Drilling Plan – KADP for Characterization Wells R-2, R-4, R-11, and R-26, Final, DOE Monitoring Well Installation at Los Alamos National Laboratory," Los Alamos, New Mexico, June 25, 2003. (Kleinfelder 2003d)

## **Appendix A**

---

*Borehole Videos  
(DVDs included)*

## **Appendix B**

---

### *Geophysical Logging Report and Montages (CD included)*

*Schlumberger Water Services  
February 2004*

## TABLE OF CONTENTS

1.0	SUMMARY .....	2
2.0	INTRODUCTION .....	4
3.0	METHODOLOGY .....	5
3.1	Acquisition procedure .....	5
3.2	Log Quality Control and Assessment .....	6
3.3	Processing Procedure .....	7
	Environmental Corrections and Raw Measurement Reprocessing .....	7
	Depth-Matching and Splicing .....	8
	Integrated Log Analysis .....	9
4.0	RESULTS .....	11
	Well Water Level 11	
	Regional Aquifer 11	
	Vadose Zone Perched Water .....	12
	Geology 13	
4.1	Summary Logs .....	16
4.2	Integrated Log Montage .....	20
	Track 1-Depth 20	
	Track 2-Basic Logs .....	20
	Track 3-Resistivity .....	20
	Track 4-Porosity 21	
	Track 5-Density 21	
	Track 6-NGS Spectral Gamma .....	22
	Track 7-CMR Porosity .....	22
	Track 8 -Pore Size Distribution .....	23
	Track 9-CMR T2 Distribution (Waveforms) .....	23
	Track 10-CMR T2 Distribution (Heated Amplitude) .....	23
	Track 11-CMR Hydraulic Conductivity .....	23
	Track 12- FMI Image (Dynamic Normalization) .....	24
	Track 13- FMI Bedding and Fractures .....	24
	Track 14- FMI Image (Static Normalization) .....	24
	Track 15- Fracture Aperture and High Resolution Porosity .....	24
	Tracks 16 to 20- Geochemical Elemental Measurements .....	25
	Track 21-ELAN Mineralogy Model Results (Dry Weight Fraction) .....	25
	Track 22-ELAN Mineralogy-Pore Space Model Results (Wet Volume Fraction)	
	25	
	Track 23-Summary Logs .....	26
	Track 24-Depth 27	
5.0	REFERENCES .....	27

## 1.0 SUMMARY

This report describes the borehole geophysical logging measurements acquired in characterization well R-26 by Schlumberger, logged at two separate times – September and October 2003 – before well completion. The report (1) summarizes the technology, measurements, and procedures employed, and (2) presents the processed results from these measurements and discusses their interpretation. The logs were acquired in two runs at two separate times as the well was drilled in an effort to maximize the amount of open hole versus cased hole measurements. The September logging suite was acquired from 20 ft. to 990 ft. bgs, when the borehole was open (uncased) below 70 ft., drilled with 12.25 in. diameter bit size, and contained 13.375 in. outer diameter steel casing above 68 ft. (as measured by the logs). The October logging suite was acquired from 655 ft. to 1378 ft. bgs, when the borehole was open below 1005 ft., drilled with 8.5 in. diameter bit size, and contained 9.625 in. outer diameter freestanding steel casing above 1005 ft. (as measured by the logs).

The primary purpose of the geophysical logging was to characterize the geologic/hydrogeologic section intersected by the well with emphasis on determining regional aquifer groundwater level, perched groundwater zones, moisture content, capacity for flow, and the stratigraphy/mineralogy of geologic units. A secondary purpose of the geophysical logging was to evaluate the borehole conditions such as borehole diameter versus depth, deviation versus depth, and degree of drilling fluid invasion. These objectives were accomplished by measuring, nearly continuously, along the length of the well: (1) total and effective water-filled porosity and pore size distribution, from which an estimate of effective water hydraulic conductivity is made, (2) bulk density (sensitive to total water- plus air-filled porosity), (3) bulk electrical resistivity at multiple depths of investigation, (4) bulk concentrations of a number of important mineral-forming elements, (5) spectral natural gamma ray, including potassium, thorium, and uranium concentrations, (6) bedding and fracture orientation, fracture aperture, and geologic texture, (7) borehole inclination and azimuth, and (8) borehole diameter.

Preliminary results of these measurements were generated in the logging truck at the time the geophysical services were performed and are documented in field logs provided onsite. However, the measurements presented in the field results are not fully corrected for borehole conditions and are provided as separate, individual logs. The field results were reprocessed by Schlumberger to (1) correct/improve the measurements, as best as possible, for borehole/formation environmental conditions, (2) perform an integrated analysis of the log measurements so that they are all coherent, and (3) combine the logs in a single presentation, enabling integrated interpretation. The reprocessed log results provide better quantitative property estimates that are consistent for all applicable measurements, as well as estimates of properties that otherwise could not be reliably estimated from the single measurements alone (e.g. total porosity inclusive of all water and air present, water saturation, mineralogy).

The geophysical log measurements from Well R-26 provide good quality results that are consistent with each other through most of the borehole. The quality of some measurements was degraded across intervals where the borehole contains large washouts and/or rugose hole. The measurements most affected by the adverse borehole conditions were ones that have a shallow depth of investigation and require close contact to the borehole wall—the bulk density, photoelectric effect, and the porosity measurements. The greatest impact on the log processing was erroneously high estimated air-filled and/or water-filled porosity in the problem zones.

Through the integrated analysis and interpretation of all the logs, the individual shortcomings of the specific measurements are reduced. Thus, the integrated log analysis results (e.g. the optimized water-filled porosity log) are the most robust single representation of the geophysical log results—providing a wealth of valuable high resolution information on the geologic and hydrogeologic environment of the R-26 locale.

Important results from the processed geophysical logs in R-26 include the following:

1. The Puye Formation fanglomerate at the bottom of the well (955–1490.5 ft bgs) is likely fully saturated with water throughout. The porosity across this interval is mostly in the range of 20–30% of the total rock volume, although there are a number of zones with higher porosity. The most porous zones (in which the logs are not obviously affected by hole conditions) appear to be 1075–1108 ft and 1186–1200 ft, with porosity mostly ranging 30–40% and a peak of over 50% at 1102 ft. Both these zones have high moveable water content (effective porosity) of 15–20% of total rock volume.
2. The high porosity glassy tuff/pumice beds and volcanoclastic sediments of the Cerro Toledo interval and Otowi Member (472–955 ft bgs) lying above the Puye Formation are likely not fully saturated with water through most of the section, although they have very high water content (30–50% of total rock volume) from 570–955 ft. The general trend is an increase in water content with depth – culminating at 52% of total rock volume at the bottom of the Guaje Pumice Bed at 955 ft. The moveable water content is relatively high as well (5–25% of total rock volume, except 40% at the bottom of the Guaje Pumice Bed). Although much of the glassy tuff/pumice interval may not be fully saturated with water, the high total and moveable water content suggests that, in general, the water is quite mobile. Likely, water in this interval is connected (in a broad sense) to the saturated Puye Formation below.
3. Three heterogeneous fanglomerate-type beds within the Cerro Toledo interval are clearly delineated by the logs at 505–524 ft, 530–544 ft, and 779–828 ft bgs. These beds have significantly lower porosity (mostly 20–30% of total rock volume) than the surrounding sediments (mostly 40–50% of total rock volume). The processed logs indicate that some zones within these beds may be fully saturated with water – particularly the interval 780–827 ft – but the moveable water content is highly variable and mostly less than 5% of total rock volume.
4. The crystalline tuff beds (60–472 ft bgs) generally have very low porosity (10–20% of total rock volume) and water content (5–10%). Some zones within this interval appear to be fully saturated with water, but the low moveable water content (5% of total rock volume) likely limits the flow of this water. The total porosity above 134 ft appears to be much higher (35–45%).
5. Fractures were identified from the electrical image log (acquired across the interval 390–1390 ft) at 412 ft, 681 ft, 687 ft, 690 ft, 700 ft, 701 ft, 705 ft, 710 ft, 870 ft, 880 ft, 882 ft, 883 ft, 947.5 ft, 950 ft, 952 ft, and 1363.5 ft. All are in the volcanic tuff sequence, except the deepest one is in the Puye Formation.
6. Clay-rich beds occur in the following zones: 1023–1026 ft, 1051–1053 ft, 1080–1114 ft, 1135–1143 ft, 1171–1177 ft, and 1187–1200 ft.

## 2.0 INTRODUCTION

Geophysical logging services were performed in characterization well R-26 by Schlumberger in September and October 2003, before initial well completion. The purpose of these services was to acquire in situ measurements that help characterize the borehole, near-borehole, and abutting geologic formation environment. The primary objective of the geophysical logging was to provide in situ evaluation of formation properties (hydrogeology and geology) intersected by the well. This information was (and is) used by scientists, engineers, and project managers in the Los Alamos Characterization and Monitoring Well Project to design the well completion, better understand subsurface site conditions, and assist in overall decision-making.

The primary geophysical logging services performed by Schlumberger in well R-26 were the

- Combinable Magnetic Resonance (CMR<sup>TM</sup>) tool to measure the nuclear magnetic resonance response of the formation, which is used to evaluate total and effective water-filled porosity of the shallow formation and to estimate pore size distribution and in-situ hydraulic conductivity;
- Compensated Neutron Tool (CNT<sup>TM</sup>) to measure volumetric water content of the formation, which is used to evaluate moist/porous zones;
- Triple detector Litho-Density (TLD<sup>TM</sup>) tool to measure formation bulk density and photoelectric factor, which are used to estimate total porosity and lithology;
- Array Induction Tool, (AIT<sup>TM</sup>) to measure formation electrical resistivity at five depths of investigation and borehole fluid resistivity, which is used to evaluate drilling fluid invasion into the formation (an indicator of relative permeability and water saturation), presence of moist zones far from the borehole wall, and presence of clay-rich zones;
- Formation Micro-Imager (FMI<sup>TM</sup>) tool to measure electrical conductivity images of the borehole wall in fluid-filled open hole and borehole diameter with a two-axis caliper – used for evaluating geologic bedding and fracturing, including strike and dip of these features and fracture apertures, and rock texture;
- General Purpose Inclination Tool (GPIT<sup>TM</sup>) to measure borehole deviation and azimuth in OH – used to evaluate borehole position versus depth and to orient FMI images;
- Natural Gamma Spectroscopy (NGS) tool to measure gross natural gamma and spectral natural gamma ray activity, including potassium, thorium, and uranium concentrations, which is used to evaluate geology/lithology, particularly the amount of clay and potassium-bearing minerals;
- Elemental Capture Spectroscopy (ECS<sup>TM</sup>) tool to measure elemental weight percent concentrations of a number of elements – used to characterize mineralogy and lithology of the formation

In addition, calibrated gross gamma ray (GR) was recorded with every service except the NGS, for the purpose of depth matching the logging runs to each other. Table 2.1 summarizes the geophysical logging runs performed in R-26.

**Table 2.1**  
**Geophysical logging services, their combined tool runs and intervals logged,**  
**as performed by Schlumberger in borehole R-26**

Date of Logging	Borehole Status	Run #	Tool 1	Tool 2	Tool 3	Depth Interval (ft)
28-Sept-2003	Open hole below 68 ft. Bit size of 12.25 in. Steel casing above 68 ft. Casing OD of 13.375 in.	1	TLD	CNT	GR	26–984 ft
Same	Same	2	NGS	AIT		20–990 ft
Same	Same	3	CMR	ECS	GR	58–988 ft
Same	Same	4	FMI	GPIT	GR	389–990 ft
14-Oct-2003	Open hole below 1007 ft. Bit size of 8.5 in. Steel casing above 1007 ft. Casing OD of 9.625 in.	5	TLD	CNT	GR	500–1482 ft
Same	Same	6	AITH	NGS		500–1484 ft
15-Oct-2003	Same	7	ECS	CMR	GR	500–1486 ft
Same	Same	8	FMI	GPIT	GR	1005–1388 ft

A description of these geophysical logging tools can be found on the Schlumberger website (<http://www.hub.slb.com/index.cfm?id=id11618>).

### 3.0 METHODOLOGY

This section describes the methods employed by Schlumberger for performed geophysical logging services in Well R-26, including the following stages/tasks:

- Measurement acquisition at the well site
- Quality assessment of logs
- Reprocessing of field data

#### 3.1 Acquisition procedure

Once the well drilling project team notified Schlumberger that R-26 was ready for geophysical well logging, the Schlumberger district in Farmington, NM, mobilized a wireline logging truck, the appropriate wireline logging tools and associated equipment, and crew to the job site. Upon arriving at the LANL site, the crew completed site entry paperwork and received a site-specific safety briefing.

After arriving at the well site, the crew proceeded to rig up the wireline logging system, including:

- Parking and stabilizing the logging truck in a position relative to the borehole that is best for performing the surveys;

- Setting up a lower and an upper sheave wheel (the latter attached to, and hanging above, the borehole from the drilling rig/mast truck);
- Threading the wireline cable through the sheaves; and
- Attaching the appropriate sonde(s) for the first run to the end of the cable.

Next, pre-logging checks and any required calibrations were performed on the logging sondes and the tool string was lowered into the borehole. If any of the tools required active radioactive sources (in this case a neutron and gamma source for the CNT/ECS and TLD, respectively), just before lowering the tool string the sources were taken out of their carrying shields and placed in the appropriate tool source-holding locations using special source handling tools. The tool string was lowered to the bottom of the borehole and brought up at the appropriate logging speed as measurements were made. At least two logging runs (one main and one repeat) were made with each tool string.

Upon reaching the surface any radioactive sources were removed from the tools and returned to their appropriate storage shields, thus eliminating any radiation hazards. Any post-logging measurement checks were performed as part of log quality control and assurance. The tool string was cleaned as it was pulled out of the hole, separated and disconnected.

The second tool string was attached to the cable for another logging run, followed by subsequent tool strings and logging runs. After the final logging run is completed the cable and sheave wheels were rigged down.

Before departure, the logging engineer printed field logs for on site distribution and sent the data via satellite to the Schlumberger data archiving center. The Schlumberger data processing center was alerted that the data were ready for post-acquisition processing.

### 3.2 Log Quality Control and Assessment

Schlumberger has a thorough set of procedures and protocols for ensuring that the geophysical logging measurements are of very high quality. This includes full calibration of tools when they are first built, regular recalibrations and tool measurement/maintenance checks, and real-time monitoring of log quality as measurements are made. Indeed, one of the primary responsibilities of the logging engineer is to ensure, before and during acquisition, that the log measurements meet prescribed quality criteria.

A tool specific base calibration that directly relates the tool response to the physical measurement using the designed measurement principle is performed on all Schlumberger logging tools when first assembled in the engineering production centers. This is accomplished through a combination of computer modeling and controlled measurements in calibration models with known physical parameters.

The base calibration is augmented through regular “master calibrations” for most Schlumberger tools – typically performed every one to six months in local Schlumberger shops (such as Farmington, NM), depending on tool design. Master calibrations consist of controlled measurements using specially designed calibration tanks/jigs and internal calibration devices that are built into the tools. The measurements are used to fine-tune the tool’s calibration parameters and to verify that the measurements are valid.

In addition, on every logging job, onsite before and after “calibrations” are executed for most Schlumberger tools directly before/after lowering/removing the tool string from the borehole. For most tools these represent a measurement verification instead of an actual calibration – used to confirm the validity of the measurements directly before acquisition and to ensure that they have not drifted or been corrupted during the logging job.

All Schlumberger logging measurements have a number of associated depth-dependent quality control (QC) logs and flags to assist with identifying and determining the magnitude of log quality problems. These QC logs are monitored in real-time by the logging engineer during acquisition and are used in the post-acquisition processing of the logs to determine the best processing approach for optimizing the overall validity of the property estimates derived from the logs.

Additional information on specific tool calibration procedures can be found on the Schlumberger web page (<http://www.hub.slb.com/index.cfm?id=id11618>).

### 3.3 Processing Procedure

After the geophysical logging job was completed in the field and the data archived, the data were downloaded to the Schlumberger processing center. There the data were processed, in the order below, to (1) correct the measurements for near-wellbore environmental conditions and redo the raw measurement field processing for certain tools using better processing algorithms, (2) depth match and splice the log curves from different logging runs, and (3) model the near-wellbore substrate lithology/mineralogy and pore fluids through integrated log analysis. Separately, the FMI electrical image was processed to produce scaled and normalized high-resolution images that were interpreted to identify geologic features and compute fracture apertures. Afterwards an integrated log montage was built to combine and compile all the processed log results.

#### Environmental Corrections and Raw Measurement Reprocessing

If required, the field log measurements were processed to correct for conditions in the well, including fluid type (water or air), presence of steel casing, and (to a much lesser extent) pressure, temperature, and water salinity. Basically these environmental corrections entail subtracting from the measurement response the known influences of the set of prescribed borehole conditions. In R-26 the log measurements requiring these corrections are the CNT porosity, TLD density, ECS elemental concentrations, and NGS spectral gamma ray logs.

Two CNT neutron porosity measurements are available – one that measures thermal (“slow”) neutrons and one that measures epithermal (“fast”) neutrons. Measurement of epithermal neutrons is required to make neutron porosity measurements in air-filled hole. In water/mud-filled hole both the CNT epithermal and thermal neutron measurements are valid, but the thermal neutron porosity has better statistical precision. Both epithermal and thermal neutron porosity measurements were made in R-26 since the borehole was partly water-filled (below 435 ft) and partly air-filled (above 435 ft) during the September logging (the log interval during the October logging was all below the well water level). The thermal neutron porosity measurement was reprocessed for borehole conditions, although the results were very similar to the field logs. For further processing and analysis (e.g. ELAN analysis), the reprocessed thermal neutron porosity log was used.

The standard open hole processing algorithm used for the TLD density measurement is influenced by the steel density in cased hole. A cased hole density algorithm was applied to the raw TLD field measurements obtained in cased hole sections of the combined September and October log intervals (comprising 30–68 ft and 981–1007 ft) to try to eliminate the casing response. While the algorithm can account for the casing per se, it cannot account for air- or water-filled gaps in the annulus between the casing and the formation—that cause erroneously low bulk density readings.

The raw ECS elemental yield measurements include the contribution of iron from steel casing and hydrogen from fluid in the borehole. The processing consists of subtracting these unwanted contributions from the raw normalized yields, then performing the normal elemental yields-to-weight fraction processing. The contribution to subtract is a constant baseline amount (or zoned constant values if there are bit/casing size changes), usually determined by comparing the normalized raw yields in zones directly below/above the borehole fluid/casing change. The ECS logs from R-26 have two short cased hole sections (30–68 ft and 981–1007 ft), for which casing corrections were applied. At the time of the September ECS logging in R-26 the borehole water level was 455 ft; no hydrogen correction was required in the air-filled section above 455 ft and the difference between the hydrogen yield above and below this depth was used to determine the baseline borehole hydrogen correction to apply below. For the October logging the entire ECS log interval was below the well water level; in this case the hydrogen baseline subtraction was determined by a trial and error comparison of the resulting estimated ECS water content with CNT and TLD porosities to check relative agreement.

The NGS spectral gamma ray logs are affected by the material (fluid, air, casing) in the borehole because different types and amounts of these materials have different gamma ray shielding properties; the NGS measures incoming gamma rays emitted by radioactive elements in the formation surrounding the borehole. The processing algorithms try to correct for the damping influence of the borehole material. The NGS logs from R-26 were reprocessed to fully account for the environmental effects of the borehole fluid (water and air), hole size, and casing (the latter above 68 ft).

The measurements cannot be fully corrected for borehole washouts or rugosity, as well as the annulus material (e.g., bentonite grout) between casing and the formation, since the specific characteristics of these features (e.g., geometry) are unknown and their effects on the measurements often too significant to account for. Thus, the compromising effects of these conditions on the measurements should be accounted for in the interpretation of the log results.

### **Depth-Matching and Splicing**

Once the logs were environmentally corrected for the conditions in the borehole and the raw measurement reprocessing was completed, the logs from different tool runs were depth-matched to each other using the AIT-NGS tool run as the base reference. Gamma ray was used as the common correlation log measurement for depth-matching the different runs. The second logging suite (October 2003) was depth-matched to the first suite (September 2003) by shifting the AIT-NGS tool run logs from the second suite to the AIT-NGS run from the first suite (using gross gamma), then depth-matching the logs from the remaining second suite tool runs to the depth-shifted AIT-NGS run (using gross gamma). Once all the logs were on depth with each other, logs

from the October logging runs (spanning the bottom 500 ft of R-26) were spliced to the equivalent logs from the September logging runs (spanning the top 1000 ft of R-26).

### Integrated Log Analysis

An integrated log analysis, using as many of the processed logs as possible, was performed to model the near-wellbore substrate lithology/mineralogy and pore fluids. This analysis was performed using the Elemental Log Analysis (ELAN\*) program (Mayer and Sibbit, 1980; Quieren et al, 1986) – a petrophysical interpretation program designed for depth-by-depth quantitative formation evaluation from borehole geophysical logs. ELAN estimates the volumetric fractions of user-defined rock matrix and pore constituents at each depth based on the known log measurement responses to each individual constituent by itself<sup>1</sup>. ELAN requires an a priori specification of the volume components present within the formation—fluids, minerals, and rocks. For each component, the relevant response parameters for each measurement are also required. For example, if one assumes that quartz is a volume component within the formation and the bulk density tool is used, then the bulk density parameter for this mineral is well known to be 2.65 g/cc.

The logging tool measurements, volume components, and measurement response parameters used in the ELAN analysis for R-26 are provided in Table 3.1. The final results of the analysis – an optimized mineral-fluid volume model – are shown on the integrated log montage (see montage on CD, inside back cover), 3<sup>rd</sup> track from the right (inclusive of the depth track). To make best use of all the measurement data and to perform the analysis across as much of the well interval as possible (25–1484 ft.), as many as possible of the processed logs were included in the analysis, with less weighting applied to less robust logs. Not all the tool measurements shown in Table 3.1 are used for the entire interval analyzed, as not all the measurements are available, or of good quality, across certain sections of the borehole. To accommodate fewer tool measurements certain model constituents are removed from the analysis in some intervals. Most notably, within the cased interval (above 68 ft) many of the minerals had to be removed from the model due to the absence of many of the logs.

The ELAN analysis was performed with as few constraints or prior assumptions as possible. A considerable effort was made to choose a set of minerals or mineral types for the model that is representative of Los Alamos area geology and its volcanic origins. No prior assumption is made about water saturation—where the boundary between saturated and unsaturated zones lies (e.g. the depth to the top of the regional aquifer or perched zones). Thus, the presence and amount of air in the pore space is unconstrained. Total porosity and water-filled porosity are also left unconstrained throughout the analysis interval. Thus, interpretations should be made from the ELAN results with the understanding that the mineral-fluid model represents a mathematically optimized solution that is not necessarily a physically accurate representation of the native geologic formation. Within this context, the ELAN model is a robust estimate of the bulk mineral-fluid composition that accounts for the combined response from all the geophysical measurements.

---

\*Mark of Schlumberger

<sup>1</sup>Mathematically this corresponds to an inverse problem – solving for constituent volume fractions from an (over)determined system of equations relating the measured log results to combinations of the tool measurement response to individual constituents

Table 3.1

Tool measurements, volumes, and respective parameters used in the R-26 ELAN analysis .

Volume Tool Measurement	Air	Capillary Bound Water	Water	Hornblende	Hypersthene	Labradorite	Silica Glass	Heavy Mafic Minerals	Augite	Montmorillonite	Pyrite	Orthoclase / Sanidine	Calcite	Quartz
Bulk density (g/cc)	-0.14	1.00	1.00	3.11	3.55	2.65	2.33	4.0	3.08	2.1	4.99	2.58 2.56		2.64
Epithermal neutron porosity (ft <sup>3</sup> / ft <sup>3</sup> )	-0.02	1.00	1.00	0.05	0.01	-0.01	0.0	0.02	-0.01	0.6	0.17	-0.01	0.0	-0.047
Thermal neutron porosity (ft <sup>3</sup> / ft <sup>3</sup> )	-0.05	1.00	1.00	0.06	0.04	-0.01	0.0	0.07	0.02	0.65	0.01	-0.01	0.0	-0.073
Volumetric photoelectric effect	0	0	0.40	12	20.2	7	4.2	65	23.8	4.4	82.1	7.3 7.0	14.1	4.8
Total CMR water- filled porosity (ft <sup>3</sup> / ft <sup>3</sup> )	0	1.0	1.0	0	0	0	0	0	0	0.425	0	0	0	0
CMR bound fluid volume (ft <sup>3</sup> / ft <sup>3</sup> )	0	1.0	0	0	0	0	0	0	0	0.425	0	0	0	0
Resistivity (ohm-m)	Very high	10	10	Very high	Very high	Very high	Very high	Very high	Very high	1.06	Very high	Very high	Very high	Very high
Dry weight silicon (lbf / lbf)	0.0	0.0	0.0	0.21	0.24	0.24	0.47	0.18	0.23	0.26	0	0.3 0.38	0	0.47
Dry weight calcium (lbf / lbf)	0.0	0.0	0.0	0.09	0.0	0.09	0.0	0.0	0.10	0.01	0.0	0.0	0.405	0.0
Dry weight iron (lbf / lbf)	0.0	0.0	0.0	0.08	0.20	0.02	0.0	0.22	0.11	0.04	0.47	0.02	0.0	0.0
Dry weight sulfur (lbf / lbf)	0.0	0.0	0.0	0.0	0.0	0.0	0.0	0.0	0.0	0.0	0.53	0.0	0.0	0.0
Dry weight titanium (lbf / lbf)	0.0	0.0	0.0	0.005	0.01	0.0	0.0	0.0	0.048	0.0	0.0	0.0	0.0	0.0
Dry weight aluminum (lbf / lbf)	0.0	0.0	0.0	0.07	0.0	0.16	0.0	0.0	0.02	0.11	0.0	0.10	0.0	0.0
Wet weight potassium (lbf / lbf)	0.0	0.0	0.0	0.01	0.0	0.0	0.0	0.0	0.003	0.005	0.0	0.102	0.0	0.0
Weight water (lbf / lbf)	0.0	1.0	1.0	0.0	0.0	0.0	0.0	0.0	0.0	0.18	0.0	0.0	0.0	0.0
Wet weight thorium (ppm)	0.0	0.0	0.0	50	25	3	2	4	20	24	0	5.5	0.0	2
Clay bound water volume (ft <sup>3</sup> / ft <sup>3</sup> )	0	0	0	0	0	0	0	0	0	0.425	0	0		0

## 4.0 RESULTS

Preliminary results from the wireline geophysical logging measurements acquired by Schlumberger in R-26 were generated in the logging truck at the time the geophysical services were performed and are documented in field logs provided onsite. However, the measurements presented in the field results are not fully corrected for undesirable (from a measurement standpoint) borehole and geologic conditions and are provided as separate, individual logs. The field log results have been processed (1) to correct/improve the measurements, as best as possible, for borehole/formation environmental conditions and (2) to depth-match the logs from different tool runs in the well and splice the top (September 2003) and bottom (October 2003) logging suites. Additional logs were generated from integrated analysis of processed measured logs, providing valuable estimates of key geologic and hydrologic properties.

The processed log results are presented as continuous curves of the processed measurement versus depth and are displayed as (1) one page, compressed summary log displays for selected directly related sets of measurements (see Figures 4.1, 4.2, and 4.3) and (2) an integrated log montage that contains all the key processed log curves, on depth and side by side (see montage on CD, inside back cover). The summary log displays address specific characterization needs, such as moisture content, water saturation, and lithologic changes. The purpose of the integrated log montage is to present, side by side, all the most salient reprocessed logs and log-derived models, depth-matched to each other, so that correlations and relationships between the logs can be identified.

Important results from the processed geophysical logs in R-26 are described below.

### Well Water Level

The standing water level in R-26 varied significantly during the September 2003 logging – dropping from 434 ft bgs at time of the first logging run to 444 ft at time of the second logging run, to 455 ft at time of the third logging run. The borehole water level was not measured during the October 2003 logging – the logging interval was completely below the water level.

### Regional Aquifer

There is strong evidence from the processed logs that the bottom of R-26, below the Guaje Pumice Bed (bottom at 956 ft) in the Puye Formation, lies within the regional aquifer. The estimated pore volume water saturation (fraction of the total pore volume containing water) computed from the ELAN analysis is very high (mostly over 85%) from 954 ft to the bottom of the log interval (1484 ft). The estimate is even higher when computed directly from bulk density and ELAN water-filled porosity for a grain density range of 2.45 g/cc to 2.65 g/cc – ranging from 90% (2.65 g/cc) to a consistent 100% (2.45 g/cc). Water-filled and total porosity<sup>2</sup> mostly ranges 20–30% across the interval, although there are a number of zones with elevated porosity:

- **968–980 ft:** Washed out zone characterized by unrealistically high total porosity (as high as 60% of total rock volume), although water-filled porosity is only 25–30%. This would

<sup>2</sup> Water-filled porosity is defined in this report as the fraction of the total rock volume occupied by water. Total porosity is defined as fraction of the total rock volume occupied by water plus air, plus any other fluid or gas (non-solid).

suggest the zone is unsaturated (estimated water saturation is less than 50%), but this condition could very well be an artifact of the huge washout.

- **997–1001 ft:** Characterized by very high total porosity (57% of total rock volume) and water-filled porosity (46%) – likely a result of a washout behind the casing across this interval at the time of logging.
- **1075–1108 ft:** Elevated porosity of 30–35%, increasing to 58% below 1100 ft. The hole condition and the log quality appear to be good across the interval (the hole does not contain any significant washouts). The zone is characterized by an increase in estimated clay content (5–20% of total volume), but high effective porosity (15–22%). A possible explanation for the very high porosity from 1100–1108 ft is that it is a pumice-rich zone within the Puye Formation.
- **1173–1175 ft:** Porosity of 50% associated with a sharp washout.
- **1186–1200 ft:** Elevated porosity of 30–43%, characterized by an increase in estimated clay content (10–30% of total volume), but high effective porosity (15–20%).
- **1422–1452 ft:** Elevated porosity of 30–35% possibly associated with a slight change in lithology (indicated by a drop in potassium content). There is a thin “tight” streak at 1490 ft.
- **1452–1483 ft (bottom of log interval):** Continuation from above of elevated total porosity (30–35%), but water-filled porosity drops 20–22% below 1475 ft. This suggests that the zone from 1475 ft might not be fully saturated, but this may well be an artifact of the bottom of the borehole being the start of the logging passes – resulting in not having coverage from all the measurements (being below the first reading of some measurements).

Estimated water-filled effective porosity (moveable water) generally varies from 7% to 15% of total rock volume across this interval, except higher where noted above. The hydraulic conductivity estimated from the ELAN integrated log analysis (largely based on the CMR moveable water measurement) generally ranges 0.1–1 gal/dat/ft<sup>2</sup>, but reaches over 3 gal/day/ft<sup>2</sup> in a few zones – most notably 1100–1108 ft and 1186–1200 ft.

### Vadose Zone Perched Water

The processed logs indicate high water-filled porosity within the porous, volcanoclastic sediments and glassy tuff/pumice sections in R-26 from 575–955 ft bgs – ranging from 30% to 52% of the total rock volume. However, the processed logs, by themselves, indicate quite strongly that most of this interval is not fully saturated with water (that is not all of the pore space is occupied by water, instead partially filled with air). The total porosity in the sediments and glassy tuffs/pumice (estimated from the ELAN integrated log analysis) ranges from 40% to over 50% of total rock volume – resulting in water saturations of generally 50–80%. The computation of water saturation directly from bulk density and ELAN water-filled porosity for a grain density of 2.45 g/cc further confirms the conclusion that the glassy tuffs/pumice are not fully saturated. The highest estimated water saturation across this interval of water-rich sediments and glassy tuff/pumice (575–955 ft) occurs in the following zones:

- **580–620 ft:** Highly variably water saturation reaching 100%, but the zone contains abrupt, large washouts – likely causing the elevated water-filled and total porosity values as high as 70%.
- **620–640 ft:** Water saturation ranges 85–90%, due to a decrease in total porosity to 30–40%, with water-filled porosity averaging 30%.
- **642–662 ft:** Water saturation reaches over 90% as a result of increased water-filled porosity as high as 42%. due to a decrease in total porosity to 30–40%, with water-filled porosity averaging 30%.
- **780–827 ft:** Water saturation reaches 100% across this “Puye-like” bed within the Cerro Toledo interval – mostly due to a marked decrease in total porosity to 30%. The actual water-filled porosity is also lower than the surrounding high porosity glassy tuff. The borehole condition across this interval is highly rugose – making the estimation of water saturation from the geophysical logs in the water-filled borehole difficult and not very reliable.
- **950–955 ft:** Water-filled porosity increases significantly to 50% within the Guaje Pumice Bed, but the total porosity also jumps to 58%. It is possible water saturation reaches 100% at the very bottom of the bed, due to pooling of water.

The estimated moveable water content is generally quite high across this water-rich sediments and glassy tuff/pumice interval – ranging 5–25% of total rock volume. Although much of the 575–955 ft interval may not be fully saturated with the water, the high total and moveable water content suggests that, in general, the water is quite mobile. Likely water in this interval is connected (in a broad sense) to the saturated Puye Formation below.

Water-filled porosity drops off significantly above 575 ft (except in a washout at 475–485 ft) – averaging about 15–23% of total rock volume from 465–575 ft, 5–10% from 134–465 ft, and 10–20% from 25–134 ft. The total porosity drops significantly as well in the crystalline tuff interval 125–450 ft, ranging mostly 10–20% of total rock volume. Correspondingly, estimated water saturation reaches 100% in a number of places across this low porosity interval – most notably 370–440 ft – but the effective porosity is 5% or less. The apparent increase in water-filled porosity at the top of the well (above 134 ft) is coincident with a significant increase in total porosity (35–50%) – resulting in a low estimate of water saturation. The borehole is significantly washed out across this interval, as well, which may be partly responsible for the elevated porosity.

## Geology

The processed geophysical log results clearly delineate the geologic material and formation contacts intersected by R-26. The generalized geologic stratigraphy observed from the logs across the logged interval is as follows (depth below ground surface):

- **33–68 ft: Clay-rich zone in cased hole** – characterized by clay content of 30% of total volume, but the elevated clay derived from the log measurements could well be due to bentonite used to seal the casing

- **68–134 ft: Porous volcanic tuff** – characterized by high total porosity (40% of total rock volume), high sanidine content and moderate silica mineral/glass content
- **134–465 ft: Low porosity volcanic tuff** – characterized by low total porosity (10–20% of total rock volume), high sanidine and silica mineral/glass content
- **465–505 ft: Porous volcanic tuff and Upper Cerro Toledo interval** – characterized by high total porosity (40–50% of total rock volume), high sanidine and silica mineral/glass content
- **505–524 ft: Heterogeneous bed within Cerro Toledo interval** – characterized by relatively low total porosity (20–25% of total rock volume), high potassium feldspar, plagioclase and silica mineral/glass content
- **524–530 ft: Porous zone** – characterized by high total porosity (30–50% of total rock volume), high sanidine and silica mineral/glass content
- **530–544 ft: Heterogeneous bed within Cerro Toledo interval** – characterized by relatively low total porosity (20–25% of total rock volume), high potassium feldspar, plagioclase and silica mineral/glass content
- **544–779 ft: Porous zone in Cerro Toledo interval** – characterized by high total porosity (40–50% of total rock volume), high sanidine and silica mineral/glass content
- **779–865 ft: Heterogeneous bed within Cerro Toledo interval** – characterized by highly variable porosity (20–40% of total rock volume), high potassium feldspar and silica mineral/glass content, and lesser plagioclase content
- **865–930 ft: Porous volcanic tuff** – characterized by high total porosity (40–50% of total rock volume), high sanidine and silica mineral/glass content
- **930–955 ft: Very porous volcanic pumice bed** – characterized by very high total porosity (58% of total rock volume), high sanidine and silica glass content
- **955–968 ft: Heterogeneous fanglomerate** – characterized by moderate total porosity (20–30% of total rock volume), high potassium feldspar, plagioclase and silica mineral/glass content
- **968–980 ft: Washout in heterogeneous fanglomerate** – characterized by unrealistically high total porosity (50–60% of total rock volume), high potassium feldspar, plagioclase and silica mineral/glass content
- **980–1010 ft: Heterogeneous fanglomerate** – characterized by relatively high total porosity (25–35% of total rock volume), high potassium feldspar and silica mineral/glass content, and the presence of clay (although the latter could be an artifact of the log measurement being made through casing in this interval)
- **1023–1026 ft: Thin clay-rich bed** – characterized by relatively high total porosity (35% of total rock volume), an indication of clay (clearly visible on the high resolution FMI image), high potassium feldspar, plagioclase and silica mineral/glass content

- **1026–1050 ft: Heterogeneous fanglomerate** – characterized by relatively low total porosity (20–25% of total rock volume), high potassium feldspar, plagioclase and silica mineral/glass content
- **1051–1053 ft: Thin clay-rich bed** – characterized by relatively high total porosity (35% of total rock volume), moderate clay, potassium feldspar, plagioclase and silica mineral/glass content
- **1053–1080 ft: Heterogeneous fanglomerate** – characterized by relatively low total porosity (20–25% of total rock volume), high potassium feldspar, plagioclase and silica mineral/glass content
- **1080–1114 ft: Clay-rich zone** – characterized by high total porosity (30–55% of total rock volume), moderate clay, potassium feldspar, plagioclase and silica mineral/glass content
- **1114–1135 ft: Heterogeneous fanglomerate** – characterized by relatively low total porosity (20–25% of total rock volume), high potassium feldspar, plagioclase and silica mineral/glass content
- **1135–1143 ft: Clay-rich zone** – characterized by relatively high total porosity (30–35% of total rock volume), moderate clay, potassium feldspar, plagioclase and silica mineral/glass content
- **1143–1171 ft: Heterogeneous fanglomerate** – characterized by relatively low total porosity (20–25% of total rock volume), high potassium feldspar, plagioclase and silica mineral/glass content
- **1171–1177 ft: Clay-rich zone** – characterized by high total porosity (50% of total rock volume), moderate clay, potassium feldspar, plagioclase and silica mineral/glass content
- **1177–1187 ft: Heterogeneous fanglomerate** – characterized by relatively low total porosity (20–25% of total rock volume), high potassium feldspar, plagioclase and silica mineral/glass content
- **1187–1200 ft: Clay-rich zone** – characterized by high total porosity (30–45% of total rock volume), moderate clay, potassium feldspar, plagioclase and silica mineral/glass content
- **1200–1233 ft: Heterogeneous fanglomerate** – characterized by relatively low total porosity (20–25% of total rock volume), high potassium feldspar, plagioclase and silica mineral/glass content
- **1233–1236 ft: Thin clay-rich bed** – characterized by moderate total porosity (30% of total rock volume), moderate clay, potassium feldspar, plagioclase and silica mineral/glass content
- **1236–1417 ft: Heterogeneous fanglomerate** – characterized by relatively low total porosity (20–25% of total rock volume), high potassium feldspar, plagioclase and silica mineral/glass content

- **1417–1423 ft: Clay-rich zone** – characterized by moderate total porosity (30% of total rock volume), moderate clay, potassium feldspar, plagioclase and silica mineral/glass content
- **1423–1483 ft (bottom of log interval): Heterogeneous, high porosity fanglomerate** – characterized by relatively high total porosity (30–38% of total rock volume), high plagioclase and silica mineral/glass content

#### 4.1 Summary Logs

Three summary log displays have been generated for R-26 to highlight the key hydrogeologic and geologic information provided by the processed geophysical log results:

- Porosity summary log showing continuous hydrogeologic property logs, including total and moveable water content and water saturation – to highlight hydrologic information obtained from the integrated log results (Figure 4.1)
- Density and clay content summary showing a continuous logs of formation bulk density and estimated grain density, as well as photoelectric factor (sensitive to mineralogy) and estimated clay volume – to highlight key geologic rock matrix information obtained from the log results (Figure 4.2)
- Spectral natural gamma ray and lithology summary showing a high vertical resolution, continuous volumetric analysis of formation mineral and pore fluid composition (based on an integrated analysis of the logs) and key lithologic/stratigraphic correlation logs from the spectral gamma ray measurement (concentrations of gamma-emitting elements) – to highlight the geologic lithology, stratigraphy and correlation information obtained from the log results (Figure 4.3)

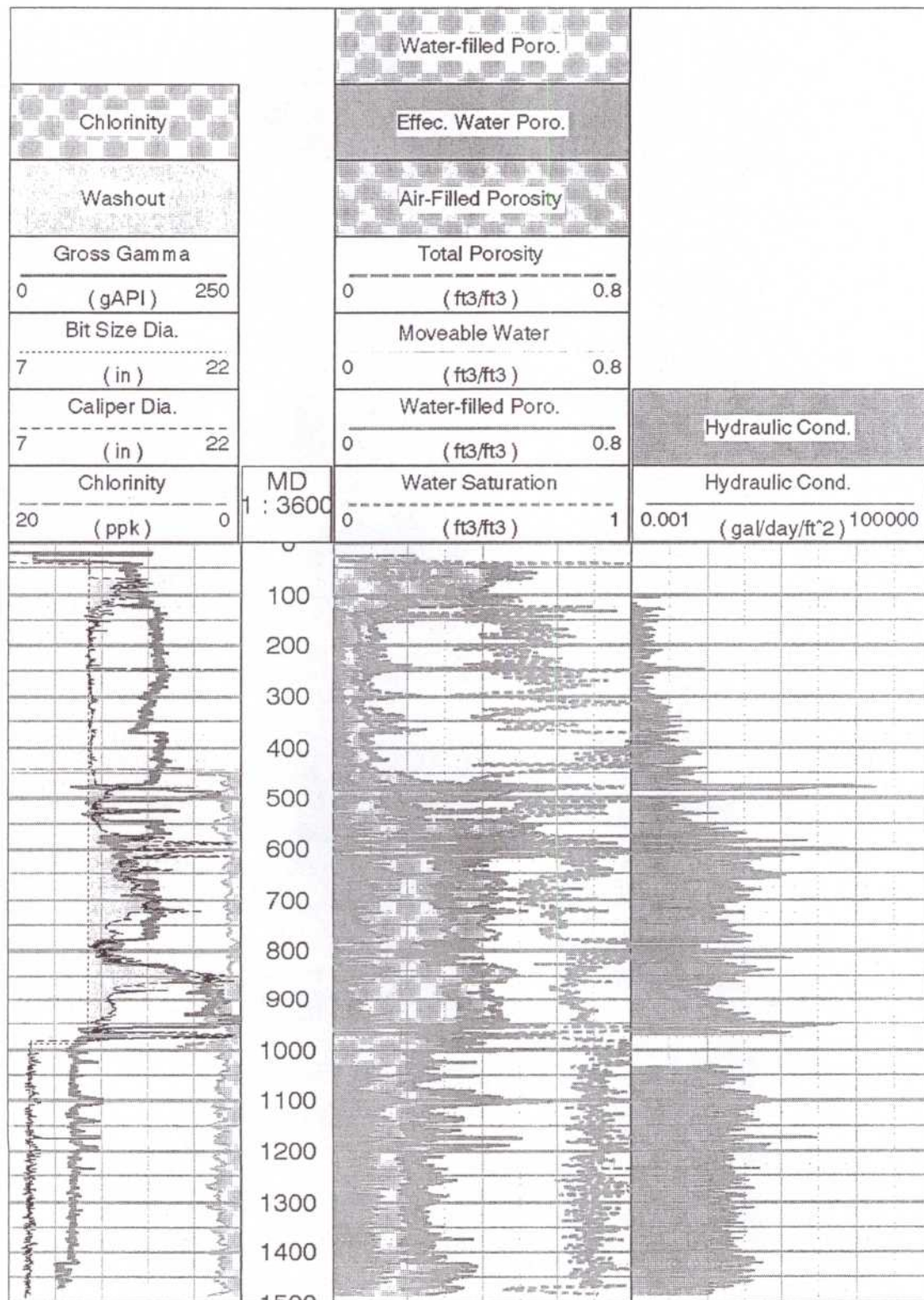


Figure 4.1. Summary porosity logs in R-26 borehole from processed geophysical logs, interval 25–1484 ft, with caliper, gross gamma, apparent chlorinity, water saturation, and water hydraulic conductivity logs. Porosity, water saturation, and hydraulic conductivity logs are derived from the ELAN integrated log analysis.

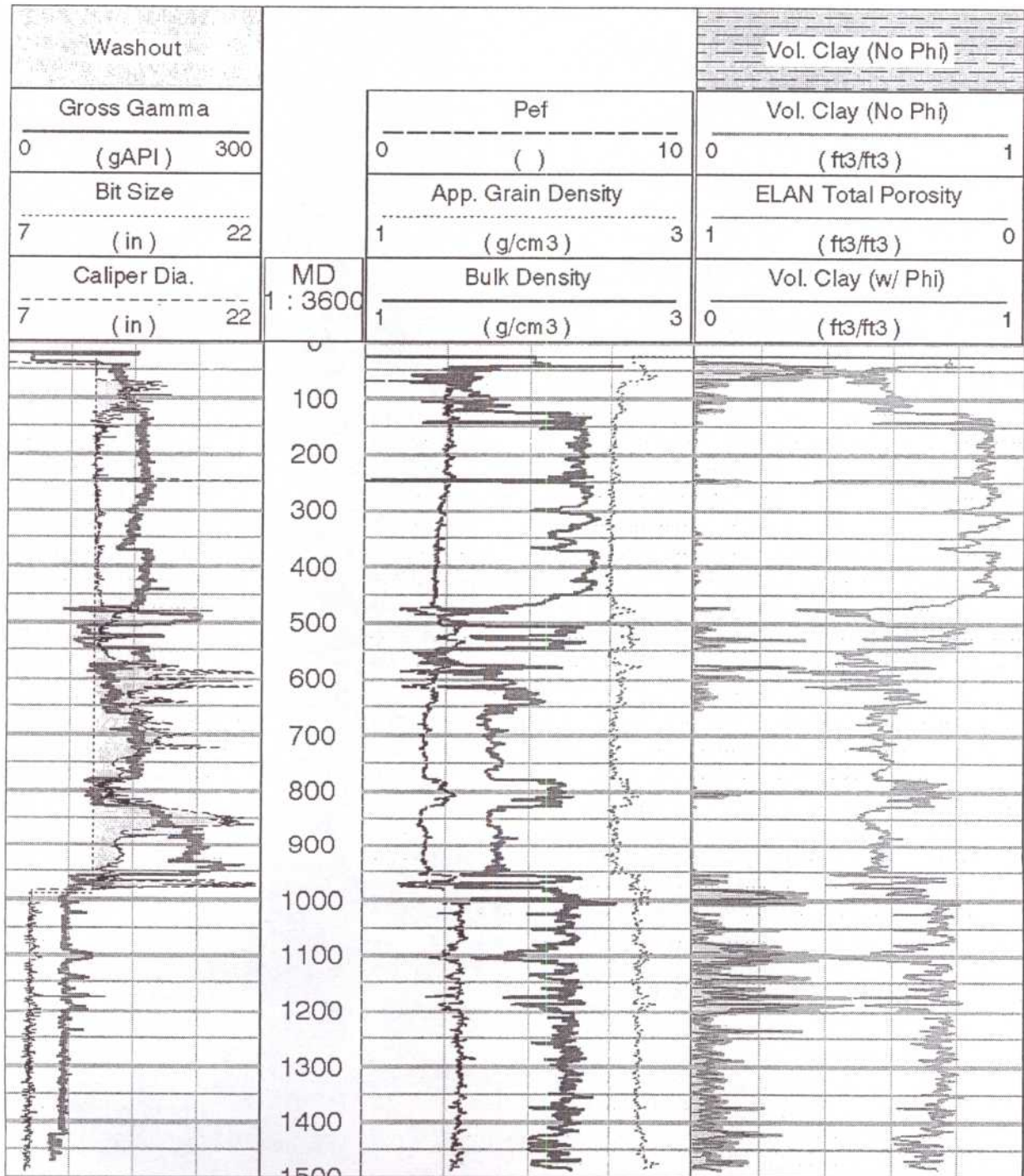


Figure 4.2. Summary bulk density and volume clay logs in R-26 borehole from processed geophysical logs, interval 25–1486 ft. Also shown – caliper, gross gamma, apparent grain density, and total porosity logs (the latter two derived from the ELAN analysis).

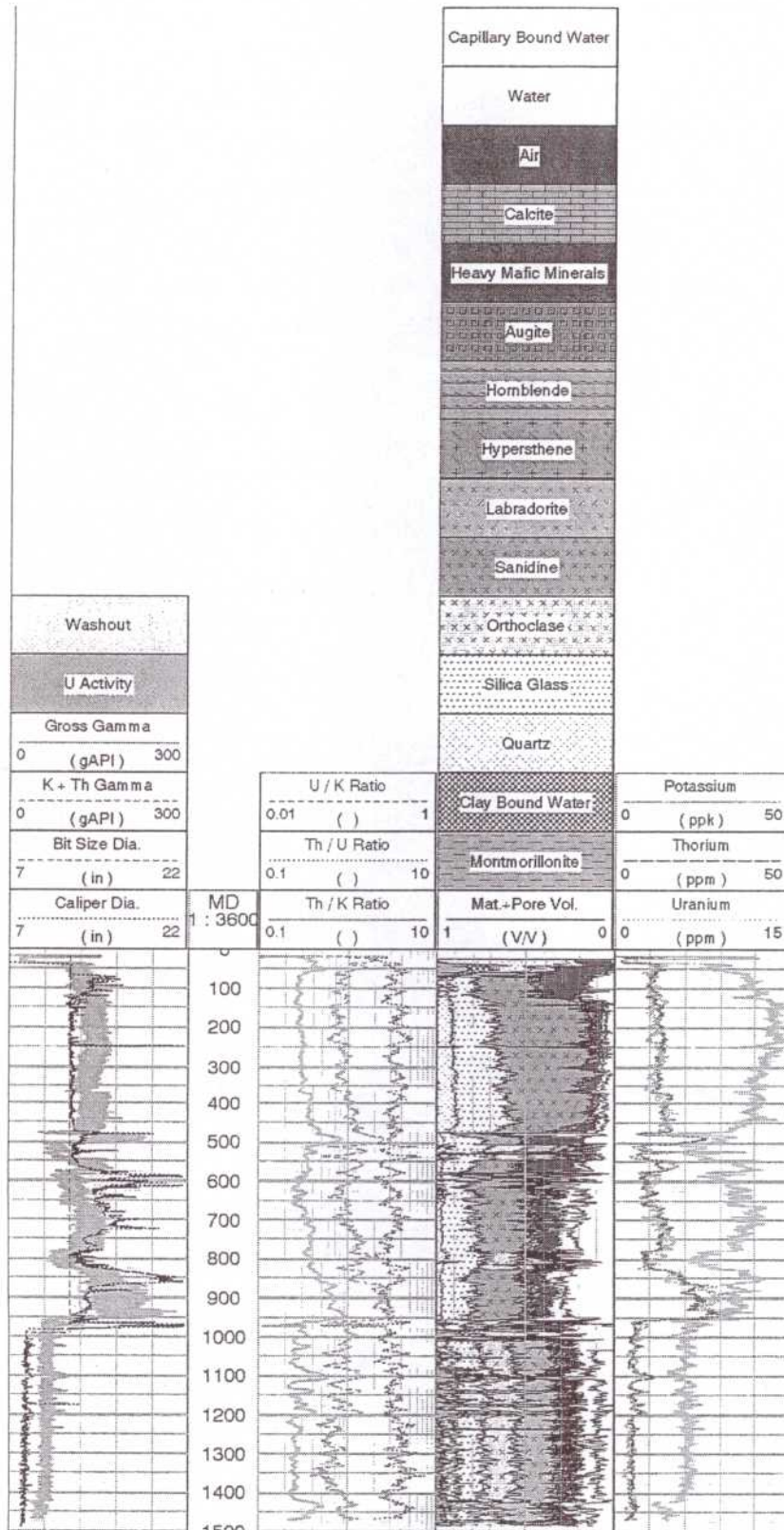


Figure 4.3. Summary spectral natural gamma ray logs and ELAN mineralogy/lithology and pore fluid model from R-26 borehole, interval 25–1484 ft. Caliper log is also shown.

## 4.2 Integrated Log Montage

This section summarizes the integrated geophysical log montage for R-26. The montage is provided in Appendix D. A description of each log curve in the montage follows—organized under the heading of each track, starting from track 1 on the left-hand side of the montage. Note that the descriptions in this section focus on what the curves are and how they are displayed; the specific characteristics and interpretations of the R-26 geophysical logs are provided in the previous section.

### Track 1—Depth

The first track on the left contains the depth below ground surface in units of feet, as measured by the geophysical logging system during the AIT logging run of September 2003 and the AIT logging run of October 2003 (the latter run depth-matched to former). All the geophysical logs are depth-matched to the spectral gross gamma measurement run with the AIT.

### Track 2—Basic Logs

The second track on the left (inclusive of the depth track) presents basic curves:

- gamma ray (thick black), recorded in API units and displayed on a scale of 0 to 250 API units;
- two calipers from the FMI (thin dotted and dashed pink) and one from the TLD (thin solid pink) with bit size as a reference (dashed-dotted black) to show washout (pink shading), recorded as hole diameter in inches and displayed on a scale of 11 to 21 in.;
- spontaneous potential or SP (dashed red – valid only below the borehole water level), recorded in millivolts and displayed on a relative scale;
- bulk chlorinity (dashed green with green shading), recorded in parts per thousand (ppk) and displayed on a scale of 5 to 0 ppk (left to right);
- borehole deviation displayed as a tadpole every ten feet (light blue dots and connected line segments) – the “head” marks the angular deviation from vertical at that particular depth, on a scale of zero to 5 degrees, and the “tail” shows the azimuth of the deviation, true north represented by the tail facing straight towards the top of the page.

Two gamma ray curves from the NGS are presented:

- total gross gamma (thick solid black curve) and
- gross gamma minus the contribution of uranium (dashed black).

### Track 3—Resistivity

The third track displays the resistivity measurements from the AIT, spanning most of the open hole section. All the resistivity logs are recorded in units of ohmmeters and displayed on a logarithmic scale of 2 to 2000 ohm-m.

Six electrical resistivity logs from the AIT are displayed:

- Borehole fluid resistivity (solid orange curve)—only valid in water-filled hole
- Bulk electrical resistivity at five median depths of investigation—10 in. (black solid), 20 in. (long-dashed blue), 30 in. (short-dashed red), 60 in. (dashed-dotted green), and 90 in. (solid purple)—each having a two-foot vertical resolution.

The area between the 10 in. and 90 in. resistivity curves, representing radial variations in bulk resistivity (potentially from invasion of drilling fluids), is shaded:

- blue when the 10 in. resistivity is greater than the 90 in. resistivity (labeled “resistive invasive”) and
- yellow when the 90 in. resistivity is greater than the 10 in. resistivity (labeled “conductive invasive”).

A high vertical resolution (~8 in.), shallow-reading (~2 in.) micro-resistivity log from the MCFL is also displayed in this track (solid pink curve).

#### Track 4—Porosity

The fourth track displays the primary porosity log results. All the porosity logs are recorded in units of volumetric fraction and displayed on a linear scale of 0.75 (left side) to negative 0.1 (right side). Specifically, these logs consist of

- CNT air-filled epithermal neutron porosity (solid sky blue curve)—epithermal neutron porosity processed for air-filled hole and, thus, valid (and visible) only in the air-filled borehole (above 833 ft);
- CNT water-filled thermal neutron porosity (solid sky blue curve)—thermal neutron porosity valid only in the water-filled borehole;
- CMR total water-filled porosity (solid black);
- CMR effective water-filled porosity (dashed green);
- CMR bound water porosity (light blue area shading)—representing by the area between the CMR total and effective water-filled porosities;
- Total porosity derived from bulk density and neutron porosity using 2.65 g/cc (dotted red curve), 2.45 g/cc (long-dashed red curve), and 2.25 g/cc (dashed red curve)—with red shading between the 2.25 and 2.65 g/cc saturation curves to show the range; and
- ELAN total water and air-filled porosity (dashed-dotted cyan)—derived from the ELAN integrated analysis of all log curves to estimate optimized matrix and pore volume constituents.

#### Track 5—Density

The fifth track displays the:

- bulk density (thick solid maroon curve) on a scale of 1 to 3 grams per cubic centimeter (g/cc);
- Pe (long-dashed black curve) on a scale of 0 to 10 non-dimensional units;

- density correction (dashed orange curve) on a scale of -0.75 to 0.25 g/cc; and
- apparent grain density (dashed-dotted brown curve), derived from the ELAN analysis, on a scale of 2 to 4 g/cc.

Grey area shading is shown where the  $P_e$  increases above 3 (indicating the presence of heavy, possibly mafic, minerals) and orange shading is shown where the density correction is greater than the absolute value of 0.25 (indicating the density processing algorithm had to perform a major correction to the bulk density calculation).

### Track 6—NGS Spectral Gamma

The sixth track from the left displays the spectral components of the NGS measurement results as wet weight concentrations:

- potassium (solid green curve) in units of parts per thousand (ppk) and on a scale of -50 to 50 ppk;
- thorium (dashed brown) in units of parts per million (ppm) and on a scale of 50 to -50 ppm; and
- uranium (dotted blue) in units of parts per million (ppm) and on a scale of 20 to 0 ppm.

### Track 7—CMR Porosity

Track 7 displays various CMR water-filled porosities along with measurement quality flags—valid only in the open hole section. The porosity and measurement quality logs are presented on a scale of 0.5 to zero volume fraction and discrete blocks originating from the left side, respectively. Specifically, the CMR logs shown in this track are:

- Total water-filled porosity (solid black curve)—representing the total water volume fraction measured by the CMR;
- Three millisecond (ms) porosity (short-dashed brown)—representing the water volume fraction corresponding to the portion of the CMR measured T2 distribution that is above 3 ms, a cutoff that is considered to be representative of the break between clay-bound water (less than 3 ms) and all other types of water (greater than 3 ms);
- Effective water-filled, or free fluid, porosity (solid pink)—representing the water volume fraction that is moveable (can flow), based on a 33 ms T2 distribution cutoff that is considered representative of the break between bound water (less than 33 ms) and moveable water (greater than 33 ms) in clastic rocks;
- Clay-bound water (brown area shading between total and 3 ms porosity logs)—representing the water volume fraction that is bound within clays;
- Capillary-bound water (pink area shading between 3 ms and effective porosity logs)—representing the water volume fraction that is bound within matrix pores by capillary forces;

- CMR wait-time flag (red area shading)—activates when there is significant measurement response at late T2 times, corresponding to large amounts of completely free (“bathtub”) water and often associated with washouts or very large pores;
- CMR measurement noise flag (yellow and orange area shading)—activates when there is potentially detrimental amounts of measurement noise detected by the tool, at moderate (yellow) and high (orange) levels.

### **Track 8 –Pore Size Distribution**

Track 8 displays the water-filled pore size distribution as determined by the CMR—shown as binned water-filled porosities and valid only in the open hole section. The binned porosity logs are presented on a scale of 0.5 to zero volume fraction with colored area shading corresponding to the different bins:

- Clay-bound water—brown area shading;
- Micro pore and small pore water (the sum comprising capillary-bound water)—gray and blue area shading, respectively;
- Medium pore, large pore, and late decay (the sum comprising effective water-filled porosity)—yellow, red, and green area shading, respectively.

### **Track 9—CMR T2 Distribution (Waveforms)**

The CMR T2 distribution is displayed in Track 9 as green waveform traces at discrete depths. The horizontal axis, corresponding to relaxation time in milliseconds, is on a logarithmic scale from 0.3 to 3000 ms. Also plotted are the:

- T2 logarithmic mean (solid blue curve) and
- T2 cutoff time used for differentiating between bound and free water (solid red line)—a constant 33 ms in this case.

### **Track 10—CMR T2 Distribution (Heated Amplitude)**

Track 10 displays the T2 distribution in another way—on a heated color scale where progressively “hotter” color (green to yellow to red) corresponds to increasing T2 amplitude. The remaining aspects of the display are the same as in Track 9, except that the T2 logarithmic mean is shown as a solid white curve and the T2 cutoff is not displayed.

### **Track 11—CMR Hydraulic Conductivity**

Track 11 displays several estimates of hydraulic conductivity (K) derived from the CMR measurement and the ELAN integrated log analysis (the latter primarily sensitive to the CMR measurement of moveable water), presented on a logarithmic scale of  $10^{-4}$  to  $10^6$  gallons per day per feet squared (gal/day/ft<sup>2</sup>):

- A K versus depth estimate derived from using the SDR permeability equation applied to the processed CMR results, converted to hydraulic conductivity (dashed purple curve);

- A K versus depth estimate derived from using the Timur-Coates permeability equation with total and moveable water content derived from the ELAN analysis, converted to hydraulic conductivity (solid blue curve); and
- An intrinsic K versus depth estimate (assuming full saturation) using the Timur-Coates permeability equation with total and effective porosity values derived from the ELAN analysis, converted to hydraulic conductivity (dotted cyan).

### **Track 12– FMI Image (Dynamic Normalization)**

Track 12 displays the FMI image, processed with dynamic normalization so that small-scale electrical resistivity features are amplified in the image. (With dynamic normalization the range of electrical resistivity amplitudes – colors in the image – is normalized across a small moving depth window.) The image is fully oriented and corresponds to the inside of the borehole wall unwrapped, such that the left-hand side represents true north, half-way across the image is south, and the right-hand side is north again. The four color tracks in the image correspond to portions of the borehole wall contacted by the four FMI caliper pads; the blank space in between is the portion of the borehole wall not covered by the pads.

Also displayed are the interpreted bed boundaries (thin blue sinusoids) and electrically conductive fractures (bold purple sinusoids).

### **Track 13– FMI Bedding and Fractures**

Track 13 displays the interpreted bed boundaries and fractures picked from the FMI image, shown in two ways:

- Individually as tadpoles at the depths the bedding plane or fracture crosses the midpoint of the borehole – where the “heads” (circles/triangles) represent the dip angle and the “tails” (line segments) represent the true dip azimuth (direction the bed is dipping towards). Bed boundaries are shown as circular headed blue and black tadpoles and electrically conductive fractures are shown as red circular headed and black triangular headed tadpoles.
- Summed as dip azimuth rose histograms (green colored fan plots for bed boundaries) – where the number of bed boundaries having a dip direction within a particular sector are summed, thus highlighting the predominant dip directions.

### **Track 14– FMI Image (Static Normalization)**

Track 14 displays the FMI image again, but in a different way – processed with static normalization to highlight larger scale features and trends. (With static normalization the range of electrical resistivity amplitudes – colors in the image – is normalized across the entire length of the log interval.)

### **Track 15– Fracture Aperture and High Resolution Porosity**

Track 15 displays the estimated hydraulic aperture of any interpreted electrically conductive fractures (red circles on logarithmic scale of 0.0001 to 1 inch) – computed using an FMI image scaled to the AIT shallow resistivity. Also displayed is the high resolution thermal neutron

porosity log (solid blue) and the high resolution density porosity (solid red), the latter computed assuming a matrix grain density of 2.65 g/cc and pore fluid density of 1.0 g/cc. Both these logs have an 8 in depth resolution. Where the density porosity is greater than the neutron porosity the area between the two logs is shaded red. The red shading is an indication of air in the pore space (less than 100% water saturation).

### **Tracks 16 to 20– Geochemical Elemental Measurements**

The narrow tracks 16 to 20 present the geochemical measurements iron (Fe) and silicon (Si), sulfur (S) and calcium (Ca), potassium (K) and estimated aluminum (Al), titanium (Ti) and gadolinium (Gd), and hydrogen (H) and bulk chlorinity (Cl) —from left to right respectively, in units of dry matrix weight fraction (except H wet weight fraction, Cl and K in ppk).

### **Track 21–ELAN Mineralogy Model Results (Dry Weight Fraction)**

Track 21 displays the results from the ELAN integrated log analysis (the matrix portion)—presented as dry weight fraction of mineral types chosen in the model:

- Montmorillonite clay (brown/tan)
- Quartz (yellow with small black dots)
- Silica glass (orange)
- Orthoclase or other potassium feldspar (lavender)
- Sanidine (violet)
- Labradorite or other plagioclase feldspar (pink)
- Hypersthene (purple)
- Hornblende (forest green)
- Augite (maroon)
- Heavy mafic/ultramafic minerals, such as magnetite or olivine (dark green)
- Pyrite (cross-hatched red).

### **Track 22–ELAN Mineralogy-Pore Space Model Results (Wet Volume Fraction)**

Track 22 displays the results from the ELAN integrated log analysis—presented as wet mineral and pore fluid volume fractions:

- Montmorillonite clay (brown/tan)
- Clay-bound water (checkered gray-black)
- Quartz (yellow with small black dots)
- Silica glass (yellow with large black dots)
- Orthoclase or other potassium feldspar (lavender)
- Sanidine (violet)

- Labradorite or other plagioclase feldspar (pink)
- Pyrite (tan with large black squares).
- Hypersthene (purple)
- Hornblende (forest green)
- Augite (maroon)
- Heavy mafic minerals, such as magnetite (dark army green)
- Air (red)
- Moveable water (white)
- Capillary-bound water (light blue).

### Track 23—Summary Logs

Track 23, the second track from the right, displays several summary logs that describe the fluid and air-filled volume measured by the geophysical tools, including water saturation:

- Optimized estimate of total volume fraction water from the ELAN analysis (solid dark blue curve and area shading);
- Optimized estimate of moveable volume fraction water (effective porosity in fully saturated conditions) from the ELAN analysis (dashed cyan curve and green area shading);
- Optimized estimate of total volume fraction of air-filled porosity from the ELAN analysis (solid red curve and dotted red area shading);
- Optimized estimate of water saturation (percentage of pore space filled with water) from the ELAN analysis (dashed-dotted purple curve);
- Water saturation as calculated directly from the bulk density and geochemical estimated porosity using a grain density of 2.65 g/cc (dotted light blue curve), 2.45 g/cc (long-dashed light blue curve), and 2.25 g/cc (dashed light blue curve)—with light blue shading between the 2.25 and 2.65 g/cc saturation curves to show the range;
- Integrated estimated relative water flow from the CMR log that mimics a flow meter (spinner) acquired under flowing conditions (solid green line coming from left-hand side at bottom of logged interval);
- Potential for water flow indicator from the CMR log (block cyan coming from the right-hand side of the track).

The porosity curves scale from 0 to 1 total volume fraction, left to right; the water saturation scales from 0 to 1 volume fraction of pore space, from left to right. The relative water flow is on a scale of 0 to 1 relative volumetric flow rate from left to right. The flow indicator is a binary-valued flag that rises to halfway through the first division from the right on the x-axis when the CMR measurement indicates a potential for flow.

## **Track 24—Depth**

The final track on the right, same as the first track on the left, displays the depth below ground surface in units of feet, as measured by the geophysical logging system during the AIT-NGT logging run.

## **5.0 REFERENCES**

Kenyon, B., R. Kleinberg, C. Straley, G. Gubelin, and C. Morris: 1995. "Nuclear Magnetic Resonance Imaging— Technology for the 21st Century." *Oilfield Review*, v. 7, n. 3, p. 19–33.

Mayer, C. and A. Sibbit, 1980. "GLOBAL, A New Approach to Computer-Processed Log Interpretation." Paper SPE 9341 presented at the 1980 SPE Annual Technical Conference and Exhibition.

Quirein, J., S. Kimminau, J. LaVigne, J. Singer, and F. Wendel. 1986. "A Coherent Framework for Developing and Applying Multiple Formation Evaluation Models." Paper DD in 27th Annual Logging Symposium Transactions: Society of Professional Well Log Analysts.

Schlumberger, Log Interpretation Charts 1998 (SMP-7006).

Schlumberger, Log Interpretation Principles/Applications 1989 (SMP 7017)

Schlumberger, Log Quality Control Manual. 1997

## **Appendix C**

---

### *Groundwater Analytical Results*

## GROUNDWATER ANALYTICAL RESULTS

During drilling operations at R-26, alluvial groundwater was not encountered. Perched groundwater was encountered in the R-26 corehole at depths of 173 and 241 ft bgs. An upper saturated zone was encountered in the R-26 borehole at 604 ft bgs. A screening groundwater sample was collected from the open corehole at 240 ft on September 15, 2003. This groundwater may have flowed down from the 173-ft zone above. The groundwater sample from the R-26 corehole was collected using a bailer and analyzed for inorganic constituents and high explosive compounds. Analytical results for the corehole sample are provided in Table 1. Two piezometers were installed at depths of 150 to 180 ft bgs and 230 to 250 ft bgs for collecting additional groundwater samples. To date, no samples have been collected from the piezometers. A groundwater sample was not collected from the 604-ft zone during drilling of the borehole; however, this zone was sampled during well development between depths of 651.8 and 669.9 ft bgs (upper screened interval). A groundwater sample was collected from the regional aquifer between 1421.8 and 1445 ft bgs (lower screened interval) on November 14, 2003. These groundwater samples were analyzed for cations, anions, metals, and low-level tritium, and the results are presented in Tables 2 and 3.

Core samples were collected from the alluvium and Tshirege Member of the Bandelier Tuff. Thirteen samples of core were collected from the vadose (unsaturated) zone during drilling from 5 to 250 ft bgs. Approximately 500 g to 1000 g of core or cuttings samples were placed in appropriate sample jars in protective plastic bags before they were analyzed by EES-6, Coastal Science Laboratories, and Severn-Trent Laboratories (STL), Inc. These samples were analyzed for high explosive compounds, cations, anions, metals, and radionuclides for characterization purposes. The results will be reported in the investigation report for the Cañon de Valle watershed.

## GEOCHEMISTRY OF SAMPLED WATERS FROM WELL R-26

Groundwater samples were collected after well development from both the upper saturated zone within the Cerro Toledo interval (651.8 to 669.9 ft bgs) and the regional aquifer (1421.8 to 1445 ft bgs) within the upper Puye Formation. Groundwater samples from the upper saturated zone and the regional aquifer were collected by using a submersible pump during well development. Analytical results for these two samples are provided in Tables 2 and 3. Temperature, turbidity, and pH were not determined onsite during sampling of the upper saturated zone and regional aquifer. Both filtered (metals, trace elements, and major cations and anions) and nonfiltered (tritium, total organic carbon, radionuclides, and stable isotopes) samples were collected for chemical and radiochemical analyses. Aliquots of the samples were filtered through a 0.45- $\mu$ m Gelman filter. Groundwater samples were acidified with analytical-grade  $\text{HNO}_3$  to a pH of 2.0 or less for metal and major cation analyses at EES-6. Alkalinity was determined at EES-6 using standard titration techniques.

Groundwater samples were analyzed by EES-6 using techniques specified in the US Environmental Protection Agency (EPA) SW-846 manual. Ion chromatography (IC) was the analytical method for bromide, chloride, fluoride, nitrate, nitrite, oxalate, perchlorate, phosphate, and sulfate. The method detection limit (MDL) for perchlorate using IC is 0.002 ppm or mg/L (2 ppb or 2  $\mu$ g/L). Perchlorate was also analyzed by General Engineering Laboratories (GEL) using the liquid chromatography/mass spectrometry/mass spectrometry (LC/MS/MS) method. This

method is more sensitive than the IC method, having an MDL of 0.00005 mg/L (0.050 µg/L) and a reporting limit or quantitation limit of 0.0002 mg/L (0.2 µg/L). Inductively coupled (argon) plasma emission spectroscopy (ICPES) was used for calcium, magnesium, potassium, silica, and sodium. Aluminum, antimony, arsenic, barium, beryllium, cadmium, chromium, cobalt, copper, iron, lead, manganese, mercury, nickel, selenium, silver, thallium, vanadium, uranium, and zinc were analyzed by inductively coupled (argon) plasma mass spectrometry (ICPMS). The precision limits (analytical error) for major ions and trace elements were generally less than  $\pm 10\%$  using ICPES and ICPMS. High explosive compounds were analyzed by using the LC/MS/MS method.

Radionuclide activity in groundwater was determined by alpha spectrometry for americium, plutonium, and uranium isotopes; gas proportional counting for strontium-90; and gamma spectrometry for cesium-137 and other gamma-emitting isotopes. GEL performed the above radiometric analyses. Concentrations of tritium were determined by electrolytic enrichment at the University of Miami. Stable isotopes of oxygen (oxygen-18 and oxygen-16,  $\delta^{18}\text{O}$ ) and hydrogen (hydrogen and deuterium,  $\delta\text{D}$ ) were analyzed by Geochron Laboratories (Cambridge, Massachusetts) using isotope ratio mass spectrometry (IRMS). Stable isotopes of nitrogen (nitrogen-15 and nitrogen-14,  $\delta^{15}\text{N}$ ) were analyzed by Coastal Science Laboratories, Inc. (Austin, Texas) using IRMS. Analytical results for nitrogen stable isotopes are pending for R-26.

**Table 1**  
**Hydrochemistry of Perched Groundwater from Open Corehole R-26**  
**(filtered samples except as noted)**

<b>Depth (ft)</b>	<b>240</b>
<b>Geologic Unit</b>	<b>Cerro Toledo Interval</b>
<b>Date Sampled</b>	<b>09/15/03</b>
pH	7.73 (Lab)
Temperature (°C)	Not reported
Specific Conductance (µS/cm)	Not reported
Turbidity (NTU)	Not reported
Alkalinity (ppm CaCO <sub>3</sub> /L)	83.8
Al (ppm)	0.035
Sb (ppm)	0.001
As (ppm)	0.0009
B (ppm)	0.018
Ba (ppm)	0.007
Be (ppm)	[0.001], U
HCO <sub>3</sub> (ppm)	90.0
Br (ppm)	0.05
Cd (ppm)	[0.001], U
Ca (ppm)	9.77
Cl (ppm)	5.27
ClO <sub>4</sub> (mg/L) (LC/MS/MS)	Not analyzed
ClO <sub>4</sub> (ppm) (IC)	Not decipherable

Cr (ppm)	0.0010
Co (ppm)	0.0059
Cu (ppm)	0.0081
F (ppm)	0.16
Fe (ppm)	[0.01], U
Pb (ppm)	0.0003
Mg (ppm)	2.86
Mn (ppm)	0.062
Hg (ppm)	0.010
Mo (ppm)	0.061
Ni (ppm)	[0.001], U
NO <sub>3</sub> (ppm) (as N)	0.60
NO <sub>2</sub> (ppm) (as N)	0.01
C <sub>2</sub> O <sub>4</sub> (ppm) (oxalate)	0.05
PO <sub>4</sub> (ppm) (as P)	0.18
K (ppm)	9.09
Se (ppm)	[0.001], U
Ag (ppm)	[0.001], U
Na (ppm)	23.1
SiO <sub>2</sub> (ppm)	32.7
Sr (ppm)	0.043
SO <sub>4</sub> (ppm)	2.46
Tl (ppm)	[0.001], U
U (ppm)	0.0022
V (ppm)	0.001
Zn (ppm)	0.003
TOC (ppm), non filtered	Not analyzed
RDX (µg/L), non filtered	0.019
HMX (µg/L), non filtered	0.0634
TDS (ppm) (calculated)	185

Note: U = not detected. Silica concentrations were calculated from measured silicon (ICPES). Bicarbonate concentrations were calculated from measured alkalinity. TOC = total organic carbon.

Table 2

**Hydrochemistry of the Upper Saturated Zone and Regional Aquifer  
in Completed Well R-26 (samples filtered, except as noted)**

<b>Depth (ft)</b>	<b>651.8 to 669.9</b>	<b>1421.8 to 1445</b>
<b>Geologic Unit</b>	<b>Cerro Toledo Interval</b>	<b>Upper Puye Formation</b>
<b>Date Sampled</b>	<b>11/16/03</b>	<b>11/14/03</b>
<b>pH</b>	6.99 (Lab)	7.07 (Lab)
<b>Temperature (°C)</b>	Not reported	Not reported
<b>Specific Conductance (µS/cm)</b>	Not reported	Not reported

Turbidity (NTU)	Not reported	Not reported
Alkalinity (ppm CaCO <sub>3</sub> /L)	46.1	46.3
Al (ppm)	0.85	0.90
Sb (ppm)	[0.001], U	[0.001], U
As (ppm)	0.0009	0.0008
B (ppm)	0.008	0.009
Ba (ppm)	0.010	0.010
Be (ppm)	[0.001], U	[0.001], U
HCO <sub>3</sub> (ppm)	56.3	56.5
Br (ppm)	0.02	0.02
Cd (ppm)	[0.001], U	[0.001], U
Ca (ppm)	7.53	7.51
Cl (ppm)	1.12	1.13
ClO <sub>4</sub> (mg/L) (LC/MS/MS)	0.000215	0.000218
ClO <sub>4</sub> (ppm) (IC)	[0.002], U	[0.002], U
Cr (ppm)	0.0013	0.0015
Co (ppm)	[0.001], U	[0.001], U
Cu (ppm)	[0.001], U	[0.001], U
F (ppm)	0.08	0.08
Fe (ppm)	0.14	0.21
Pb (ppm)	0.0004	0.0006
Mg (ppm)	2.93	2.90
Mn (ppm)	0.0040	0.0062
Hg (ppm)	[0.00005], U	[0.00005], U
Mo (ppm)	[0.001], U	[0.001], U
Ni (ppm)	[0.001], U	[0.001], U
NO <sub>3</sub> (ppm) (as N)	0.38	0.37
NO <sub>2</sub> (ppm) (as N)	[0.01], U	[0.01], U
C <sub>2</sub> O <sub>4</sub> (ppm) (oxalate)	[0.01], U	[0.01], U
PO <sub>4</sub> (ppm) (as P)	0.08	0.06
K (ppm)	2.11	2.11
Se (ppm)	[0.001], U	[0.001], U
Ag (ppm)	[0.001], U	[0.001], U
Na (ppm)	9.35	9.27
SiO <sub>2</sub> (ppm)	66.8	67.8
Sr (ppm)	0.042	0.043
SO <sub>4</sub> (ppm)	1.09	1.13
Tl (ppm)	[0.001], U	[0.001], U
U (ppm)	0.0005	0.0005
V (ppm)	0.007	0.007
Zn (ppm)	0.041	0.17
TDS (ppm) (calculated)	152	154

Note: U = not detected. Silica concentrations were calculated from measured silicon (ICPES). Bicarbonate concentrations were calculated from measured alkalinity.

**Table 3**  
**Hydrochemistry of the Upper Saturated Zone and Regional Aquifer**  
**in Completed Well R-26**  
**(non-filtered samples)**

<b>Depth (ft)</b>	<b>651.8 to 669.9</b>	<b>1421.8 to 1445.0</b>
<b>Geologic Unit</b>	<b>Cerro Toledo Interval</b>	<b>Upper Puye Formation</b>
<b>Date Sampled</b>	<b>11/16/03</b>	<b>11/14/03</b>
Tritium (pCi/L)	[0.10], U	[0.19], U
Am-241 (pCi/L)	[0.0054], U	[0.0163], U
Cs-137 (pCi/L)	[-1.51], U	[0.383], U
Pu-238 (pCi/L)	[0.0148], U	[-0.0050], U
Pu-239,240 (pCi/L)	[0.0049], U	[0.0050], U
Sr-90 (pCi/L)	[0.0276], U	[-0.0694], U
U-234 (pCi/L)	0.371	0.351
U-235 (pCi/L)	[0.0327], U	[0.0312], U
U-238 (pCi/L)	0.185	0.229
RDX (mg/L)	[0.000104], U	[0.000104], U
HMX (mg/L)	[0.000104], U	[0.000104], U
TOC (ppm)	2.01	2.17
$\delta^{15}\text{N}$ (‰)	Results pending	Results pending
$\delta\text{D}$ (‰)	-88	-87
$\delta^{18}\text{O}$ (‰)	-12.0	-12.0

*Note:* U = not detected, ‰ = permil, and TOC = total organic carbon.

## **Appendix D**

---

### *Lithology Log*

## Lithologic Descriptions of Core and Drill Cuttings at Borehole R-26

Geologic Unit	Lithologic Description	Sample Interval (ft)	Elevation Range (ft above msl)
Qal, alluvium	No core recovery. Note: rock core samples examined for lithologic description in the interval from 5.0 to 105.0 ft bgs for this lithlog	0.0-5.0	7641.6-7636.6
	Unconsolidated material. Olive brown (2.5 YR 4/2), sandy gravel (GW) with cobbles and silt, non-plastic; core damp.	5.0-13.0	7636.6-7628.6
	No core recovery.	13.0-14.0	7628.6-7627.6
	Same material as above; weathered tuff plugging sampler shoe.	14.0-16.0	7627.6-7625.6
	No core recovery.	16.0-16.5	7625.6-7625.1
	Volcanic tuff, light brown (7.5 YR 6/4), devitrified, moderately weathered, medium dense, 30% quartz and sanidine phenocrysts (1-2 mm), 20% pumice (up to 2.5 cm), trace dacite xenoliths.	16.5-18.5	7625.1-7623.1
	No core recovery.	18.5-19.0	7623.1-7622.6
	Volcanic tuff, red brown (2.5 YR 4/4), severely weathered tuff composed of 5% pumice, 5-10% quartz and sanidine phenocrysts, clasts of dacite (5.0-7.5 cm), core damp.	19.0-24.0	7622.6-7617.6
	Volcanic tuff. Same material as above, with cobbles up to 7.5 cm.	24.0-25.0	7617.6-7616.6
	Volcanic tuff. Cobbles up to 7.5 cm.	25.0-29.0	7616.6-7612.6
	Volcaniclastic sediments, reddish gray (5YR 4/2), sandy clay with silt (SC), non-plastic to low plasticity. Composed of crystals and dacite fragments; core damp.	29.0-31.0	7612.6-7610.6
	No core recovery.	31.0-32.5	7610.6-7609.1
	Volcaniclastic sediments. Same material as above with larger (up to 10 cm) dacite fragments.	32.5-35.0	7609.1-7606.6
	Volcaniclastic sediments, red brown (2.5 YR 4/4), sandy gravel (GP) with silt and clay, non-plastic, gravel 40%, sand 30%, silt 20%. Composed of dacite gravels (up to 5 cm), fine to coarse sand. Large (up to 10 cm) dacite gravel clasts stuck in geobarrel at 41 ft bgs; core damp to moist.	35.0-45.0	7606.6-7596.6
	Volcaniclastic sediments. Large dacite fragment plugging barrel. Same material as above.	45.0-50.0	7596.6-7591.6
	Volcanic tuff, yellow brown (10YR 5/8), predominantly coarse-grained sand composed of pumice fragments and quartz and sanidine crystals, 20% ash, some devitrified pumice; core damp to moist.	50.0-51.3	7591.6-7590.3
Qbt 4, Unit 4 Tshirege Member of the Bandelier Tuff	Volcanic tuff, pink (7.5 YR 7/4), fine-grained ash matrix. Yellow phenocryst-rich vitric pumice occurrence at 54 ft bgs. <b>Note: base of alluvium and contact with underlying Unit 4 of the Tshirege Member of the Bandelier Tuff is interpreted to be at 60 ft bgs.</b>	51.3-63.5	7590.3-7578.1
	Volcanic tuff, pale red (10YR 6/4), nonwelded to partially welded, slightly weathered. Composed of 20% white to light gray devitrified pumice, 10-20% quartz and sanidine phenocrysts (up to 2 mm), and 60-70% fine-grained ash matrix; core dry to damp.	63.5-65.0	7578.1-7576.6
	Volcanic tuff, light red (10R 6/6). Similar to above, reddish brown to light gray pumice increasing in abundance to 25-30% by volume. Coloration change to pale red (10R 5/4) in the interval 66.2-66.9 ft bgs.	65.0-70.0	7576.6-7571.6
	Volcanic tuff, similar to above, phenocrysts increasing in abundance (35-40%).	70.0-75.0	7571.6-7566.6
	Volcanic tuff, light red (10R 6/6). Similar to above; slight increase in degree of welding, partially welded.	75.0-80.0	7566.6-7561.6
	Volcanic tuff, light red (10R 6/6). Similar to above, partially welded.	80.0-85.0	7561.6-7556.6
	Volcanic tuff. Increase in pumice ratio to 5 to 1.	85.0-90.0	7556.6-7551.6
	Volcanic tuff. Same material as above, slight decrease in welding.	90.0-95.0	7551.6-7546.6
	Volcanic tuff, light red (10R 6/6). Similar to above.	95.0-100.0	7546.6-7541.6

## Lithologic Descriptions of Core and Drill Cuttings at Borehole R-26 (Continued)

Geologic Unit	Lithologic Description	Sample Interval (ft)	Elevation Range (ft above msl)
	Volcanic tuff. Same material as above, becoming more dense at 103.6 ft bgs. Note: drill cuttings were collected and are described in the R-26 interval from 105 ft to the bottom of the borehole at 1,485 ft bgs.	100.0-105.0	7541.6-7536.6
	Volcanic tuff, light brownish gray (5YR 6/1) to grayish orange (10YR 7/4), crystal rich, moderately to strongly welded. +10F (i.e., plus No. 10 sieve-size fraction): 20-30% quartz and sanidine crystals, 1-2% unidentified dark mafic minerals; 1-2% lithic fragments (up to 1 mm); strong Fe-oxide staining. +35F (i.e., plus No. 35 sieve-size fraction): 70-75% quartz and sanidine crystals, 25-30% welded tuff fragments. WR (i.e., unsieved whole rock sample): clayey.	105-110	7536.6-7531.6
Qbt 3t, Unit 3t, Tshirege Member of the Bandelier Tuff	Volcanic tuff, moderate yellowish brown (10YR 5/4), crystal rich, strongly welded. +10F: no sample recovery. +35F 85-95% quartz and sanidine crystals; 10-15% welded crystal-tuff fragments. Note: base of Unit 4 and contact with underlying Unit 3t of the Tshirege Member of the Bandelier Tuff is interpreted to be at 120 ft bgs.	110-125	7531.6-7516.6
	Volcanic tuff, light brownish gray (5YR 6/1), moderately to strongly welded. +10F: welded crystal tuff fragments composed of 15-25% quartz and sanidine phenocrysts; 3-7% ferromagnesian phenocrysts (1-2 mm); 3-5% intermediate volcanic lithic fragments (1-2 mm); fragments exhibiting local Fe-oxide staining and white clay lining vugs. +35F: 30-40% free quartz and sanidine crystals; 60-70% welded tuff fragments.	125-140	7516.6-7501.6
	Volcanic tuff, yellowish gray (5Y 8/1), moderately to strongly welded. +10F: welded crystal tuff fragments composed of 30-40% quartz, sanidine, and minor ferromagnesian crystals; 3-5% dacite lithic fragments (up to 1mm), chips locally stained with Fe-oxide. +35F: 20-30% free quartz and sanidine crystals; 70-80% welded tuff fragments.	140-150	7501.6-7491.6
	No cuttings returned; no sample available for examination.	150-155	7491.6-7486.6
	Volcanic tuff, pale yellowish brown (10YR 6/2), moderately to strongly welded. +10F: crystal-rich welded tuff fragments composed of 35-40% quartz, sanidine, and minor oxidized ferromagnesian phenocrysts; 2-3% white lithic fragments in an aphanitic groundmass of welded ash. +35F: 15-20% free quartz and sanidine crystals; 80-85% welded tuff fragments.	155-165	7486.6-7476.6
	Volcanic tuff, medium gray (N5 6/2), strongly welded. +10F: welded crystal tuff fragments composed of 35-40% quartz, sanidine, and minor ferromagnesian phenocrysts in an aphanitic matrix of welded ash. +35F: 15-20% free quartz and sanidine crystals; 80-85% welded tuff fragments.	165-180	7476.6-7461.6
	Volcanic tuff, brownish gray (5YR 4/1), strongly welded. +10F: crystal-rich welded tuff fragments composed of 35-40% quartz, sanidine, and minor oxidized pyroxene(?) phenocrysts in an aphanitic groundmass of welded ash. +35F: 15-20% free quartz and sanidine crystals; 80-85% welded tuff fragments.	180-195	7461.6-7446.6
	Volcanic tuff, light gray (N7) to very light gray (N8), strongly welded. +10F: welded crystal tuff fragments composed of 15-20% quartz, sanidine, and minor oxidized pyroxene(?) phenocrysts in an aphanitic groundmass of welded ash. +35F: 10-15% free quartz and sanidine crystals; 80-90% welded tuff fragments.	195-210	7446.6-7431.6
	Volcanic tuff, medium light gray (N6), strongly welded. +10F: welded crystal tuff fragments composed of 40-50% quartz, sanidine, and minor oxidized ferromagnesian phenocrysts in a siliceous, aphanitic groundmass of welded ash. White fines (clay) coating chip fragments. +35F: 5-10% free quartz and sanidine crystals; 90-95% welded tuff fragments.	210-225	7431.6-7416.6

## Lithologic Descriptions of Core and Drill Cuttings at Borehole R-26 (Continued)

Geologic Unit	Lithologic Description	Sample Interval (ft)	Elevation Range (ft above msl)
	Volcanic tuff, light brownish gray (5YR 6/1) to medium light gray (N6), strongly welded. +10F: welded crystal tuff fragments composed of 15-20% quartz, sanidine, and minor oxidized ferromagnesian phenocrysts and minor lithic fragments in a siliceous aphanitic groundmass of welded ash; local Fe-oxide staining. White fines (clay) coating tuff fragments. +35F: 10-15% free quartz and sanidine crystals; 85-90% welded tuff fragments.	225-230	7416.6-7411.6
	Volcanic tuff, medium light gray (N6), moderately to strongly welded. +10F: welded crystal tuff fragments composed of 20-30% quartz, sanidine, and minor oxidized ferromagnesian (biotite) phenocrysts in an aphanitic groundmass of welded ash; local Fe-oxide staining. +35F: 100% welded crystal tuff fragments.	230-240	7411.6-7401.6
	No cuttings returned; no sample available for examination.	240-245	7401.6-7396.6
	Volcanic tuff, pale yellowish brown (10YR 6/2), moderately welded, weathered appearance. +10F: welded crystal tuff fragments composed of 5-10% quartz, sanidine, and minor oxidized ferromagnesian phenocrysts in a fine-grained groundmass of welded ash; local Fe-oxide staining. +35F: 100% welded crystal tuff fragments.	245-255	7396.6-7386.6
	Volcanic tuff, medium dark gray (N4), moderately to strongly welded. +10F: welded crystal tuff fragments composed of 50-60% quartz, sanidine, and minor oxidized ferromagnesian phenocrysts in an aphanitic groundmass of welded ash. WR sample: very fine yellowish gray (5Y 6/1) ash coating chips.	255-280	7386.6-7361.6
	Volcanic tuff, light gray (N7) to medium light gray (N6), strongly welded. +10F: welded crystal tuff fragments composed of 15-20% quartz, sanidine, and minor ferromagnesian phenocrysts; trace volcanic lithics (up to 1 mm); aphanitic groundmass of welded ash. +35F: 5% free quartz and sanidine crystals; 95% welded tuff fragments.	280-300	7361.6-7341.6
Qbt 3, Unit 3, Tshirege Member of the Bandelier Tuff	Volcanic tuff, medium light gray (N6), moderately to strongly welded. +10F: welded crystal tuff fragments composed of 15-20% quartz, sanidine, and minor ferromagnesian phenocrysts; 2-5% volcanic lithics (1-3 mm); fine-grained groundmass exhibits sugary texture; local Fe-oxide staining. +35F: 30-40% free quartz and sanidine crystals; 60-70% welded tuff fragments.	300-305	7341.6-7336.6
	Insufficient recovery for sample collection and description.	305-315	7336.6-7326.6
	Volcanic tuff, medium gray (N5), crystal-rich, strongly welded. +10F: welded crystal tuff fragments composed of 40-60% quartz, sanidine, and minor ferromagnesian phenocrysts; fine-grained groundmass; local Fe-oxide staining.	315-325	7326.6-7316.6
	Volcanic tuff, medium light gray (N6), strongly welded. +10F: welded crystal tuff fragments composed of 30-35% quartz, sanidine, and minor ferromagnesian (pyroxene?) phenocrysts; 1% aphyric volcanic lithics (2-5 mm); aphanitic groundmass. +35F: 50% free quartz and sanidine crystals; 50% welded tuff fragments. WR sample: 50% pale yellowish brown (10YR 6/2) fines; 50% crystals and tuff fragments.	325-340	7316.6-7301.6
	No cuttings returned; no sample available for examination.	340-345	7301.6-7296.6
	Volcanic tuff, light brownish gray (5YR 6/1), strongly welded. +10F: welded crystal tuff fragments composed of 30-40% quartz, sanidine, and minor ferromagnesian phenocrysts; fine-grained groundmass. +35F: 70-80% free quartz and sanidine crystals; 20-30% welded tuff fragments.	345-360	7296.6-7281.6

## Lithologic Descriptions of Core and Drill Cuttings at Borehole R-26 (Continued)

Geologic Unit	Lithologic Description	Sample Interval (ft)	Elevation Range (ft above msl)
Qbt 2, Unit 2, Tshirege Member of the Bandelier Tuff	Volcanic tuff, medium light gray (N6), strongly welded. +10F: welded crystal tuff fragments composed of 30-40% quartz, sanidine, and minor ferromagnesian phenocrysts; 1-2% volcanic lithics (up to 1 cm); aphanitic groundmass. +35F: 70-80% free quartz and sanidine crystals; 20-30% welded tuff fragments. WR sample: 50% pale light brownish gray fines; 50% welded tuff fragments. Note: base of Unit 3 and contact with underlying Unit 2 of the Tshirege Member of the Bandelier Tuff is interpreted to be at 365 ft bgs.	360-370	7281.6-7271.6
	Volcanic tuff, pale brown (5YR 5/2), moderately welded. +10F: 50% welded crystal tuff fragments composed of quartz, sanidine, and minor ferromagnesian (hornblende?) phenocrysts in aphanitic groundmass of welded ash; 50% dacite lithic fragments with varicolored (yellow, white, green) clay filling vugs; Fe-oxide staining common. +35F: 70-80% free quartz and sanidine crystals; 20-30% welded tuff fragments.	370-375	7271.6-7266.6
	Volcanic tuff, brownish gray (5YR 4/1), strongly welded. +10F: welded crystal tuff fragments composed of 50-60% quartz, sanidine, and minor ferromagnesian phenocrysts and trace felsic volcanic lithics in an aphanitic groundmass. +35F: 30-40% free quartz and sanidine crystals; 60-70% welded tuff fragments. WR sample: 50% pale light brownish gray fines; 50% welded tuff fragments.	375-385	7266.6-7256.6
	No cuttings returned; no sample available for examination.	385-390	7256.6-7251.6
	Volcanic tuff, medium gray (N5), strongly welded. +10F: welded crystal tuff fragments composed of 20-25% quartz, sanidine, and minor ferromagnesian phenocrysts and 1-2% volcanic lithics in an aphanitic groundmass. WR sample: yellowish gray, clayey.	390-410	7251.6-7231.6
	Volcanic tuff, light brownish gray (5YR 6/1), strongly welded. +10F: welded crystal tuff fragments composed of 30-40% quartz, sanidine, and minor ferromagnesian phenocrysts and 1-2% volcanic lithics (up to 2 mm) in an aphanitic groundmass. +35F: 50% free quartz and sanidine crystals; 50% welded tuff fragments. WR sample: 50% light brownish gray fines; 50% welded tuff fragments.	400-410	7231.6-7221.6
	No cuttings returned; no sample available for examination.	410-415	7221.6-7216.6
	Volcanic tuff, mottled coloration light brownish gray (5YR 6/1) to medium gray (N5), strongly welded. +10F: welded crystal tuff fragments composed of 40-50% quartz, sanidine, and minor ferromagnesian phenocrysts and 3-5% volcanic lithics (up to 3 mm) in an aphanitic groundmass. +35F: 50-60% free quartz and sanidine crystals; 40-50% welded tuff fragments.	415-425	7216.6-7206.6
	No cuttings returned; no sample available for examination.	425-430	7206.6-7201.6
	Volcanic tuff, medium gray (N5), strongly welded. +10F: 90% welded crystal tuff fragments made up of quartz, sanidine, and minor ferromagnesian phenocrysts (30-40% volume) and black and dark gray volcanic lithics (5-10% volume, up to 2 mm) in an aphanitic groundmass. Free lithic fragments (10% volume, up to 1.0 cm) composed of various intermediate volcanic rocks (up to 1.0 cm). +35F: 20-30% free quartz and sanidine crystals; 70-80% welded tuff fragments.	430-450	7201.6-7181.6
Qbt 1v	Volcanic tuff, light brownish gray (5YR 6/1), strongly welded. +10F: welded crystal tuff fragments composed of 50-60% quartz, sanidine, and minor ferromagnesian phenocrysts and 20-30% medium gray (N5) volcanic lithics (up to 5 mm) in an aphanitic groundmass of welded ash. +35F: 40-50% free quartz and sanidine crystals; 50-60% welded tuff fragments.	450-465	7181.6-7166.6
	No cuttings returned; interpreted to be Unit 1v	465-470	7166.6-7161.6

## Lithologic Descriptions of Core and Drill Cuttings at Borehole R-26 (Continued)

Geologic Unit	Lithologic Description	Sample Interval (ft)	Elevation Range (ft above msl)
Qct, Cerro Toledo Interval	Volcanic tuff, light brownish gray (5YR 6/1), strongly welded. +10F: welded crystal tuff fragments composed of 50-60% quartz, sanidine, and minor ferromagnesian phenocrysts and 20-30% medium gray (N5) volcanic lithics (up to 5 mm) in an aphanitic groundmass of welded ash. WR sample: light grayish brown (5YR 6/1), 70-75% fines, 25-30% free quartz and sanidine crystals/welded tuff fragments. Note: base of Unit 1v of the Tshirege Member of the Bandelier Tuff and contact with underlying Cerro Toledo interval is interpreted to be at 472 ft bgs. This sample is likely contaminated with tuff fragments of the Bandelier Tuff from above.	470-475	7161.6-7156.6
	Volcanic tuff, light brownish gray (5YR 6/1), strongly welded. +10F: welded crystal tuff fragments composed of 50-60% quartz, sanidine, and minor ferromagnesian phenocrysts and 20-30% medium gray (N5) volcanic lithics (up to 5 mm) in an aphanitic groundmass of welded ash. WR sample: light grayish brown (5YR 6/1) 80-90% fines, 10-15% free quartz and sanidine crystals; 5-10% welded tuff fragments. This sample is likely contaminated with tuff fragments of the Bandelier Tuff from above.	475-485	7156.6-7146.6
	No cuttings returned; no sample available for examination.	485-490	7146.6-7141.6
	Volcaniclastic sediments, grayish orange pink (5YR 7/2), silty sand (SM), very fine to coarse sand, gravel clasts (5-10% volume, up to 6 mm) angular to subrounded, poor sample recovery. +10F: detrital constituents made up of welded tuff fragments and minor white cherts.	490-495	7141.6-7136.6
	Volcaniclastic sediments, grayish orange pink (5YR 7/2), silty sand with gravel (SM), very fine to coarse sand, gravel clasts (10-15% volume, up to 1.0 cm) subangular, poor sample recovery. +10F: detrital constituents composed of 5-10% welded tuff fragments, 10-15% white porphyritic rhyolite, 80-85% dacite, trace black vitrophyre.	495-500	7136.6-7131.6
	Insufficient sample recovery. Sample appears similar to that of interval 495-500 ft.	500-510	7131.6-7121.6
	No cuttings returned; no sample available for examination.	510-515	7121.6-7116.6
	Volcaniclastic sediments, very pale orange (10YR 8/2), gravelly silt (ML), very fine to medium sand, gravel clasts (15-20% volume, up to 1.0 cm) subangular to subrounded, commonly broken. +10F: detrital constituents composed of 75-85% porphyritic dacite, 10-15% vitrophyre of intermediate volcanic composition, 5-10% porphyritic rhyolite.	515-520	7116.6-7111.6
	No cuttings returned; no sample available for examination.	520-530	7111.6-7101.6
	Volcaniclastic sediments, medium light gray (N6) to yellowish gray (5Y 8/1), poorly graded gravel with silt and sand (GP-GM), fine to coarse sand, gravel clasts (0.5-5 cm) subangular to subrounded, commonly broken. +10F: detrital constituents composed of 40-50% hornblende-dacite, 40-50% other aphanitic rocks of intermediate volcanic composition, trace white vitric pumice, trace black vitrophyre (obsidian); clasts commonly stained with Fe-oxides.	530-545	7101.6-7086.6
	Volcaniclastic sediments, grayish orange (10YR 7/4), silty sand with gravel (SM), very fine to coarse sand, gravel clasts (up to 1.0 cm) angular to subrounded. +10F: varied detrital constituents composed mostly of porphyritic dacite and rhyolite; 1-2% obsidian, 1-2% flow-banded rhyolite; 8-15% gray and red-brown vitrophyre.	545-560	7086.6-7071.6
	Volcaniclastic sediments, grayish orange (10YR 7/4), silty sand (SM), very fine to coarse sand, gravel clasts (up to 1.0 cm) broken to subrounded. +10F: varied detrital constituents composed of hornblende-dacite, andesite, and black vitrophyre.	560-565	7071.6-7066.6
	No cuttings returned; no sample available for examination.	565-570	7066.6-7061.6

## Lithologic Descriptions of Core and Drill Cuttings at Borehole R-26 (Continued)

Geologic Unit	Lithologic Description	Sample Interval (ft)	Elevation Range (ft above msl)
	Volcaniclastic sediments, very pale orange (10YR 8/2), poorly graded sand with gravel (SP), predominantly medium sand, gravel clasts (up to 8 mm) subangular to subrounded. +10F: detrital constituents composed of 50% white to pale orange pumices, partly vitric; 50% volcanic lithic clasts including dacite and gray aphanitic varieties of intermediate composition.	570-580	7061.6-7051.6
	Volcaniclastic sediments, very pale orange (10YR 8/2), silt with sand (ML), fine to coarse sand (15-20% volume) grains subangular to subrounded. +10F: coarse sand (less than 5 mm) made up of varied dacite, andesite, and quartz crystals. +35F: 60-70% quartz and sanidine crystals, 30-40% varied volcanic lithics, trace pumice.	580-595	7051.6-7036.6
	Volcaniclastic sediments, very pale orange (10YR 8/2), silty sand (SM). WR: fine to coarse sand composed of quartz and sanidine crystals plus volcanic lithic fragments.	595-600	7036.6-7031.6
	Volcaniclastic sediments, grayish orange (10YR 7/4), well-graded sand (SW) with silt, fine to very coarse sand grains subangular to rounded. +10F: very coarse sand composed of quartz and sanidine crystals and volcanic lithics (dacite, other intermediate volcanic rocks, welded tuff, vitrophyre).	600-615	7031.6-7016.6
	Volcaniclastic sediments, grayish orange (10YR 7/4), well-graded sand (SW) with gravel, fine to very coarse sand, gravel clasts (up to 1 cm) angular to subangular. +10F: detrital clasts dominantly dacite, lesser amounts of andesite, medium gray vitrophyre, and welded tuff; Fe-oxide staining of clasts common.	615-625	7016.6-7006.6
	Volcaniclastic sediments, very pale orange (10YR 8/2) to pale yellowish brown (10YR 6/2), well-graded sand (SW) with gravel, fine to very coarse sand, gravel clasts up to 2 cm. +10F: detrital clasts composed of varied volcanic constituents including indurated ash flow tuff, andesite, dacite, and vitrophyre.	625-645	7006.6-6986.6
	Volcaniclastic sediments, grayish orange (10YR 7/42), silty sand (SM) with gravel, fine to coarse sand, gravel clasts (up to 1.5 cm) are angular and broken. +10F: detrital clasts composed mainly of hornblende dacite with lesser amounts of porphyritic rhyolite, vitrophyre, and welded tuff.	645-655	6986.6-6976.6
	No cuttings returned; no sample available for examination.	655-660	6976.6-6971.6
	Volcaniclastic sediments, very pale orange (10YR 8/2) to pale yellowish brown (10YR 6/2), well-graded sand (SW) with gravel, very fine to very coarse sand, gravel clasts angular to rounded (up to 5 cm). +10F: detrital clasts composed of 80-85% vitric pumice and indurated ash-flow tuff fragments; 5-10% indurated sandstone clasts; and 5% volcanic rocks of intermediate composition.	660-680	6971.6-6951.6
	Volcaniclastic sediments, medium dark gray (N4) to medium light gray (N6), well-graded sand (SW), very fine to very coarse sand, gravel clasts (3-5% volume) generally broken (up to 1.0 cm). +10F: clasts composed of 80-90% hornblende-dacite, 3-5% andesite, 5-7% vitrophyre and trace white pumice; weak local Fe-oxide staining.	680-690	6951.6-6941.6
	Volcaniclastic sediments, pale yellowish brown (10YR 6/2) to grayish orange pink (5YR 7/2), well-graded sand (SW), very fine to coarse sand, gravel clasts (5-10% volume) angular to subangular. +10F: detrital clasts composed of 20-25% hornblende-dacite, 20-25% andesite, 30-40% brown vitreous pumice, 15-20% indurated ash-flow tuff fragments, 5-10% vitrophyre.	690-700	6941.6-6931.6
	Volcaniclastic sediments, varicolored grayish orange pink (5YR 7/2) to light brown (5YR 6/4), well graded sand (SW), very fine to coarse sand, gravel clasts (5-10% volume, up to 1 cm) angular to subangular. +10F: detrital pebbles composed of 20-25% hornblende-dacite, 20-25% andesite, 30-40% brown vitreous pumice, 15-20% indurated ash-flow tuff fragments, 5-10% vitrophyre.	700-710	6931.6-6921.6

## Lithologic Descriptions of Core and Drill Cuttings at Borehole R-26 (Continued)

Geologic Unit	Lithologic Description	Sample Interval (ft)	Elevation Range (ft above msl)
	Volcaniclastic sediments, grayish orange pink (5YR 7/2), silt (ML). +10F: detrital pebbles (up to 1.2 cm) composed of 80-85% vitric pumice that is Fe-oxide +/- Mn-oxide stained and 15-20% varied volcanic lithics (i.e., hornblende-biotite-dacite, pumice, trace vitrophyre).	710-715	6921.6-6916.6
	Volcaniclastic sediments, light brown (5YR 6/4), silt (ML). +10F: subrounded to rounded pebbles (up to 1.0 cm) composed of 100% vitric pumice that is Fe-oxide +/- Mn-oxide stained.	715-720	6916.6-6911.6
	Volcaniclastic sediments, varicolored grayish orange pink (5YR 7/2) to medium gray (N5), fine to coarse sand (SW), gravel clasts (5-10% volume, up to 1.0 cm) generally broken. +10F: 80% varied volcanic lithics (i.e., hornblende-biotite-dacite, rhyolite, andesite, minor vitrophyre), 20% orange-colored vitric pumice. Note: percent detrital pumices increasing to 50-70% in lower 15 ft of the interval.	720-740	6911.6-6891.6
	Volcaniclastic sediments, grayish orange pink (5YR 8/4), silty sand (SM), predominantly fine sand. +10F: detrital clasts composed of 50-75% vitric pumice that is Fe-oxide +/- Mn-oxide stained and 25-50% varied volcanic lithics including rhyolite, hornblende-biotite-dacite, and vitrophyre.	740-755	6891.6-6876.6
	Volcaniclastic sediments, varicolored grayish orange pink (5YR 7/2) to medium gray (N5), clayey sand (SC), predominantly very coarse sand, gravel clasts (5% volume, 0.2-0.7 cm) are generally broken. +10F: detrital clasts composed of 60-70% orange pumice and 25-40% varied volcanic lithics including dark brown vitrophyre, rhyolite, and dacite. Note: increase in lithic content to 50% and increase in vitrophyre abundance at 760 ft.	755-765	6876.6-6866.6
	Volcaniclastic sediments, varicolored grayish orange pink (5YR 7/2) to medium gray (N5), clayey sand (SC), fine to medium sand, gravel clasts (5-10% volume, 0.2-1.1 cm) are generally broken. +10F: detrital clasts composed of 50-80% pumice and 20-50% varied volcanic lithics including dark brown vitrophyre, rhyolite, and dacite; local Mn-oxide staining on pumice clasts.	765-785	6866.6-6846.6
	Volcaniclastic sediments, grayish orange pink (5YR 8/4), silty sand (SM), predominantly fine sand. +10F: detrital clasts composed of 50-75% vitric pumice that is Fe-oxide +/- Mn-oxide stained and 25-50% varied volcanic lithics including rhyolite, hornblende-biotite-dacite, and vitrophyre.	785-800	6846.6-6831.6
	Volcaniclastic sediments, medium light gray (N6), sand (SW) with gravel, abundant broken gravel clasts (30-40% volume, 0.3-1.5 cm) exhibiting subrounded fresh surfaces. +10F: detrital clasts composed of varied volcanic lithics including rhyolite, andesite, hornblende-dacite, and vitrophyre.	800-815	6831.6-6816.6
	Volcaniclastic sediments, varicolored to light gray (N7), gravel (GW) with sand, medium to coarse sand, abundant broken gravel clasts (70% volume, 0.5-2.0 cm). +10F: detrital clasts composed of varied volcanic lithics including rhyolite, andesite, hornblende-biotite-dacite, vesicular basalt, and vitrophyre; local Fe-oxide staining of clasts.	815-825	6816.6-6806.6
	Volcaniclastic sediments, medium light gray (N6), sand with gravel (SW), fine to coarse sand, broken to subrounded gravel clasts (8% volume, 0.5-2.0 cm). +10F: detrital clasts composed of varied volcanic lithics including rhyolite, andesite, hornblende-biotite-dacite, vesicular basalt, and vitrophyre; local Fe-oxide staining of clasts.	825-840	6806.6-6791.6
	Volcaniclastic sediments, varicolored to medium light gray (N6), sand (SW) with gravel, fine to coarse sand, broken to subrounded gravel clasts (15% volume, 0.3-1.0 cm). +10F: detrital clasts composed of varied volcanic lithics including rhyolite, rhyodacite and vitrophyre with lesser pumice, andesite, and dacite; strong Fe-oxide staining of clasts.	840-845	6791.6-6786.6

## Lithologic Descriptions of Core and Drill Cuttings at Borehole R-26 (Continued)

Geologic Unit	Lithologic Description	Sample Interval (ft)	Elevation Range (ft above msl)
	Volcaniclastic sediments, varicolored medium light gray (N6) to grayish orange pink (5YR 7/2), sand with clay and gravel (SP-SC), fine to coarse sand, broken to subrounded gravel clasts (8% volume, 0.3-1.3 cm). +10F: detrital clasts composed of orange sugary pumice (35-40% volume) and vitrophyre; other volcanic lithics (60-65% volume) include rhyolite, andesite, and hornblende-biotite-dacite; local Fe-oxide and Mn-oxide staining of pumices.	845-850	6786.6-6781.6
	Volcaniclastic sediments, varicolored grayish orange pink (5YR 7/2) to medium light gray (N6), clayey (SC), very fine to coarse sand, broken to subrounded gravel clasts (15% volume, 0.3-0.8 cm). +10F: detrital clasts composed of 60% pumice and 40% volcanic lithics including porphyritic andesite, hornblende-biotite-dacite, and vitrophyre; local Fe-oxide staining of pumice clasts.	850-860	6781.6-6771.6
	No cuttings returned; no sample available for examination.	860-865	6771.6-6766.6
Qbo, Otow Member of the Bandelier Tuff	Volcanic tuff, grayish orange pink (5YR 7/2) to light gray (N6), poorly welded. +10F: composed of 50% orange vitric pumice, 50% lithic fragments (up to 1.5 cm) including dacite, andesite and lesser vitrophyre. +35F: 15-20% pumice fragments, 70-75% quartz and sanidine crystals, and 10-15% lithics.	865-870	6766.6-6761.6
	Volcanic tuff, grayish orange pink (5YR 7/2) to light gray (N6), poorly welded. +10F: composed of 50-80% white pumice, 20-50% lithic fragments including vitrophyre, biotite-dacite, and andesitic vitrophyre. +35F: 10-15% pumice fragments, 70-75% quartz and sanidine crystals, and 10-15% lithics.	870-900	6761.6-6731.6
	No cuttings returned; no sample available for examination.	900-905	6731.6-6726.6
	Volcanic tuff, very light gray (N8) to medium dark gray (N4), poorly welded, lithic-rich. +10F: composed mostly of lithic fragments including andesite, vitrophyre, rhyolite, porphyritic dacite and minor pumice. +35F: 10-15% pumice fragments, 60-65% quartz and sanidine crystals, and 20-25% lithics.	905-910	6726.6-6721.6
	Volcanic tuff, very light gray (N8), poorly welded. +10F: very little sample return. +35F: 2-5% pumice fragments, 70-75% quartz and sanidine crystals, and 25-30% lithics.	910-920	6721.6-6711.6
	Volcanic tuff, very light gray (N8) to grayish orange pink (5YR 7/2), poorly welded, broken fragments up to 0.7 cm. +10F: very little sample return. +35F: 40% pumice fragments, 30% quartz and sanidine crystals, and 30% lithics.	920-930	6711.6-6701.6
	Volcanic tuff, pinkish gray (5YR 8/1), poorly welded to nonwelded, broken fragments up to 2.2 cm. WR sample: has texture of clayey sand. +10F: very little sample returns. +35F: 50-60% pumice fragments, 25-30% quartz and sanidine crystals, and 10-15% volcanic lithics.	930-935	6701.6-6696.6
Qbog, Guaje Pumice Bed	Volcanic tuff, pinkish gray (5YR 8/1) to grayish red (10R 4/2), nonwelded, lithic-rich. +10F: contains variety of lithic fragments (0.3-0.6 cm) including altered andesite, white vitric and Fe-oxide-stained pumice, and hornblende-biotite-dacite. +35F: 40-45% pumice fragments, 40-45% quartz and sanidine crystals, and 10% volcanic lithics.	935-940	6696.6-6691.6
	Volcanic tuff, pinkish gray (5YR 8/1) to grayish red (10R 4/2), nonwelded, lithic-rich. +10F: contains variety of lithic fragments (0.3-0.6 cm) including altered andesite, white vitric and Fe-oxide-stained pumice, and hornblende-biotite-dacite. +35F: 40-45% pumice fragments, 40-45% quartz and sanidine crystals, and 10-50% volcanic lithics.	940-945	6691.6-6686.6
	Volcanic tuff, very light gray (N8), nonwelded, pumice-rich. +10F: very little sample returns +35F: mostly pumice fragments, 35% quartz and sanidine crystals, minor lithic fragments. Increase in lithic fragments noted in interval 110-115 ft.	945-950	6686.6-6681.6

## Lithologic Descriptions of Core and Drill Cuttings at Borehole R-26 (Continued)

Geologic Unit	Lithologic Description	Sample Interval (ft)	Elevation Range (ft above msl)
Tpf, Puye Fanglomerate	Volcanic tuff, very light gray (N8) to white (N9), pumice-rich, lithic-rich, moderately welded, vitric. +10F: 70-75% white vitric pumice fragments, 25-30% lithic (vitrophyre, dacite, andesite, rhyolite) fragments. +35F: 60-65% vitric pumice fragments, 25-30% quartz and sanidine crystals, 5-10% lithic fragments. Probable Guaje Pumice Bed contamination from above. <b>Note: base of Guaje Pumice Bed and contact with underlying Puye Formation is interpreted to be at 955 ft bgs.</b>	950-960	6681.6-6671.6
	Volcaniclastic sediments, light brownish gray (5YR 6/1), sand with silt and clay (SP-SM). +10F: no sample returns. +35F: 25-30% pumice, 30-35% quartz and sanidine crystals, 40-45% volcanic lithic fragments.	960-965	6671.6-6666.6
	Volcaniclastic sediments, light brownish gray (5YR 6/1), sand with silt and clay (SP-SM), very fine to coarse sand, gravel clasts up to 1.8 cm. +10F: very little sample returns. +35F: 65% lithic fragments including porphyritic dacite, andesite, rhyodacite and vitrophyre. <b>Note: reddish brown clay at 975 ft bgs.</b>	965-980	6666.6-6651.6
	Volcaniclastic sediments, light brownish gray (5YR 6/1), sand with silt and clay (SP-SM). +10F: no sample return. +35F: 80% hornblende-biotite-plagioclase dacite, 20% other volcanic lithics (andesite, vitrophyre, rhyodacite, minor pumice).	980-985	6651.6-6646.6
	Volcaniclastic sediments, varicolored to pale yellowish brownish (10YR 6/2), poorly graded sand with silt and gravel (SP-SM), subrounded to broken clasts up to 0.7 cm. +10F: varied volcanic lithics including vitrophyre, dacite, andesite, trace rhyodacite, and poorly welded ash flow tuff.	985-990	6646.6-6641.6
	Volcaniclastic sediments, varicolored to pale yellowish brownish (10YR 6/2), poorly graded sand with silt and gravel (SP-SM), subrounded to broken clasts up to 0.7 cm. +10F: mainly dacite with lesser amounts of vitrophyre, andesite, trace rhyodacite, and poorly welded ash flow tuff.	990-1000	6641.6-6631.6
	No cuttings returned; no sample available for examination.	1000-1005	6631.6-6626.6
	Volcaniclastic sediments, varicolored to pale yellowish brownish (10YR 6/2), poorly graded sand (SP), coarse sand grains subangular to subrounded. +10F: grains (up to 5 mm) dacite, rhyodacite, and andesite. +35F: 80-85% dacite and rhyodacite, 15-20% quartz and sanidine crystals.	1005-1025	6626.6-6606.6
	Volcaniclastic sediments, moderate yellowish brown (10YR 4/2), silty, clayey sand (SC-SM), angular grains up to 5 mm. +10F: grains dominantly composed of dacite with other volcanics of intermediate composition. +35F: grains similar in composition to that of +10F.	1025-1040	6606.6-6591.6
	Volcaniclastic sediments, moderate reddish brown (10YR 4/6), silty, clayey sand (SC-SM), angular grains up to 5 mm. +10F: grains dominantly composed of hornblende-biotite-dacite with other volcanics of intermediate composition. +35F: grains similar in composition to that of +10F sample.	1040-1050	6591.6-6581.6
	Volcaniclastic sediments, pale yellowish brown (10YR 6/2), well graded sand (SW) with clay, angular to subrounded grains up to 5 mm. +10F: grains dominantly composed of hornblende-dacite and porphyritic rhyolite, Fe-oxide staining common. +35F: grains similar in composition to that of +10F sample.	1050-1055	6581.6-6576.6
	Volcaniclastic sediments, pale yellowish brown (10YR 6/2), well graded sand (SW) with clay, angular to subrounded grains up to 5 mm. +10F: grains composed of dacite, andesite, vitrophyre, trace white chert. +35F: grains similar in composition to that of +10F sample.	1055-1075	6576.6-6556.6
	Volcaniclastic sediments, light brownish gray (5YR 6/1), poorly graded sand with silt (SP-SM), very fine to fine sand, angular to subrounded grains up to 5 mm. +10F: grains composed of andesite, dacite, vitrophyre; 2-5% Fe-oxide staining. +35F: grains similar in composition to that of +10F sample.	1075-1090	6556.6-6541.6

## Lithologic Descriptions of Core and Drill Cuttings at Borehole R-26 (Continued)

Geologic Unit	Lithologic Description	Sample Interval (ft)	Elevation Range (ft above msl)
	Volcaniclastic sediments, light brownish gray (5YR 6/1), poorly graded sand with silt (SP-SM), very fine to fine sand, angular to subrounded grains up to 5 mm. +10F: (very little sample returns) grains composed of andesite, dacite, vitrophyre; 2-5% Fe-oxide staining. +35F: grains of similar in composition to that of +10F sample, minor pale yellow orange chert fragments.	1090-1105	6541.6-6526.6
	Volcaniclastic sediments, pale yellowish brown (10YR 6/2), poorly graded sand with silt (SP-SM), very fine to fine sand, grains angular to subrounded. +10F: grains composed of andesite, dacite, and orange-pink clay-altered pumice and/or indurated tuff.	1105-1115	6526.6-6516.6
	Volcaniclastic sediments, pale yellowish brown (10YR 6/2), poorly graded sand with silt (SP-SM), very fine to fine sand, grains angular to subrounded. +10F: grains composed of andesite and dacite with significantly increased abundance (60-70% volume) of orange-pink clay-altered biotite-bearing tuff; minor well-indurated sandstone clasts. Note: poor sample returns for +10F in the interval 1120-1125 ft bgs.	1115-1125	6516.6-6506.6
	Volcaniclastic sediments, pale yellowish brown (10YR 6/2), poorly graded sand (SP), very fine to fine sand, grains angular to subangular. +10F: (poor sample returns) grains composed of dacite, other intermediate volcanic rocks, with tuff fragments. +35F: similar in composition to that of +10F sample.	1125-1145	6506.6-6486.6
	Volcaniclastic sediments, pale brown (5YR 5/2), poorly graded sand with silt (SP-SM), very fine to fine sand, grains angular to subrounded. +10F: grains composed of varied volcanic constituents including dacite, andesite, vitrophyre, porphyritic rhyolite, and white biotite-bearing tuff. Note: poor sample returns for +10F at 1150 to 1165 ft bgs.	1145-1165	6486.6-6466.6
	Volcaniclastic sediments, pale yellowish brown (10YR 6/2), poorly graded sand (SP), fine sand grains angular to subangular. +10F: grains composed of dacite, porphyritic rhyolite, orange and white tuff fragments, and indurated sandstone. +35F: similar composition to +10F sample.	1165-1180	6466.6-6451.6
	Volcaniclastic sediments, pale yellowish brown (10YR 6/2), poorly graded sand with silt (SP-SM), fine sand grains angular to subangular. +10F: no sample returns. +35F: grains composed of intermediate volcanics and vitrophyre.	1180-1195	6451.6-6436.6
	Volcaniclastic sediments, light brownish gray (5YR 6/1), poorly graded sand (SP), very fine to fine sand grains mostly angular. +10F: grains composed of hornblende-dacite and trace porphyritic rhyolite. +35F: angular intermediate volcanic grains.	1195-1200	6436.6-6431.6
	Volcaniclastic sediments, grayish orange pink (5YR 7/2), poorly graded sand (SP), fine sand grains angular to subangular. +10F: (poor sample returns) grains composed of intermediate volcanic rocks, obsidian, quartz, altered tuff. Note: sample lacking in obsidian in the interval 1205-1210 ft bgs.	1200-1210	6431.6-6421.6
	Volcaniclastic sediments, grayish orange pink (5YR 7/2), poorly graded sand with silt (SP-SM), very fine to fine sand grains mostly angular. +10F: (poor sample returns) grains composed of intermediate volcanic rocks. +35F: similar in composition to that of +10F sample.	1210-1225	6421.6-6406.6
	Volcaniclastic sediments, pale yellowish brown (10YR 6/2), poorly graded sand (SP) to sand with silt (SP-SM), very fine to fine sand grains mostly angular. +10F: very little sample returns. +35F: grains composed of intermediate volcanic rocks.	1225-1255	6406.6-6376.6
	Volcaniclastic sediments, pale yellowish brown (5YR 6/1), poorly graded sand (SP) to sand with silt (SP-SM), very fine to fine sand grains angular to subangular (up to 5 mm). +10F: grains composed predominantly of intermediate volcanic composition. +35F: grains composed of dacite and intermediate volcanic rocks, trace quartz. Note: poor sample returns for +10F at 1260 to 1280 ft bgs.	1255-1285	6376.6-6346.6

## Lithologic Descriptions of Core and Drill Cuttings at Borehole R-26 (Continued)

Geologic Unit	Lithologic Description	Sample Interval (ft)	Elevation Range (ft above msl)
	Volcaniclastic sediments, brownish gray (5YR 4/1) to pale brown (5YR 5/2), poorly graded sand (SP), fine to medium sand grains angular to subangular. +10F: no sample returns. +35F: grains of intermediate and felsic volcanic composition, minor abundances of quartz and vitrophyre.	1285-1305	6346.6-6326.6
	Volcaniclastic sediments, pale brown (5YR 5/2) to pale yellowish brown (10YR 6/2), poorly graded sand (SP), very fine to fine sand, grains angular to subangular. +10F: no sample returns. +35F: grains of intermediate and felsic volcanic composition.	1305-1330	6326.6-6301.6
	Volcaniclastic sediments, pale brown (5YR 5/2) to pale yellowish brown (10YR 6/2), poorly graded sand (SP), fine to medium sand, grains angular to subangular. +10F: poor sample returns. +35F: light-colored grains of intermediate and felsic volcanic composition.	1330-1360	6301.6-6271.6
	Volcaniclastic sediments, pale yellowish brown (10YR 6/2), poorly graded sand with silt (SP-SM), very fine to fine sand, grains angular to subangular. +10F: very poor sample returns. +35F: light-colored grains of intermediate and felsic volcanic composition.	1360-1380	6271.6-6251.6
	Volcaniclastic sediments, pale yellowish brown (10YR 6/2), poorly graded sand (SP), very fine to fine sand, grains angular to subangular. +10F: very poor sample returns; reddish brown clay noted at 1395 to 1400 ft bgs. +35F: light-colored grains of intermediate and felsic volcanic composition.	1380-1400	6251.6-6231.6
	Volcaniclastic sediments, light brownish gray (5YR 6/1), poorly graded sand (SP), fine to medium sand, grains angular to subangular (up to 3 mm). +10F: (poor sample returns) grains composed of intermediate volcanic rocks; trace reddish brown clay. +35F: grains of intermediate and felsic volcanic composition, vitrophyre, altered volcanic tuff.	1400-1405	6231.6-6226.6
	Volcaniclastic sediments, light brownish gray (5YR 6/1), poorly graded sand (SP), very fine to fine sand, grains angular to subangular. +10F: poor sample returns. +35F: grains of intermediate and felsic volcanic composition, vitrophyre, altered volcanic tuff.	1405-1420	6226.6-6221.6
	Volcaniclastic sediments, light brownish gray (5YR 6/1), poorly graded sand with silt (SP-SM), very fine to fine sand, grains angular to subangular. +10F: poor sample returns. +35F: grains predominantly of intermediate and felsic volcanic composition.	1420-1430	6221.6-6211.6
	No cuttings returned; no sample available for examination.	1430-1440	6211.6-6201.6
	Volcaniclastic sediments, grayish orange pink (5YR 7/2), poorly graded sand with silt (SP-SM), very fine to fine sand, grains angular to subangular. +10F: grains composed of intermediate volcanic composition and minor gray-orange indurated sandstone. +35F: grains of similar in composition to that of +10F: sample with trace vitrophyre.	1440-1445	6201.6-6196.6
	Volcaniclastic sediments, light brownish gray (5YR 6/1), well graded sand (SW), very fine to medium sand, grains angular to subrounded (up to 3 mm). +10F: grains composed of light gray and orange-pink hornblende-dacite intermediate volcanic composition and minor gray-orange indurated sandstone. +35F: grains of similar in composition to that of +10F: sample.	1445-1455	6196.6-6186.6
	Volcaniclastic sediments, light brownish gray (5YR 6/1), poorly graded sand (SP), very fine to fine sand, grains angular to subangular. +10F: grains composed of light gray and orange-pink hornblende-dacite intermediate volcanic composition. +35F: grains of dacite, other intermediate volcanics, vitrophyre, and indurated tuff.	1455-1460	6186.6-6181.6
	Volcaniclastic sediments, light gray (N8), poorly graded sand (SP), very fine to medium sand, grains angular to subangular. +10F: grains composed of dacite and other intermediate volcanic composition. +35F: grains of hornblende-biotite-dacite, other intermediate volcanics, vitrophyre, and indurated tuff.	1460-1490.5	6181.6-6151.1
	TOTAL BOREHOLE DEPTH (TD) IS AT 1,490.5 FT BGS.		

## Lithologic Descriptions of Core and Drill Cuttings at Borehole R-26 (Continued)

Geologic Unit		Lithologic Description		Sample Interval (ft)	Elevation Range (ft above msl)
GW	Well-graded gravel	GP-GM	Poorly graded gravel with silt to silty gravel, transitional		
GP	Poorly graded gravel	SP-SC	Poorly graded sand with clay to clayey sand, transitional		
GM	Silty gravel	SP-SM	Poorly graded sand with silt to silty sand, transitional		
SW	Well-graded sand	SC-SM	Clayey sand to silty sand, transitional		
SP	Poorly graded sand				
SM	Silty sand				
SC	Clayey sand				

## REFERENCE

ASTM D 2488-90. Standard Practice and Identification of Soils (Visual-Manual Procedure)

Note: The term "per cent" (%), as used in the above descriptions, refers to relative abundance by volume for a given sample component.

Note: Contact locations are based on cuttings retrieval. There is general agreement between this borehole log and the geophysics report.

Note: Grain size descriptions are based on analysis of the cuttings. FMI logs indicate that a much larger grain size is present throughout much of the Puye Formation.

## **Appendix E**

---

### *Aquifer Testing Report and Aquifer Test Data*

# R-26 PUMPING TEST ANALYSIS

## INTRODUCTION

This section describes the analysis of constant-rate pumping tests and shut-in tests conducted on R-26. The primary objective of the analysis was to determine the hydraulic properties of the sediments screened in R-26.

R-26 is completed with two screens, one installed from 651.8 to 669.9 ft bgs (Screen 1) and one from 1421.8 to 1445 ft bgs (Screen 2). Prior to testing, a snug fitting packer had been installed beneath Screen 1 to hydraulically separate the shallow and deep screen zones. The packer was not an inflatable packer, but rather was constructed with a solid neoprene ring bonded to a steel coupling. It was not designed for high-pressure applications and, therefore, provided only partial resistance to movement of water between the screen zones.

With the packer in place, the static water level measured in Screen 1 was approximately 607 ft bgs. When the packer was removed to allow a camera survey of the well, the resulting *composite* water level revealed by the down-hole camera was also 607 ft bgs. The lack of a discernable water level change suggested that the deep zone was exceedingly tight compared to the upper zone and, thus, the upper zone dominated the hydraulics of the combined system. The testing program for R-26 was designed around this assumption.

Three tests were conducted on R-26, one test on Screen 1 and two tests on Screen 2. Screen 1 was tested using conventional constant-rate pumping and recovery procedures. During this testing, the well was open to both zones, because it was believed that the deep zone would have negligible effect on the hydraulic response (subsequently confirmed). Screen 2 was tested initially by shutting it in and pumping it briefly. The information from this preliminary test was used to design a long-term isolation test.

Testing of Screen 1 (both zones open) began on February 16, 2004. The test consisted of two trial pumping periods, a day and a half shut down for background monitoring, 24 hours of pumping and 24 hours of recovery. An inflatable packer was set above Screen 1 to eliminate casing storage effects during the tests. The packer was installed at approximately 635 ft bgs. The pump was positioned well below the packer, with the bottom of the pump shroud at approximately 780 ft bgs. This design was incorporated in anticipation of preliminary testing of Screen 2, which was planned to immediately follow the Screen 1 test.

Two trial tests were conducted in Screen 1 on February 16. Trial 1 was conducted at a rate of 16 gpm for 72 minutes from 3:52 pm to 5:04 pm, and was followed by 28 minutes of recovery. Trial 2 was conducted at a rate of 16 gpm for 31 minutes from 5:32 pm to 6:03 pm. Following this test, recovery was monitored for more than a day and a half from 6:02 pm on February 16 until 8:36 am on February 18. This data set served as recovery for the trial 2 test and as background data.

The 24-hour test on Screen 1 was begun at a rate of 15.7 gpm at 8:36 am on February 18. By mid-afternoon, it was observed that the pumping rate was declining steadily (to less than 15 gpm) and that the gauge pressure in the discharge line was also declining. The only explanation for these simultaneous observations was that the drawdown in the well was increasing

substantially – possibly to a level well below the bottom of the screen. (Note that it was not possible to monitor the pumping water level during the test when using the inflatable packer and isolated down-hole MiniTROLL pressure transducer, so it was necessary to infer what was occurring from the available indirect evidence.) Based on the observed reductions in pumping rate and discharge line pressure, it was concluded that the well screen had become dewatered and that the drawdown would continue to increase, unchecked, until the pump cavitated.

Therefore, the pump was shut off at 6:01 pm for 61 minutes and restarted at 7:02 pm at a reduced rate of 7 gpm. During the temporary shut down, the packer was deflated and re-inflated to release any air that may have entered the well through the well screen. Pumping continued until 8:50 am on February 19. By the end of the pumping period, the discharge rate had declined to 6.8 gpm. Following pump shutdown, recovery measurements were made for 1465 minutes until 9:15 am on February 20.

The 24-hour Screen 1 pumping test procedures are summarized as follows:

1. Pumped at 15.7 gpm (eventually declining to 14.8 gpm) for 565 minutes from 8:36 am to 6:01 pm on February 18.
2. Shut down for 61 minutes from 6:01 pm to 7:02 pm.
3. Pumped at 7.0 gpm (declining to 6.8 gpm) for 828 minutes from 7:02 pm February 18 to 8:50 am February 19.
4. Monitored recovery from 8:50 am February 19 to 9:15 am February 20.

The Screen 2 testing occurred in two phases – a preliminary shut-in and brief pumping event, and long-term isolation and monitoring. The preliminary test was run on February 20 and was accomplished with the pump and packer string used to test Screen 1. To test Screen 2, the pump/packer string was lowered 105 feet, placing the packer and the bottom of the pump shroud at approximately 740 feet and 885 ft bgs, respectively. Testing consisted of setting the packer, monitoring shut-in head for 52 minutes, pumping for 15 minutes, shutting down and monitoring for an additional 53 minutes.

The packer was inflated at 11:22 am. After 52 minutes, the pump was started at 12:14 pm. It was expected that Screen 2 would produce little flow and that most of the pumped water would come from casing storage between the inflatable packer and the top of the pump – an available water volume of about 78 gallons. After 15 minutes of pumping, cavitation occurred and the pump was shut down at 12:29 pm. Monitoring continued for another 53 minutes until 1:22 pm, when the packer was deflated. A total water volume of 58 gallons was removed from the well during pumping – 18 gallons less than the volume drained from casing storage. It is probable that antecedent drainage of a portion of the drop pipe had emptied about 18 gallons of volume, and the pump had to refill the drained volume before discharge reached the surface. Consistent with this, when the pump was started, only air was produced at the surface for the first couple of minutes of operation.

Results of the preliminary test were used to guide the choice of final testing procedures for Screen 2. The preliminary test confirmed that the deep zone yield was exceedingly low and that the zone would not support continuous pumping. It also showed that the deep zone static water level was significantly below that of the upper screened zone. Based on this information, the

decision was made to simply isolate Screen 2 using the inflatable packer and monitor the decay response of the water levels following packer inflation.

The submersible pump used to test Screens 1 and 2 was removed and an inflatable packer was re-run into R-26 to a depth of about 713 feet, with a 1 7/8-inch OD tailpipe (stinger pipe) extending to around 720 feet. The packer was inflated at 2:20 pm on February 22. Water levels were monitored until 8:00 am on March 6, providing a data record of 12.7 days duration.

## BACKGROUND DATA

The background water level data collected in conjunction with running the pumping test allow the analyst to see what water level fluctuations occur naturally in the aquifer and help distinguish between water level changes caused by conducting the pumping test and changes associated with other causes.

Background water level fluctuations have several causes, among them barometric pressure changes, operation of other wells in the aquifer, earth tides, and long-term trends related to weather patterns. The background data hydrograph from the R-26 tests was compared to barometric pressure data from the area to determine if a correlation existed.

Previous pumping tests have demonstrated a barometric efficiency for most wells of between 90 and 100 percent. Barometric efficiency is defined as the ratio of water level change to barometric pressure change, expressed as a percentage. In the early pumping tests conducted as part of this project, down hole pressure was monitored using a *vented* transducer. This equipment measures the *difference* between the total absolute pressure applied to the transducer and the barometric pressure, this difference being the true height of water above the transducer.

Later pumping tests in the project, including the R-26 pumping test, utilized a *non-vented* transducer for the background monitoring. This device simply records the total absolute pressure on the transducer, that is, the sum of the water height plus the barometric pressure. This results in an attenuated "apparent" hydrograph in a barometrically efficient well. Take as an example a 90 percent barometrically efficient well. When monitored using a vented transducer, an *increase* in barometric pressure of 1 unit causes a *decrease* in recorded down-hole pressure of 0.9 units, because the water level is forced downward 0.9 units by the barometric pressure change. However, using a non-vented transducer, the total measured pressure *increases* by 0.1 units (the combination of the barometric pressure increase and the water level decrease). Thus, the resulting apparent hydrograph changes by a factor of 100 minus the barometric efficiency, and in the same direction as the barometric pressure change, rather than in the opposite direction.

When the non-vented transducer is used in combination with an inflatable packer, the output is the same as what would be measured without the packer. Because the packer isolates the water in the well from atmospheric pressure, the changing barometric pressure has no direct effect on the water level. The only effect is the indirect effect on the aquifer as a whole. Using the example of a 90 percent barometrically efficient well, an increase in barometric pressure of 1 unit would cause a general aquifer pressure increase of 0.1 units (100 percent minus the barometric efficiency). Thus, the barometric effect is muted and, again, the "apparent" water level hydrograph recorded by the non-vented transducer in conjunction with an inflatable packer is indistinguishable from that recorded by a non-vented transducer without an inflatable packer.

Barometric pressure data were obtained from the Los Alamos National Laboratory TA-54 tower site from RRES-Meteorology and Air Quality. The TA-54 measurement location is at an elevation of 6548 feet above mean sea level (amsl), whereas the wellhead elevation is 7642 feet amsl. Furthermore, the static water level in R-26 was about 607 ft bgs, making the water table elevation 7035 feet amsl. Therefore, the measured barometric pressure data from TA-54 had to be adjusted to reflect the pressure at the elevation of the water table within R-26.

The following formula was used to adjust the measured barometric pressure data:

$$P_{WT} = P_{TA54} \exp \left[ -\frac{g}{3.281R} \left( \frac{E_{R26} - E_{TA54}}{T_{TA54}} + \frac{E_{WT} - E_{R26}}{T_{WELL}} \right) \right]$$

where,

$P_{WT}$  = barometric pressure at the water table inside R4

$P_{TA54}$  = barometric pressure measured at TA-54

$g$  = acceleration of gravity, in m/sec<sup>2</sup> (9.80665 m/sec<sup>2</sup>)

$R$  = gas constant, in J/Kg/degree Kelvin (287.04 J/Kg/degree Kelvin)

$E_{R26}$  = land surface elevation at R-26, in feet (7642 feet)

$E_{TA54}$  = elevation of barometric pressure measuring point at TA-54, in feet (6548 feet)

$E_{WT}$  = elevation of the water level in R-26, in feet (7035 feet)

$T_{TA54}$  = air temperature near TA-54, in degrees Kelvin (assigned a value of 33 degrees Fahrenheit, or 273.7 degrees Kelvin)

$T_{WELL}$  = air temperature inside R-26, in degrees Kelvin (assigned a value of 63 degrees Fahrenheit, or 290.4 degrees Kelvin)

This formula is an adaptation of an equation provided by RRES-Meteorology and Air Quality. It can be derived from the ideal gas law and standard physics principles. An inherent assumption in the derivation of the equation is that the air temperature between TA-54 and the well is temporally and spatially constant, and that the temperature of the air column in the well is similarly constant.

The corrected barometric pressure data reflecting pressure conditions at the water table were compared to the apparent water level hydrograph to discern the correlation between the two.

## THICK AQUIFER RESPONSE

A complicating aspect of the R-well pumping tests is that the wells are partially penetrating. The typical well design incorporates a relatively short well screen (a few feet to tens of feet in length) installed within a massively thick aquifer (many hundreds of feet or more).

As a result, during pumping, the cone of depression expands not only horizontally, but also vertically, throughout the test. As the cone intercepts a greater and greater aquifer thickness, the data plot reflects a steadily flattening slope, corresponding to the continuously increasing vertical height of the zone of investigation. As a result, later data tend to produce a greater calculated

transmissivity than do early data. This complicates the analysis because, for any given slope (or transmissivity value), it is not possible to know what the corresponding aquifer thickness is (vertical extent of the cone of depression).

If an aquitard is encountered at depth, limiting the vertical growth of the cone of depression, the data curve may reach a steady slope, reflecting the transmissivity of the sediments above the aquitard. In that case, a definitive transmissivity can be determined and the hydraulic conductivity can be calculated by dividing the transmissivity by the saturated thickness above the aquitard (if that dimension is known). If no aquitard is encountered, the drawdown curve gets steadily flatter, reflecting a continuum of transmissivities corresponding to the effective depth of the cone of depression at any given time.

### Importance of Early Data

When pumping or recovery first begins, the vertical extent of the cone of depression is limited to approximately the well screen length. For most R-well pumping tests, these first few moments of pumping are the only time that the effective height of the cone of depression is known with certainty. Thus, the early data potentially offer the best opportunity to obtain hydraulic conductivity information, because conductivity would equal the earliest-time transmissivity divided by the well screen length.

Unfortunately, in the R-wells, casing storage effects dominate the early-time data, hindering the effort to determine the transmissivity of the screened interval. The duration of casing storage effects can be estimated using the following equation (Schafer, 1978).

$$t_c = \frac{0.6(D^2 - d^2)}{\frac{Q}{s}}$$

where,

- $t_c$  = duration of casing storage effect, in minutes
- $D$  = inside diameter of well casing, in inches
- $d$  = outside diameter of column pipe, in inches
- $Q$  = discharge rate, in gpm
- $s$  = drawdown observed in pumped well at time  $t_c$ , in feet

In some instances, it may be possible to eliminate casing storage effects by setting an inflatable packer above the tested screen interval prior to conducting the test. Therefore, this option was implemented for the R-26 pumping test. As described later, using the packer was effective at preventing casing drainage during the test, thereby eliminating casing storage effects.

### TIME-DRAWDOWN METHODS

Time-drawdown data can be analyzed using a variety of methods. Among them is the Theis method. The Theis equation describes drawdown around a well as follows:

$$s = \frac{114.6Q}{T} W(u) \quad (1)$$

where,

$$W(u) = \int_u^{\infty} \frac{e^{-x}}{x} dx \quad (2)$$

and

$$u = \frac{1.87r^2 S}{Tt} \quad (3)$$

and where,

- $s$  = drawdown, in feet
- $Q$  = discharge rate, in gpm
- $T$  = transmissivity, in gpd/ft
- $S$  = storage coefficient (dimensionless)
- $t$  = pumping time, in days
- $r$  = distance from center of pumpage, in feet

To use the Theis method of analysis, the time-drawdown data are plotted on log-log graph paper. Then, Theis curve matching is performed using the Theis type curve – a plot of the Theis well function  $W(u)$  versus  $1/u$ . Curve matching is accomplished by overlaying the type curve on the data plot and, while keeping the coordinate axes of the two plots parallel, shifting the data plot to align with the type curve, effecting a match position. An arbitrary point, referred to as the match point, is selected from the overlapping parts of the plots. Match point coordinates are recorded from the two graphs, yielding four values –  $W(u)$ ,  $1/u$ ,  $s$ , and  $t$ . Using these match point values, transmissivity and storage coefficient are computed as follows:

$$T = \frac{114.6Q}{s} W(u) \quad (4)$$

$$S = \frac{Tut}{2693r^2} \quad (5)$$

where,

- $T$  = transmissivity, in gpd/ft
- $S$  = storage coefficient
- $Q$  = discharge rate, in gpm
- $W(u)$  = match point value
- $s$  = match point value, in feet
- $u$  = match point value
- $t$  = match point value, in minutes

An alternative solution method applicable to time-drawdown data is the Cooper-Jacob method (1946), a simplification of the Theis equation (1935) that is mathematically equivalent to the

Theis equation for most pumped well data. The Cooper-Jacob equation describes drawdown around a pumping well as follows:

$$s = \frac{264Q}{T} \log \frac{0.3Tt}{r^2 S} \quad (6)$$

where,

$s$  = drawdown, in feet  
 $Q$  = discharge rate, in gpm  
 $T$  = transmissivity, in gpd/ft  
 $t$  = pumping time, in days  
 $r$  = distance from center of pumpage, in feet  
 $S$  = storage coefficient (dimensionless)

The Cooper-Jacob equation is a simplified approximation of the Theis equation and is valid whenever the  $u$  value is less than about 0.05.

For small radius values (e.g., corresponding to borehole radii),  $u$  is less than 0.05 at very early pumping times and, therefore, is less than 0.05 for nearly all measured drawdown values. Thus, for pumped wells, the Cooper-Jacob equation usually can be considered a valid approximation of the Theis equation. (Note: an exception to this can occur when the transmissivity is exceedingly low. If the transmissivity is sufficiently small, some of the very early time measurements may not meet the  $u$ -value criterion.)

According to the Cooper-Jacob method, the time-drawdown data are plotted on a semilog graph, with time plotted on the logarithmic scale. Then a straight line of best fit is constructed through the data points and transmissivity is calculated using:

$$T = \frac{264Q}{\Delta s} \quad (7)$$

where,

$T$  = transmissivity, in gpd/ft  
 $Q$  = discharge rate, in gpm  
 $\Delta s$  = change in head over one log cycle of the graph, in feet

Because the R-wells are severely partially penetrating, another solution considered for determining aquifer parameters is the Hantush equation for partially penetrating wells (1961a, b). The Hantush equation is as follows:

$$s = \frac{Q}{4\pi T} \left( W(u) + \frac{2b^2}{\pi^2(l-d)(l'-d')} \sum_{n=1}^{\infty} \frac{1}{n^2} \left[ \sin \frac{n\pi d}{b} - \sin \frac{n\pi d'}{b} \right] \left[ \sin \frac{n\pi l'}{b} - \sin \frac{n\pi d'}{b} \right] W \left( u, \sqrt{\frac{K_z}{K_r}} \frac{n\pi r}{b} \right) \right) \quad (8)$$

where, in consistent units,  $s$ ,  $Q$ ,  $T$ ,  $t$ ,  $r$ ,  $S$ , and  $u$  are as previously defined and

- $b$  = aquifer thickness
- $d$  = distance from top of aquifer to top of well screen in pumped well
- $l$  = distance from top of aquifer to bottom of well screen in pumped well
- $d'$  = distance from top of aquifer to top of well screen in observation well
- $l'$  = distance from top of aquifer to bottom of well screen in observation well
- $K_z$  = vertical hydraulic conductivity
- $K_r$  = horizontal hydraulic conductivity

In this equation,  $W(u)$  is the Theis well function and  $W(u, \beta)$  is the Hantush well function for leaky aquifers. For single-well tests,  $d = d'$  and  $l = l'$ .

## RECOVERY METHODS

Recovery data were analyzed by the several methods. One of the methods used was the Theis Recovery Method. This is a semi-log analysis method similar to the Cooper-Jacob procedure.

In this method, residual drawdown is plotted on a semi-log graph versus the ratio  $t/t'$ , where  $t$  is the time since pumping began and  $t'$  is the time since pumping stopped. A straight line of best fit is constructed through the data points and  $T$  is calculated from the slope of the line as follows:

$$T = \frac{264Q}{\Delta s} \quad (7)$$

The recovery data are particularly useful compared to time-drawdown data. Because the pump is not running, spurious data responses associated with dynamic discharge rate fluctuations are eliminated. The result is that the data set is generally "smoother" and easier to analyze.

Recovery data also were analyzed using the Cooper-Jacob and Hantush methods described above. In applying these procedures, simple recovery (difference between residual drawdown and maximum drawdown observed at the end of the pumping period) was plotted versus recovery time ( $t'$ ). Such a plot can be considered analogous to a time-drawdown plot and is accurate for early and middle data. For late data, however, this approach can sometimes lose accuracy. The reason for possible loss of accuracy is explained as follows.

Theoretically, recovery time must be plotted against *calculated recovery*, which is defined as the difference between the observed residual drawdown and the drawdown that would have occurred had pumping continued (also called extrapolated drawdown):

$$s_c = s_e - s_r \quad (9)$$

where,

- $s_c$  = calculated recovery
- $s_e$  = extrapolated drawdown
- $s_r$  = observed residual drawdown

Substituting simple recovery for calculated recovery is done by substituting the drawdown observed at the end of the pumping period for  $s_e$  in the above equation. At early-to-middle recovery times, this substitution introduces little error; but at late times, the discrepancy could

become substantial if the extrapolated drawdown deviates significantly from the drawdown observed at the end of the pumping period. Note that in wells where the pumping water level stabilizes during the test, the extrapolated drawdown and the drawdown observed at the end of the pumping test are identical, and no error is introduced by substituting simple recovery for calculated recovery.

Although plotting calculated recovery is theoretically correct, determining the values of extrapolated drawdown to use in computing calculated recovery is problematic. Often, the time-drawdown data are erratic, or biased by changing well efficiency, and can't be extrapolated readily. Even when the time-drawdown data are not erratic, extrapolating the drawdown trend presupposes that future drawdown changes will be similar to those observed during the pumping period. Alternatively, extrapolated drawdown can be determined by mathematical formula, but this approach presupposes particular aquifer coefficients and conceptual model of the well/aquifer system. Thus, regardless of the method used to extrapolate drawdown beyond the pumping period, the validity of the extrapolated values is in doubt. Furthermore, when calculated recovery is used in the graphical procedure, the resulting analysis does not provide independent information on aquifer parameters, but simply reflects the mathematical content of the extrapolation process.

To summarize, either simple recovery or calculated recovery may be plotted against recovery time and analyzed using time-drawdown methods. However, for late times both methods can produce errors. At late time, simple recovery may provide a poor approximation of the calculated recovery. Similarly, obtaining calculated recovery, by extrapolating the time-drawdown trend beyond the pumping period, can introduce a mathematical bias in the data.

## **SPECIFIC CAPACITY METHOD**

The specific capacity of the pumped well can be used to obtain a lower-bound value of hydraulic conductivity. The hydraulic conductivity is computed using formulas that are based on the assumption that the pumped well is 100 percent efficient. The resulting hydraulic conductivity is the value required to sustain the observed specific capacity. If the actual well is less than 100 percent efficient, it follows that the actual hydraulic conductivity would have to be greater than calculated to compensate for well inefficiency. Thus, because the efficiency is unknown, the computed hydraulic conductivity value represents a lower bound. The actual conductivity is known to be greater than or equal to the computed value.

For fully penetrating wells, the Cooper-Jacob equation can be iterated to solve for the lower-bound hydraulic conductivity. However, the Cooper-Jacob equation (assuming full penetration) ignores the contribution to well yield from permeable sediments above and below the screened interval. To account for this contribution, it is necessary to use a computation algorithm that includes the effects of partial penetration. One such approach was introduced by Brons & Marting (1961) and augmented by Bradbury & Rothchild (1985).

Brons and Marting introduced a dimensionless drawdown correction factor,  $s_p$ , approximated by Bradbury and Rothchild as follows:

$$s_p = \frac{1 - \frac{L}{b}}{\frac{L}{b}} \left[ \ln \frac{b}{r_w} - 2.948 + 7.363 \frac{L}{b} - 11.447 \left( \frac{L}{b} \right)^2 + 4.675 \left( \frac{L}{b} \right)^3 \right] \quad (10)$$

In this equation,  $L$  is the well screen length, in feet. Incorporating the dimensionless drawdown parameter, the conductivity is obtained by iterating the following formula:

$$K = \frac{264Q}{sb} \left( \log \frac{0.3Tt}{r_w^2 S} + \frac{2s_p}{\ln 10} \right) \quad (11)$$

To apply this formula, a storage coefficient value must be assigned. Storage coefficient values for unconfined sand and gravel aquifers, such as the Puye Formation in which many of the R-wells are completed, typically range from a few percent to 20 percent or more, with the majority of the values falling between approximately 5 and 15 percent. Thus, in the absence of site-specific storage coefficient data for the Puye, a value of 0.1 is deemed to be a reasonable choice for performing calculations for unconfined conditions. When confined conditions are encountered, as in R-26 Screen 2, for example, the storage coefficient can be expected to range from about  $10^{-5}$  to  $10^{-3}$ , depending on aquifer thickness (the thicker the aquifer, the greater the storage coefficient). Typically, a value of  $5 \times 10^{-4}$  may be assigned for calculation purposes. The choice of storage coefficient is less clear for other formations on the plateau, such as the more massive Cerro Toledo interval in which Screen 1 is completed. Conditions in the Screen 1 zone are likely to be unconfined, but the porosity and specific yield of the Cerro Toledo may be expected to be less than that of the Puye. Without site-specific information on the specific yield of the Cerro Toledo, an arbitrary estimated value of 1 percent was used in the calculations. The calculation result is not particularly sensitive to the choice of storage coefficient value, so a rough estimate of the storage coefficient is adequate to support the calculations.

The analysis also requires assigning a value for the saturated aquifer thickness,  $b$ , which is generally not known. Fortunately, the calculated value of hydraulic conductivity is usually insensitive to the selected aquifer thickness value, as long as the aquifer thickness is significantly greater than the screen length. This is because saturated aquifer materials far above or below the screened interval contribute little to the yield of the well. Thus, it was expected that an approximate aquifer thickness estimate would suffice for the calculations.

An alternative specific capacity method for partially penetrating screens is a formula presented by Hvorslev (1951) that can be derived directly from Darcy's Law:

$$K = \frac{229}{L} \frac{Q}{s} \ln \left( \frac{L}{2r_w} + \sqrt{1 + \frac{L^2}{4r_w^2}} \right) \quad (12)$$

where,

$K$  = hydraulic conductivity, in gpd/ft<sup>2</sup>  
 $Q$  = discharge rate, in gpm

$L$  = well screen length, in feet  
 $s$  = drawdown, in feet  
 $r_w$  = borehole radius, in feet

This formula is derived based on the assumption of infinite aquifer thickness, above and below the well screen, and infinite pumping time. As such, it works reasonably well for short well screens completed in thick aquifers and very long pumping times. As with other specific capacity methods, the resulting  $K$  value may be considered a lower-bound estimate of the screened zone hydraulic conductivity.

Computing the lower-bound estimate of hydraulic conductivity can provide a useful frame of reference for evaluating the other pumping test calculations.

### **SCREEN 1 (651.8 to 669.9 ft bgs)**

This section presents the data obtained from the R-26 Screen 1 aquifer tests and the results of the analytical analyses. All tests were run with both well Screens 1 and 2 open, i.e., Screen 1 was not hydraulically isolated from Screen 2. However, as was verified subsequently, Screen 2 produces negligible flow and, thus, the test results may be considered applicable to Screen 1.

There were several episodes of testing that were analyzed:

1. Trial 1. R-26 was pumped at 16 gpm for 72 minutes from 3:52 pm to 5:04 pm on February 16, followed by 28 minutes of recovery.
2. Trial 2. R-26 was pumped at 16 gpm for 31 minutes from 5:32 pm to 6:03 pm on February 16, followed by a day and a half of recovery.
3. Pumping Test. R-26 was pumped at 15.7 gpm (declining to 14.8 gpm) for 565 minutes from 8:36 am to 6:01 pm on February 18.
4. Pumping Test Restart. Following a 61-minute shutdown, R-26 was pumped at 7 gpm (declining to 6.8 gpm) for 828 minutes from 7:02 pm on February 18 to 8:50 am on February 19.
5. Recovery. Recovery data were collected for 1465 minutes from 8:50 am on February 19 to 9:15 am on February 20.

### **Background Data**

Figure 1 shows the “apparent” water level hydrograph and the barometric pressure data recorded on February 17 and 18. These data were recorded well after the brief Trial 1 and Trial 2 pumping events. While the barometric pressure data showed typical diurnal and sinusoidal response, the measured aquifer pressures were very different. It appears that the upper screen zone was still recovering from the short trial pumping episodes. Recovery had not yet become complete, even more than 1.5 days following the trial pumping tests. This response was different than seen in previous R-well pumping tests performed during this phase of investigation. Such sluggish recovery response suggests aquifer boundaries and an aquifer not well connected to the main regional aquifer. The response is not unlike what would be expected in a perched aquifer of limited areal extent.

There was no discernable correlation between aquifer pressures and barometric pressure, suggesting that the Screen 1 zone is nearly 100 percent barometrically efficient. Recall that the observed lack of aquifer pressure response to changes in barometric pressure implies that, had no packer been installed, the actual water levels in the well would have responded nearly equally and opposite to changes in barometric pressure, such that the combined pressure (water head plus atmospheric pressure) would have shown negligible change (except for the steady, gradual recovery from pumping). The observed barometric pressure and aquifer pressure response indicated that barometric corrections to the pumping test data were not necessary, because barometric pressure changes had little effect on the measured pressures in the well.

### **Trial 1**

The first pumping trial consisted of 72 minutes of pumping followed by 28 minutes of recovery. Figure 2 shows the resulting recovery data plot.

The graph shows three distinct slopes. The first slope (right-hand side of graph, i.e., large values of  $t/t'$ ) shows the early data response reflecting the transmissivity of the screened interval. The calculated transmissivity was 240 gpd/ft for the 18.1-foot-thick interval, making the hydraulic conductivity 13.3 gpd/ft<sup>2</sup>, or 1.8 feet per day.

During the first minute of recovery, the data trace began to flatten, consistent with vertical expansion of the cone of depression. The transmissivity calculated from the second slope on the graph was 620 gpd/ft, corresponding to some (unknown) thickness of sediments greater than the screen length. The second slope was analyzed using the Hantush method to account for the effects of partial penetration. Figures 3, 4, and 5 show the Hantush analysis results for assumed vertical anisotropy ratios of 1.0, 0.1, and 0.01, respectively. The resulting transmissivity values ranged from 690 to 1000 ft<sup>2</sup>/day (5160 to 7480 gpd/ft), while the resulting hydraulic conductivity values ranged from 2.7 to 3.9 feet per day. The different values obtained from the analysis result from different assumed vertical anisotropy ratios (a parameter that is unknown and can't be determined from the available data). All calculations were performed for an assigned aquifer thickness of 258 feet, the observed saturated portion of the Cerro Toledo interval in R-26.

Note on Figures 3 through 5 that the early data did not fit the partial penetration type curves, but described a steeper slope. This indicates that the hydraulic conductivity of the materials immediately adjacent to the well screen is less than that of the sediments farther from the screen, either laterally or vertically. Indeed, early time analysis showed the hydraulic conductivity of the near well sediments to be 1.8 feet per day, while the Hantush analysis of subsequent data showed the average hydraulic conductivity over a broader area to be 2.7 to 3.9 feet per day.

Finally, the late data showed a steepening of the drawdown graph. This could be an indication of reduced hydraulic conductivity at distance, or the presence of negative boundaries, i.e., physical limits to the areal extent of the aquifer. Subsequent analyses, discussed below, suggested that the aquifer is limited in areal extent.

### **Trial 2**

The second pumping trial consisted of 31 minutes of pumping followed by a day and a half of recovery (which also served as background data). Figure 6 shows the resulting recovery data plot.

The graph shows the same three distinct slopes as the first trial. The first slope shows the early data response reflecting the transmissivity of the screened materials. The calculated transmissivity was 250 gpd/ft for the 18.1-foot-thick interval, making the hydraulic conductivity 13.8 gpd/ft<sup>2</sup>, or 1.8 feet per day.

The second slope shows the effect of partial penetration. Figures 7, 8, and 9 show Hantush analyses of these data for vertical anisotropy ratios of 1.0, 0.1, and 0.01, respectively. The resulting transmissivities ranged from 660 to 1040 ft<sup>2</sup>/day (4940 to 7780 gpd/ft), while the hydraulic conductivity values ranged from 2.6 to 4.0 feet per day, consistent with the results of the first trial test.

Similar to the first test, the late data showed a steep slope, reflecting boundary conditions. Note on Figure 6 that even after more than a day and a half of recovery, the water level was still more than 1.6 feet below the original static water level – this after only about an hour and a half of total preliminary pumping. This suggests that the aquifer is limited in areal extent and not well connected to the regional aquifer. A possible explanation for the observed response is perched conditions. In other words, a perched aquifer having limited areal extent would be expected to respond as observed here. Well R-26 is located in a recharge area where the downward gradients are exceedingly steep (over 30 percent). In this hydrologic setting, perching conditions would not be unexpected. Keep in mind that the pumping response does not prove or guarantee perched conditions, but is nevertheless consistent with such conditions.

Note that the steep-flat-steep data pattern in both trial 1 and trial 2 has the same form as the response associated with delayed yield in an unconfined aquifer, due to slow drainage of the sediments above the cone of depression. This idea was investigated by applying the Neuman method for partially penetrating wells in unconfined aquifers to the data set (not presented here). Using this procedure, it was not possible to arrive at a reasonable solution if parameters such as storage and vertical anisotropy ratio were constrained to plausible values. Therefore, the delayed yield hypothesis was rejected.

## **Pumping Test**

Following the extended recovery period at the end of trial 2, the 24-hour pumping test was started. As described earlier, the test consisted of 565 minutes of pumping at 15.7 gpm (declining to 14.8 gpm), a 61-minute shutdown, and 828 minutes of pumping at 7 gpm (declining to 6.8 gpm).

Figure 10 shows a linear plot of the time-drawdown response. It can be seen on the left side of the graph that the drawdown curve appeared regular (concave upward) until the water level fell into the well screen. Once dewatering of the well screen began, the water levels showed a steepening downward trend, eventually plunging into the casing below the bottom of the screen.

In general, once the pumping water level falls below the well screen, additional lowering of the water level cannot induce more flow from the aquifer, because the aquifer has already been drawn down to the maximum. What occurs next is that, because the aquifer is being pumped at a constant head (i.e., effective head at the bottom of the screen), the flow from the aquifer declines with time as the cone of depression expands. As this occurs, the pump (operating at a fixed rate) begins emptying the casing beneath the screen to make up for the loss of production from the

aquifer. Under these circumstances, it is common for the sump beneath the screen to be completely dewatered in a short time.

In R-26, the dewatering of the casing below the well screen was slowed substantially. This is because, as the sump dewatered, the vertical lift required of the pump increased, causing the pumping rate to decline. Thus, this built-in control mechanism caused the discharge rate produced by the pump to nearly mirror the flux from the aquifer. The result was that it took nearly four hours to evacuate just 57 feet of annulus between the 5-inch OD well casing and the 2-inch drop pipe, a water volume of only 34 gallons.

Once this suspected response was deduced, the pump was shut down. Figure 10 shows the water level rebound that occurred when the pump was shut off for 61 minutes, as well as the response to restarting the pump at 7 gpm.

An attempt was made to analyze the early data from the 15.7 gpm segment of the test. Figure 11 shows the time-drawdown graph of data up to the point where the water level fell into the screen. This graph showed only the second (flat) and third (steep) slopes analogous to those observed in the trial tests on Figures 2 and 6. The early steep slope was not observed in this data set. Notice that at a pumping time of 0.1 minutes, the observed water level displacement was nearly 30 feet. By comparison, inspection of Figures 3 through 5 and 7 through 9 shows displacement magnitudes of around 10 feet (plus or minus) at 0.1 minutes. The excess drawdown on Figure 11 was likely caused by a slow leak in either a coupling joint or a check valve in the drop pipe, resulting in antecedent drainage of a portion of the drop pipe. This caused the pump to start against reduced head and, therefore, pump at a greater rate than under full head conditions. As a result of the greater initial discharge rate, the early data were affected (exaggerated drawdown) and the steep early slope was absent. The Hantush method was applied to the drawdown data to calculate hydraulic conductivity values. Previous Hantush curve matching analyses for trial tests 1 and 2 were applied to data recorded between times ranging from about 1 minute to 5 or 10 minutes. Therefore the Hantush analysis of the 24-hour pumping test data set was constrained to data recorded in this same time interval. Figures 12, 13, and 14 show the analytical results for vertical anisotropy ratios of 1.0, 0.1, and 0.01, respectively. The calculated hydraulic conductivity values ranged from 2.5 to 3.9 feet per day, consistent with the results of trials 1 and 2. Note that the curve matches on Figures 12, 13, and 14 are not particularly good. Nevertheless, the analysis presented is still valid and worthwhile. The early data were affected by the initial over pumping of the well (caused by antecedent drainage of the drop pipe) and, as such, should fall above the theoretical type curve. Similarly, the late, boundary-affected data should lie above the theoretical type curve. Only those data points between the early data and the boundary-affected data would be expected to fall on the type curve. So long as the curve matches are restricted to the appropriate data segments, they may be considered valid and should be included in the analysis. Indeed, the resulting aquifer parameter values agreed well with the results of trials 1 and 2.

### **Pumping Test Restart**

Following the 61-minute shut down of the R-26 pumping test, the pump was restarted and the well was pumped for 828 minutes. The initial discharge rate was 7.0 gpm, but declined to 6.8 gpm during the test.

Figure 15 shows time-drawdown data from the restart test. On this graph, the drawdown values shown are *incremental drawdown* from the onset of restarting the pump, rather than total drawdown from the original static water level. The early data confirmed the transmissivity of the screened zone to be about 240 gpd/ft, corresponding to a hydraulic conductivity of the near-screen sediments of 13.3 gpd/ft<sup>2</sup>, or 1.8 feet per day. The Hantush solution was applied to the flat portion of the drawdown curve immediately following the initial steep portion. Figures 16, 17, and 18 show curve matching results for vertical anisotropy ratios of 1.0, 0.1, and 0.01, respectively. The resulting hydraulic conductivity values ranged from 2.0 to 2.9 feet per day.

Note on Figure 15 that the third (steep) slope seen on previous data plots was absent. Instead, the late data actually showed water level reversal, rising slightly for most of the test. This was attributable to a combination of the gradual reduction in pumping rate during the test and superposition of the ongoing water level rebound (recovery), from the previous 15.7 gpm pumping event, on the new pumping test.

### Recovery

Following the completion of the 24-hour pumping test, recovery was measured for 1465 minutes. Figure 18 shows the resulting recovery graph. The slope of the early recovery data showed a screen zone transmissivity of 180 gpd/ft, corresponding to a hydraulic conductivity of 9.9 gpd/ft<sup>2</sup>, or 1.3 feet per day. As seen in previous plots, the subsequent data showed flattening of the curve associated with vertical expansion of the cone of depression, followed by steepening associated with boundary effects.

Partial penetration effects were analyzed using the Hantush method to quantify formation properties at greater distances, laterally and vertically, from the screen zone. Figures 20, 21, and 22 show curve matching results for assumed vertical anisotropy ratios of 1.0, 0.1, and 0.01, respectively. The resulting hydraulic conductivity values ranged from 2.3 to 3.6 feet per day, considered representative of a greater volume of aquifer than the near-screen portion.

Note on Figure 19 that after more than one day of recovery, the observed water level was still more than 2.6 below the original static water level. This provides additional evidence that the aquifer is limited in areal extent, not well connected to the regional aquifer, and possibly perched.

### Specific Capacity Analysis

Specific capacity data from Screen 1 were used to compute lower-bound estimates of hydraulic conductivity. Two data sets were used for this.

First, at the beginning of the 24-hour pumping test, Screen 1 produced 15.7 gpm with 43.36 feet of drawdown after 100 minutes of pumping. The Brons and Marting formula was used to compute the lower-bound hydraulic conductivity value. Other inputs used in the calculation included a borehole radius of 0.51 feet, an aquifer thickness of 258 feet (the Cerro Toledo), a storage coefficient of 0.01 and a well screen length of 18.1 feet. (As explained earlier in the section entitled SPECIFIC CAPACITY METHODS, in the absence of site-specific field data the storage coefficient of 0.01 was selected because the fractured Cerro Toledo is expected to have a lower porosity than would a granular aquifer.) The resulting lower-bound hydraulic conductivity value was 2.4 feet per day. A second calculation was based on recovery following the 24-hour

pumping test. Following final pumping at 6.8 gpm, the water level recovered 19.97 feet after 100 minutes. The Brons and Marting method produced a lower-bound hydraulic conductivity estimate of 2.2 feet per day from this information.

The computed values of 2.4 and 2.2 feet per day were consistent with previous results, which showed a hydraulic conductivity of around 1.8 feet per day immediately adjacent to the well screen, and 2.0 to 4.0 feet per day away from the screen, depending on vertical anisotropy ratio.

At first glance, the lower-bound estimates appear contradictory in that they exceed the calculated hydraulic conductivity of the near-bore sediments of 1.8 feet per day. However, the degree of exceedance is small and can be considered insignificant compared to the expected accuracy of the various analyses. Furthermore, the hydraulic conductivity of the more distant sediments was estimated to range from 2.0 to 4.0 feet per day. Thus, when a weighted average hydraulic conductivity of the near-bore sediments and distant sediments is considered, the lower-bound hydraulic conductivity values are consistent with these, rather than contradictory.

## **SCREEN 2**

This section presents the data obtained from the R-26 Screen 2 hydraulic tests. The Screen 2 testing occurred in two phases – a brief preliminary shut-in, pumping and recovery test; and a long-term isolation test.

### **Preliminary Test**

The preliminary test involved setting a packer below Screen 1, monitoring shut-in head for 52 minutes, pumping for 15 minutes, and monitoring recovery for an additional 53 minutes.

The packer was inflated at 11:22 am on February 20. After 52 minutes, the pump was started at 12:14 pm. After 15 minutes of pumping, cavitation occurred and the pump was shut down at 12:29 pm. Monitoring continued for an additional 53 minutes, until 1:22 pm when the packer was deflated.

Figure 23 shows the heads monitored during the two-hour-long preliminary test. As shown on the graph, the shut-in head declined rapidly for about a half hour after the packer was inflated.

Prior to shut-in, the head on the deep screen zone had been maintained at or near the static water level of the Screen 1 zone for an extended period – essentially since the well was completed on October 19, 2003. This was equivalent to a long-term constant-head injection test of 126 days duration. This meant that the observed head decline following shut-in could be analyzed as a standard post-injection recovery data set. As described later, the effective injection rate was determined to be 0.099 gpm, based on data recorded during the long-term isolation test.

Note that although the effective injection rate was quite low it was nevertheless determined with a high degree of accuracy. As explained in the next section, this was accomplished by observing the rate at which water drained out of a 2-inch pipe. Thus, the rate, as determined, and the corresponding calculations of aquifer parameters can be considered roughly as reliable as those determined by more conventional means.

As shown on Figure 23, after about half an hour of shut-in, the peizometric head rose slightly and leveled off. It was surmised that the check valve above the pump had leaked, allowing a

very small quantity of water in the drop pipe to seep slowly into the Screen 2 zone. The seepage rate was sufficient to halt recovery and maintain the head.

At 12:14 pm, the pump was started and run for 15 minutes. The data points shown on Figure 23 were recorded at 3-second intervals. Note that upon starting, the peizometric head declined more than 40 feet between consecutive measurements, i.e., in less than three seconds. At that point, a full vacuum was formed beneath the packer and further head reduction required physical drainage of the annular space between the 5-inch OD well casing and the 2-inch drop pipe, resulting in a slower rate of head reduction. The water level declined to near the pump intake at which point cavitation occurred.

At 12:29 pm, the pump was shut off and recovery was measured. Based on the recovery rate and the volume of the annulus between the well casing and pump drop pipe, the refill rate was computed to be 0.28 gpm. As discussed later, the static water level for Screen 2 was determined from the long-term isolation test to be about 870 ft bgs. Thus, the 0.28-gpm refilling event occurred with minimal drawdown below the Screen 2 static level. This flow rate was not consistent with the long-term injection rate of only 0.099 gpm at high head buildup above static. It was concluded that check valve leakage, or leaky joints in the drop pipe, had allowed water to leak from the drop pipe into the Screen 2 zone.

The initial recovery data, immediately following packer inflation, were analyzed using the Cooper-Jacob and Theis methods. Figure 24 shows the Cooper-Jacob analysis of the data, revealing a very low deep zone transmissivity of 0.37 gpd/ft. For exceedingly tight sediments, the cone of depression grows very slowly, both laterally and vertically. Therefore, it was assumed that the vertical growth of the cone of depression beyond the screen zone would have been minimal during the brief recovery period. Thus, the computed transmissivity was taken to be representative of the screened interval of 23.2 feet, making the hydraulic conductivity 0.016 gpd/ft<sup>2</sup>, or 0.002 feet per day.

It was determined that the very early recovery data were not valid for the Cooper-Jacob analysis because the  $u$ -value criterion was not met. Therefore, the data were analyzed using Theis curve matching. Figure 25 shows the curve matching results, which produced a transmissivity of 0.41 gpd/ft, yielding a hydraulic conductivity of 0.018 gpd/ft<sup>2</sup>, or 0.0024 feet per day.

### **Long-Term Isolation Test**

Based on the very low yield of the deep zone, the decision was made to hydraulically isolate it by packing off Screen 1 and monitor the head decline once the influence of the Screen 1 head was removed. A packer was set on 2-inch drop pipe at a depth of about 713 ft bgs, with a 1 7/8-inch OD stinger pipe extending below the packer to approximately 720 ft bgs. The packer was inflated at 2:20 pm on February 22 and maintained until 8:00 am on March 6, providing a data record of 12.7 days duration.

Figure 26 shows the water levels measured during the Screen 2 isolation period. The first 110 feet or so of water level decline corresponded to drainage of the inside of the 2-inch pipe connected to the packer. Once the water level dropped below 720 feet (the bottom of the stinger pipe) further water level decline corresponded to drainage of the full 5-inch OD well casing.

The hydrograph on Figure 26 shows some unusual responses. First, once the water level fell below the packer into the 5-inch well casing, the rate of descent proceeded at a nearly linear rate (on February 23). Another near-linear segment occurred on February 25. There was no apparent explanation for this unusual response.

Second, the water levels reversed direction and rose periodically – tens of feet in some instances – during the monitoring period. Such water level fluctuations, especially at great depths, are exceedingly rare.

It was not known if the measured head values were valid or whether the pressure transducer had malfunctioned. To check the transducer response, at the end of the monitoring period, the transducer was manually raised and lowered prescribed distances, so that the recorded output could be compared to the known vertical displacements. The transducer readouts correctly reflected these artificially imposed head changes.

If the transducer readings on Figure 26 are valid, it is difficult to explain the large water level fluctuations during the last week of monitoring. Perhaps the proximity of R-26 to the mountain front is such that snowmelt events are able to induce rapid head changes, even at depth. Once Westbay equipment is installed in R-26, it will be important to monitor Screen 2 long term to see if similar responses are observed.

The average depth to water over the last week of monitoring was 870 ft bgs. This was taken to be a representative estimate of the static water level for the deep zone. This water level is 263 feet lower than the initial static water level observed in Screen 1.

The Figure 26 water level recession graph was expanded on Figures 27 and 28 to provide greater detail. As shown on these figures, the segment reflecting drainage of the 2-inch pipe showed the expected concave upward appearance, indicating a gradual reduction in the rate of water level decline as the head dropped.

Note that once the head reached the bottom of the stinger pipe beneath the packer, the water level stabilized for a while. This is because water in the annulus, outside the stinger pipe and beneath the packer element, which was being held above the water level by vacuum, gradually drained out as the vacuum was released because of exposure to atmospheric pressure when the water level reached the lower end of the stinger pipe. The duration of the horizontal portion of the hydrograph illustrates the length of time it took for the suspended volume of water to drain – approximately 107 minutes.

Figures 27 and 28 showed expected response for the water level descent through the 2-inch pipe and packer. Through the 2-inch pipe, the expected concave upward form was evident in the data curve. Even the subtle change in the shape of the curve associated with the water level falling through the smaller inside diameter packer assembly can be seen on the graph. This portion of the hydrograph looked normal, orderly, and consistent with expectations.

The data on Figure 28 were used to determine the rate at which water flowed into Screen 2, calculated as the volume of water that drained from the 2-inch pipe divided by the time it took to drain. Figure 29 shows the calculated injection rates. As expected, as the head dropped, the seepage rate of water into Screen 2 declined. The initial injection rate, calculated using the earliest measurements, was 0.099 gpm. This was the injection rate associated with a head

buildup in Screen 2 equal to the static water level in Screen 1. It was concluded that approximately 0.099 gpm had flowed from Screen 1 to Screen 2 since well completion. (Note that the actual flux rate would have been somewhat less than 0.099 gpm during the time that the solid neoprene packer was in place between Screens 1 and 2, because of the slight flow resistance imposed by the packer.)

As shown on Figure 29, the injection rate declined to a value of about 0.038 gpm by the time the water level reached the packer. When the water level reached the bottom of the stinger pipe, it stabilized as the suspended water between the stinger pipe and well casing drained away. The volume of water suspended in the annulus around the stinger pipe was calculated to be 4.11 gallons. The hydrograph data showed that it took 107 minutes for this volume to drain away, before water levels resumed their downward trend. This worked out to a drainage rate of  $4.11/107 = 0.038$  gpm, a good match to the observed drainage rate at the time that the water level first reached the packer.

Thus, as discussed above, the portion of the hydrograph reflecting the water level descent through the 2-inch pipe, packer and stinger pipe showed 1) the expected concave upward response indicating declining flux rate with declining head, 2) the effect of the smaller inside diameter of the packer assembly, and 3) reasonable seepage rates showing both the expected decline over time and a good match between the seepage rate at the bottom of the 2-inch pipe and the draining of the annulus outside the stinger pipe. Despite this consistent set of observations, however, once the water levels fell into the 5-inch casing, contradictory response was observed.

Figure 30 shows the water level decline inside the 5-inch casing on February 23. (A straight line has been added to the graph to demonstrate how nearly linear the measured response was.) Based on the volume of the 5-inch casing and the measured water level descent rate, the drainage rate was calculated to be 0.046 gpm. There was no explanation as to why the apparent injection rate declined to 0.038 gpm inside the 2-inch pipe and then increased to 0.046 gpm. Further, there was no explanation as to why the apparent seepage rate of 0.046 gpm was maintained nearly constant as the head declined an additional 100 feet. It is not known whether the transducer malfunctioned or whether the data are valid. However, as stated previously, attempts to assess the working order of the transducer showed it to be responding accurately.

### Specific Capacity Analysis

Information gained on the injection rate of Screen 1 water into Screen 2 was used to compute lower-bound hydraulic conductivity estimates for the Screen 2 zone. With the applied head on Screen 2 equal to the static water level in Screen 1 (approximately 607 ft bgs), the flux rate had been calculated to be 0.099 gpm. This rate (or similar) had been occurring since well completion 126 days earlier. The corresponding head buildup was  $870 - 607 = 263$  feet. The Brons and Marting formula was used to calculate a lower-bound hydraulic conductivity from this information. An arbitrary assumed aquifer thickness of 400 feet and an estimated storage coefficient of 0.0005 were used in the calculation. The resulting lower-bound hydraulic conductivity was 0.0021 feet per day. The calculation was repeated using the Hvorslev formula, yielding 0.0019 feet per day. These values were consistent with the values of 0.0020 and 0.0024 feet per day obtained from the time-recovery analysis.

## SUMMARY

The following information was determined from the pumping, recovery, and shut-in tests on R-26.

### Screen 1

1. The barometric efficiency of the Screen 1 zone was near 100 percent.
2. Implementation of the inflatable packer successfully eliminated the effects of casing storage and barometric pressure fluctuations.
3. Multiple analyses produced an average hydraulic conductivity value for the portion of the Cerro Toledo immediately adjacent to the screen of about 1.7 feet per day.
4. For portions of the aquifer farther away from the screen, multiple analyses produced average hydraulic conductivities of 2.4 feet per day for isotropic conditions, 3.1 feet per day for 10:1 anisotropy, and 3.7 feet per day for 100:1 anisotropy. The steep vertical gradient at the site suggests that values in the upper end of this range may be most reliable.
5. Analysis of specific capacity data revealed lower-bound estimates of hydraulic conductivity averaging 2.3 feet per day.
6. The data showed the tested zone to be limited in areal extent.
7. The Screen 1 interval appeared to be not well connected to the regional aquifer.
8. Evidence suggested possible perched conditions for the Screen 1 interval.

### Screen 2

1. Screen 2 was shut in after 126 days of "injection", i.e., receiving water from Screen 1, at around 0.1 gpm. The recovery response produced an average hydraulic conductivity of 0.0022 feet per day.
2. A 12.7-day isolation and water level equilibration period revealed an average static water level for Screen 2 of 870 ft bgs, 263 feet deeper than the Screen 1 static water level of 607 feet.
3. After water level equilibration, the measured water levels still fluctuated over a range of nearly 25 feet. It is not known whether these fluctuations were real or symptoms of equipment malfunction. However, checks on the equipment showed it to be working properly.
4. Long-term water level monitoring of Screen 2 will be important to see if these kinds of water level fluctuations are replicated in the future.
5. In addition to the unusual water fluctuations, other inexplicable water level response was observed. The descent of the water level through the 2-inch drop pipe and packer appeared normal, conforming to expected hydraulic response in which the rate of descent declines with decreasing head. However, once the water level dropped below the packer, into the 5-inch casing, the rate of descent appeared abnormally great (corresponding to an increase in water seepage rate from 0.038 gpm to 0.046 gpm) and, further, the rate did not fall off as the head declined. There was no apparent explanation for this very unusual observed response. It is not known whether these water level responses were real or

symptoms of equipment malfunction. However, checks on the equipment showed it to be working properly.

6. Analysis of specific capacity data revealed lower-bound estimates of hydraulic conductivity averaging 0.002 feet per day.

## REFERENCES

- Bradbury, Kenneth R. and Rothschild, Edward R., 1985. A Computerized Technique For Estimating the Hydraulic Conductivity of Aquifers From Specific Capacity Data. *Ground Water*. V. 23, no. 2, pp. 240-246.
- Brons, F. and Marting, V. E., 1961. The Effect of Restricted Fluid Entry on Well Productivity. *J. Petrol. Technol.* V. 13, no. 2, pp. 172-174.
- Cooper, H. H., Jr. and Jacob, C. E., 1946. A Generalized Graphic Method for Evaluating Formation Constants and Summarizing Well Field History, *Transactions. Am. Geophys. Union*, v. 27, No. 4, pp. 526-534.
- Hantush, M. S., 1961a. Drawdown Around a Partially Penetrating Well, *Journal of the Hyd. Div., Proceedings of the American Society of Civil Engineers*, vol. 87, no. HY5, pp. 83-98.
- Hantush, M. S., 1961b. Aquifer Tests on Partially Penetrating Wells, *Journal of the Hyd. Div., Proceedings of the American Society of Civil Engineers*, vol. 87, no. HY5, pp. 171-194.
- Hvorslev, J. M., 1951. Time Lag and Soil Permeability in Ground-Water Observations, *Bulletin 36, U. S. Corps of Engineers, Waterways Experiment Station, Vicksburg, Mississippi*.
- Schafer, David C., 1978. Casing Storage Can Affect Pumping Test Data, *Johnson Drillers' Journal*, Jan/Feb, Johnson Division, UOP Inc., St. Paul, Minnesota.
- Theis, C. V., 1935. The Relation Between the Lowering of the Piezometric Surface and the Rate and Duration of Discharge of a Well Using Groundwater Storage, *Transactions. Am. Geophys. Union*, v. 16, pp. 519-524.

Figure 1. Comparison of R-26 Screen 1 Apparent Hydrograph and Barometric Pressure

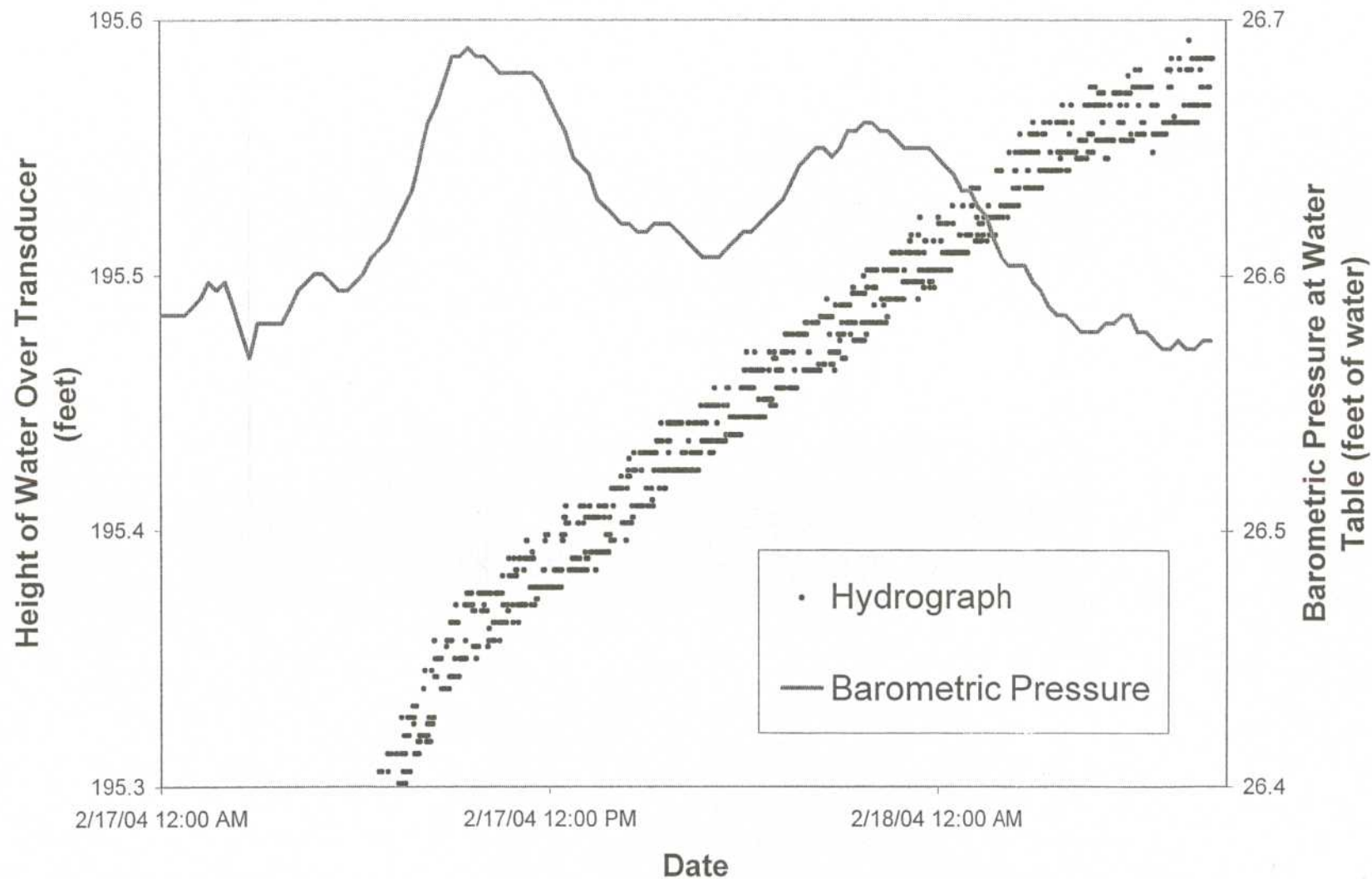


Figure 2. Well R-26 Screen 1 - Trial 1 Recovery

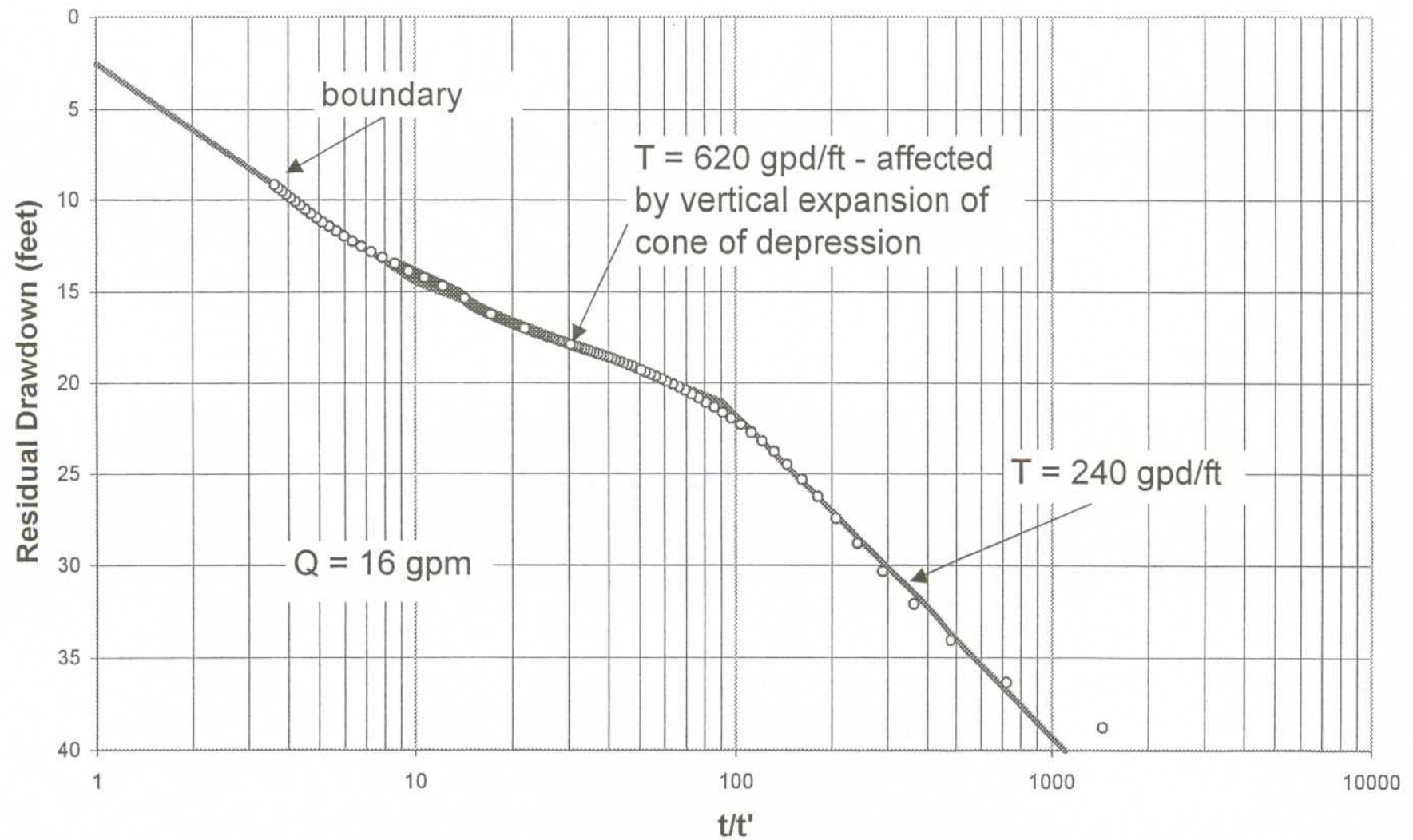


Figure 3. Well R-26 Screen 1 Trial 1 Recovery  
Hantush Solution For Anisotropy of 1.0

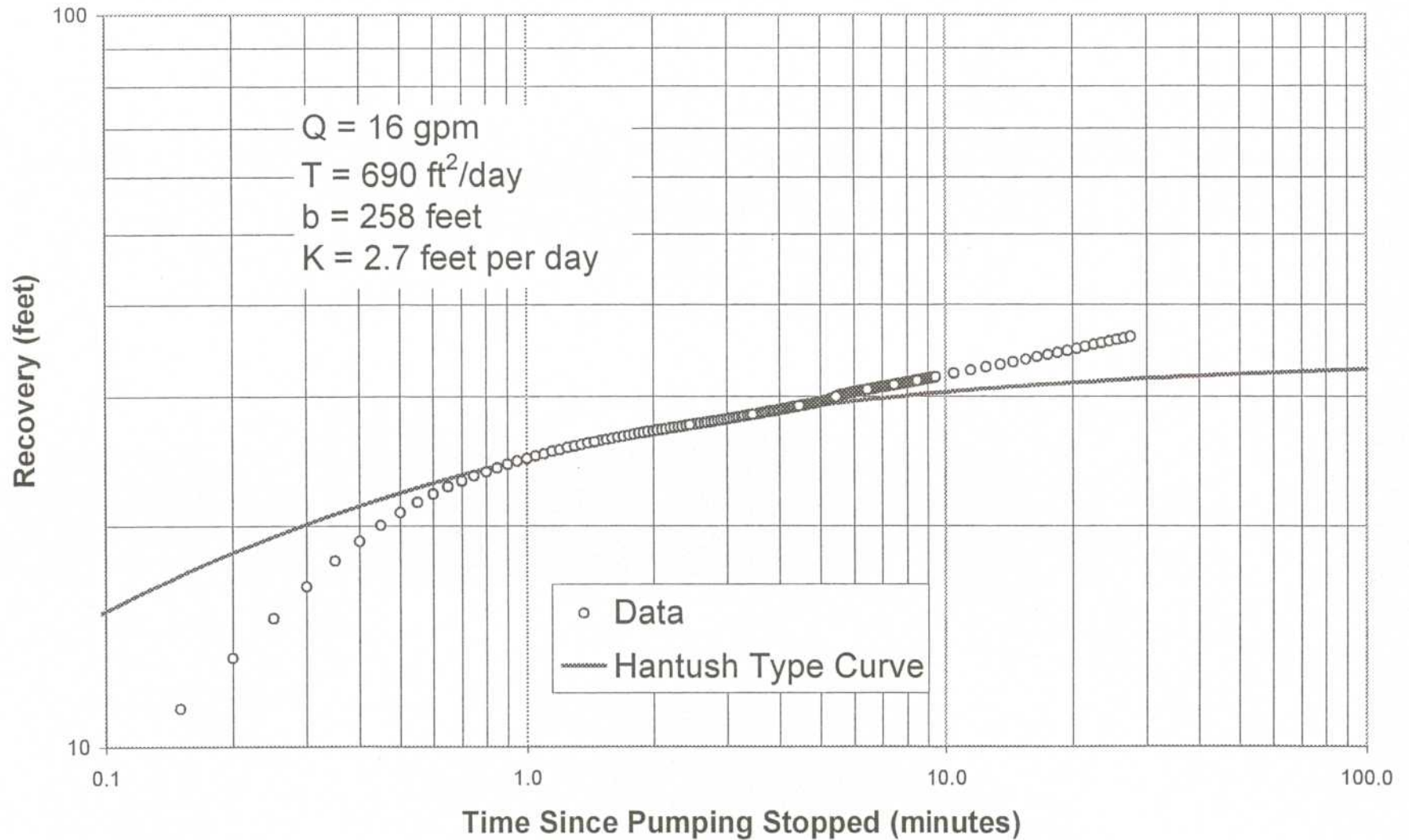


Figure 4. Well R-26 Screen 1 Trial 1 Recovery  
Hantush Solution For Anisotropy of 0.1

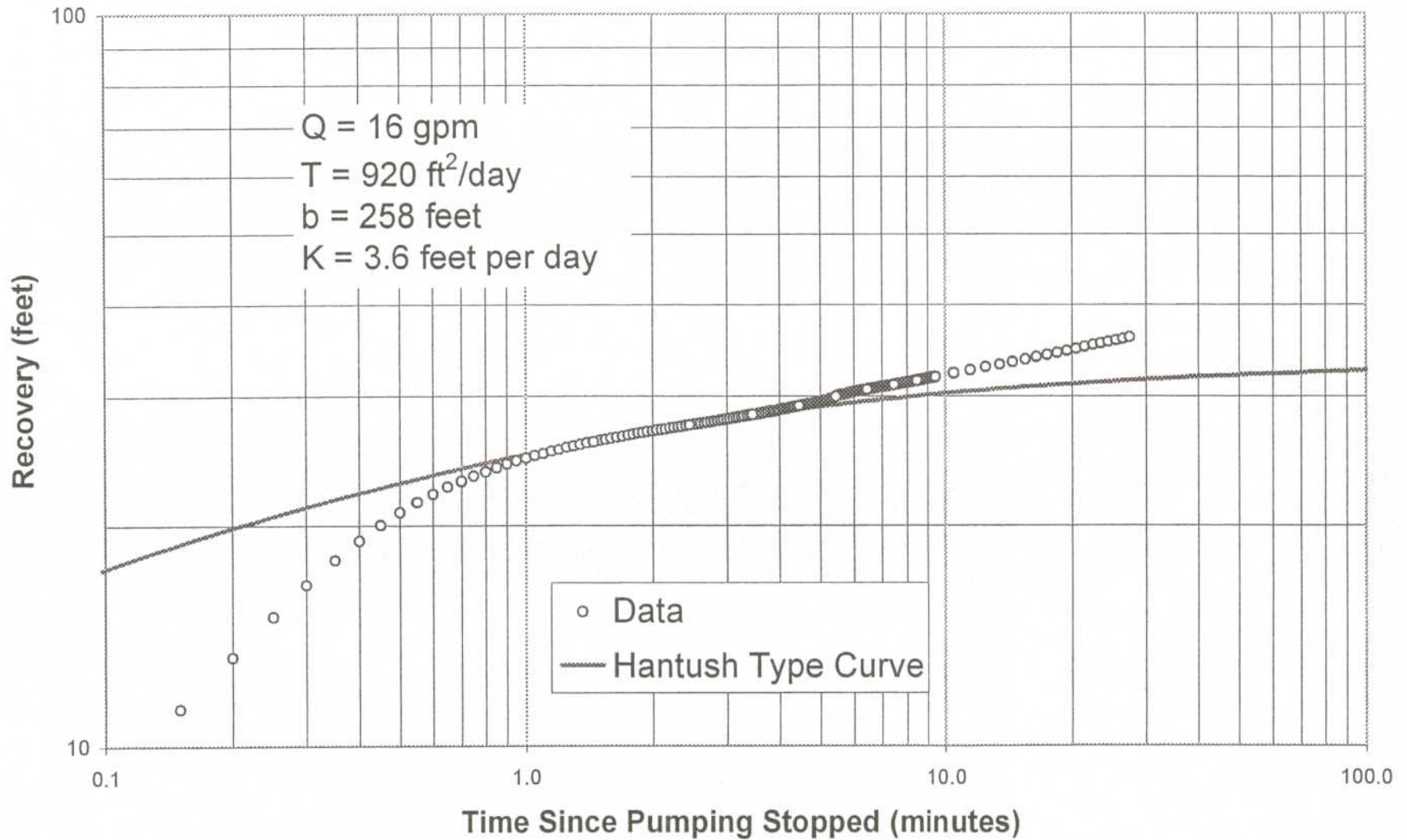


Figure 5. Well R-26 Screen 1 Trial 1 Recovery  
Hantush Solution For Anisotropy of 0.01

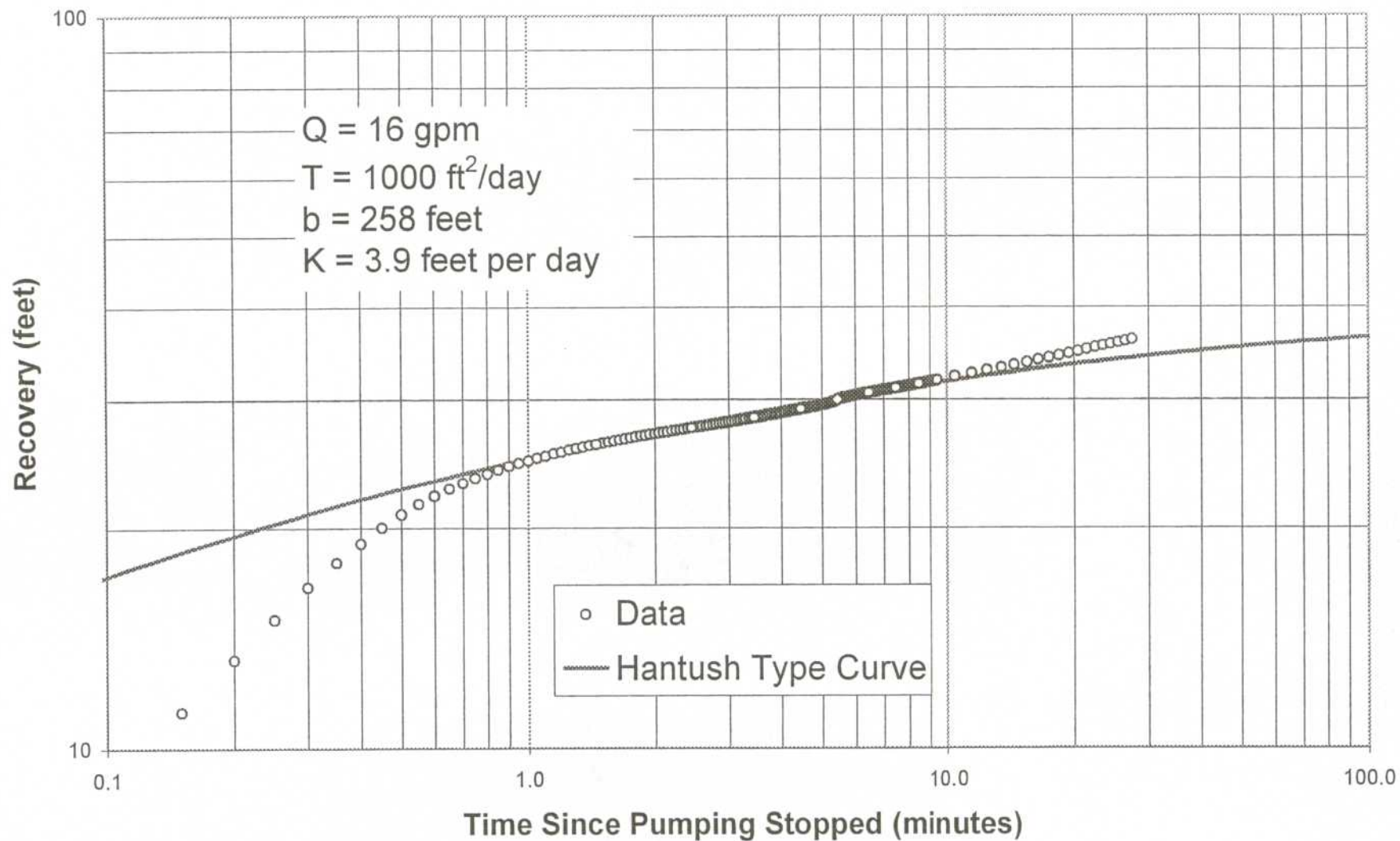


Figure 6. Well R-26 Screen 1 - Trial 2 Recovery

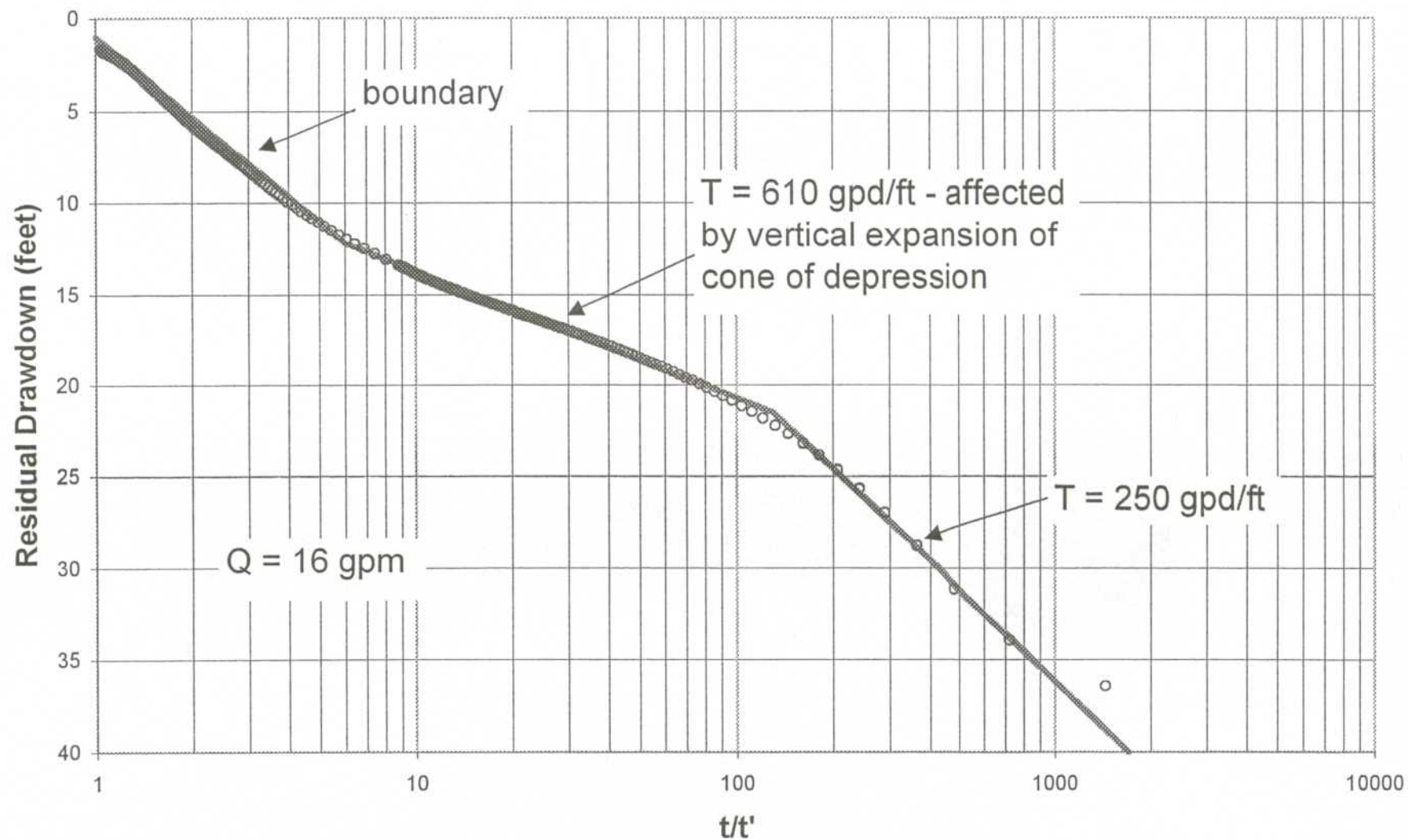


Figure 7. Well R-26 Screen 1 Trial 2 Recovery  
Hantush Solution For Anisotropy of 1.0

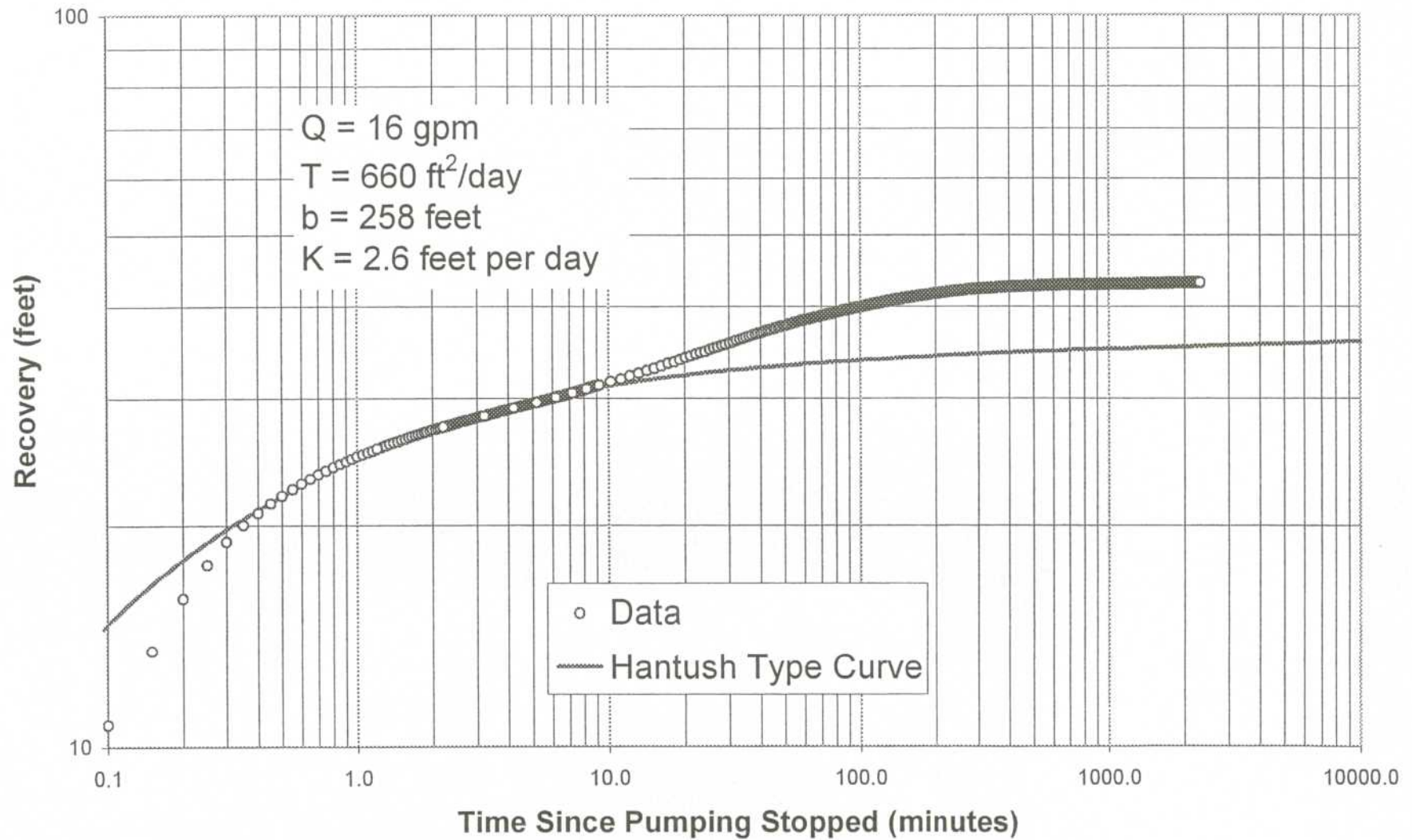


Figure 8. Well R-26 Screen 1 Trial 2 Recovery  
Hantush Solution For Anisotropy of 0.1

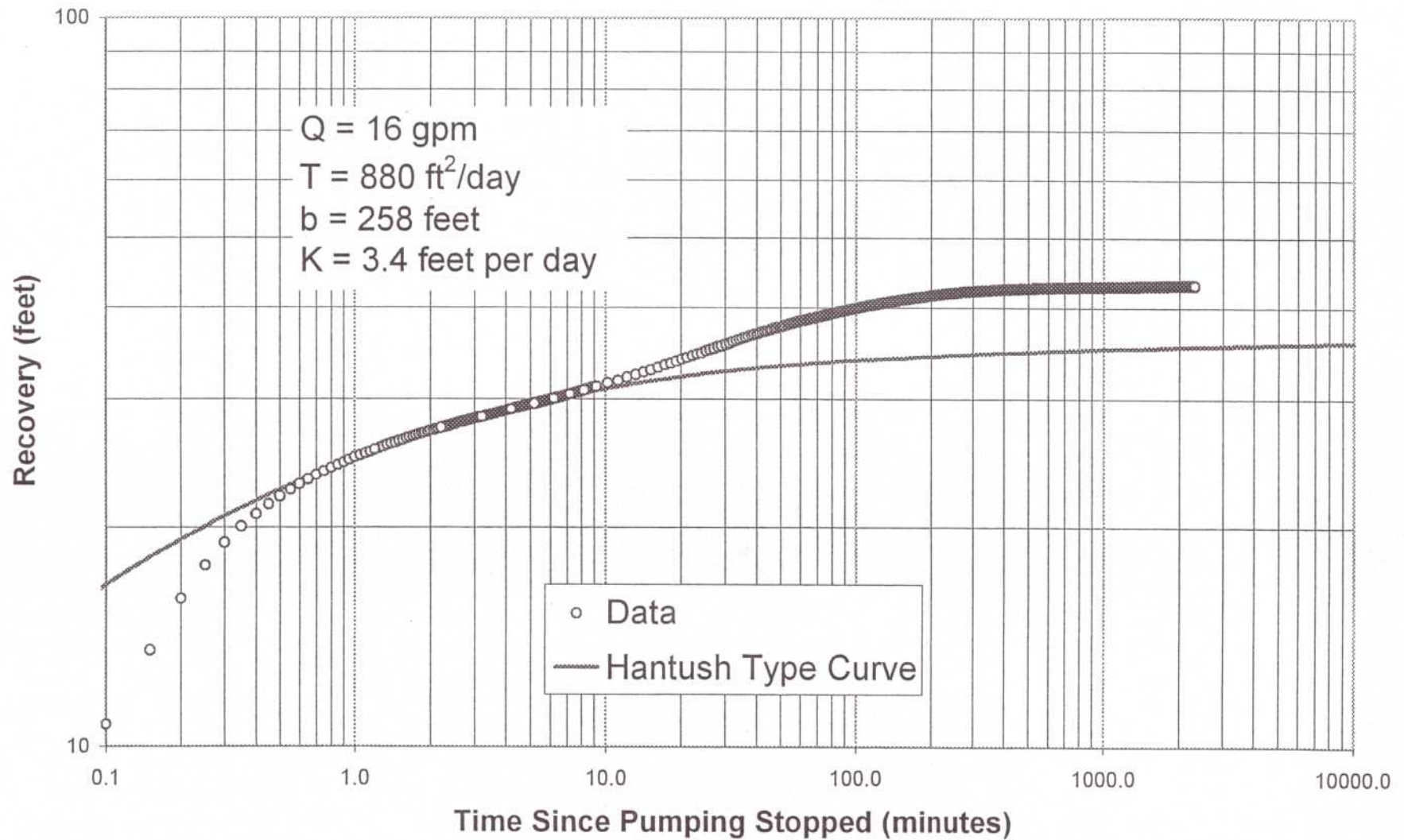


Figure 9. Well R-26 Screen 1 Trial 2 Recovery  
Hantush Solution For Anisotropy of 0.01

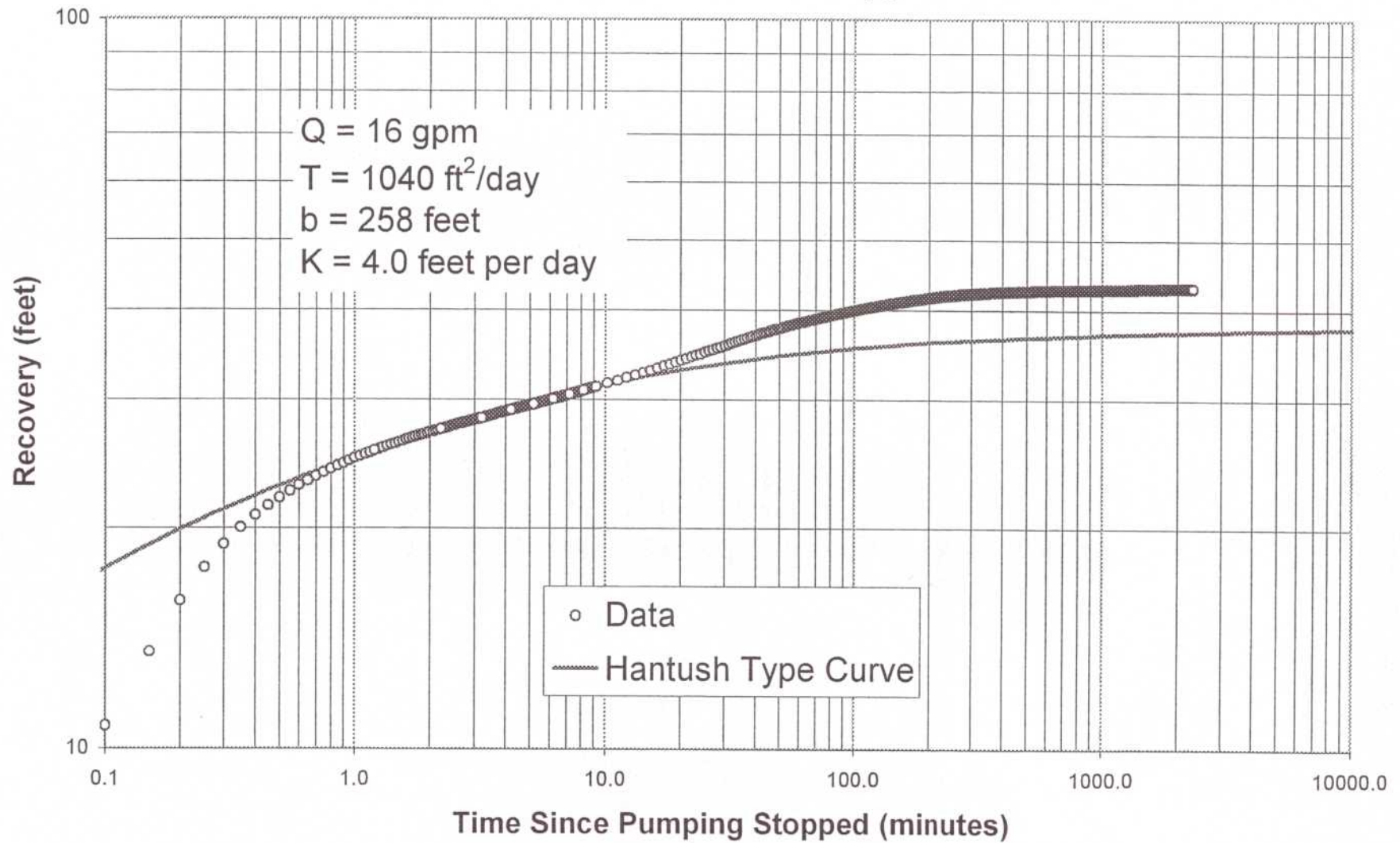


Figure 10. Well R-26 Screen 1 Drawdown - Linear Plot

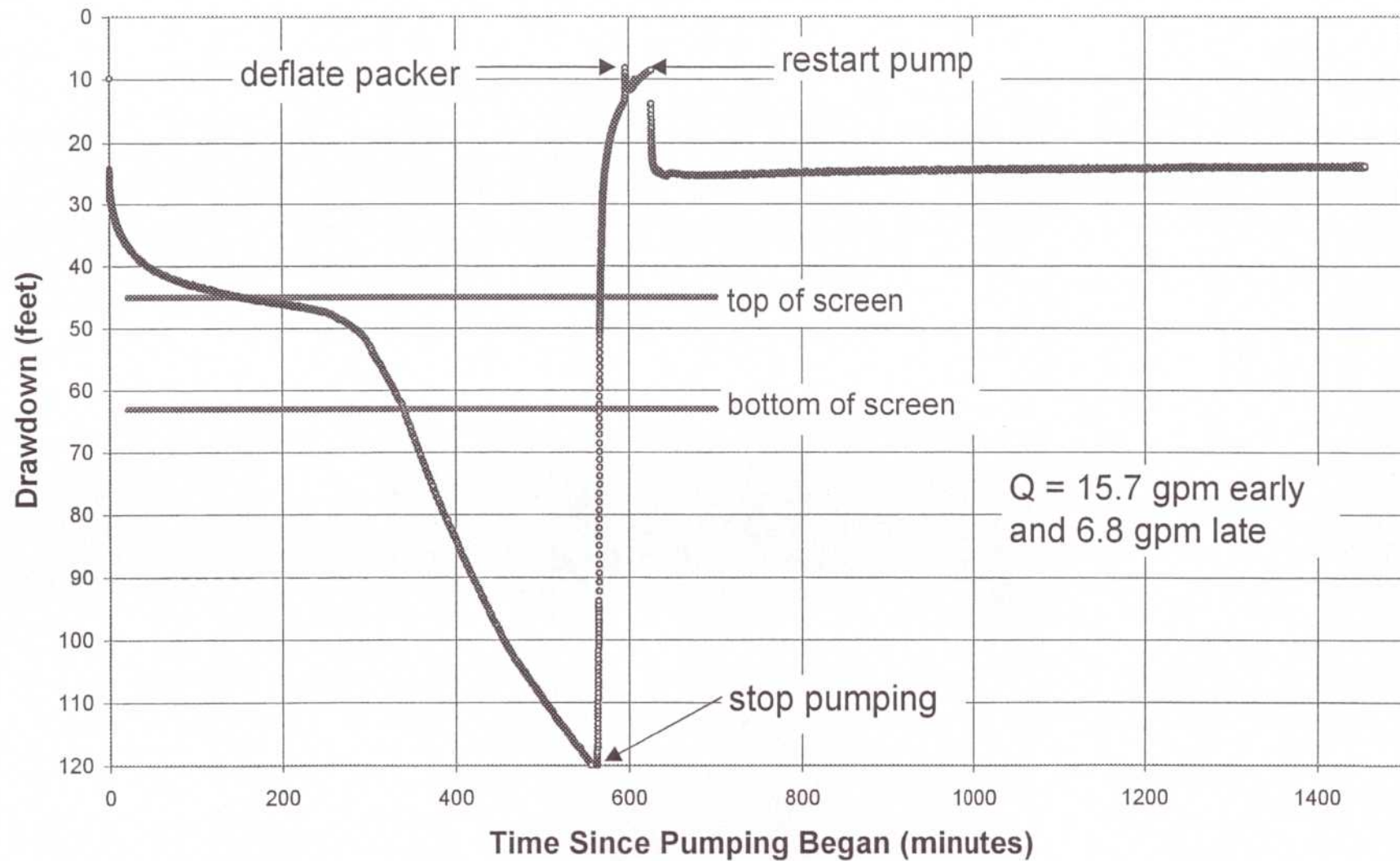


Figure 11. Well R-26 Screen 1 Drawdown - Expanded Scale

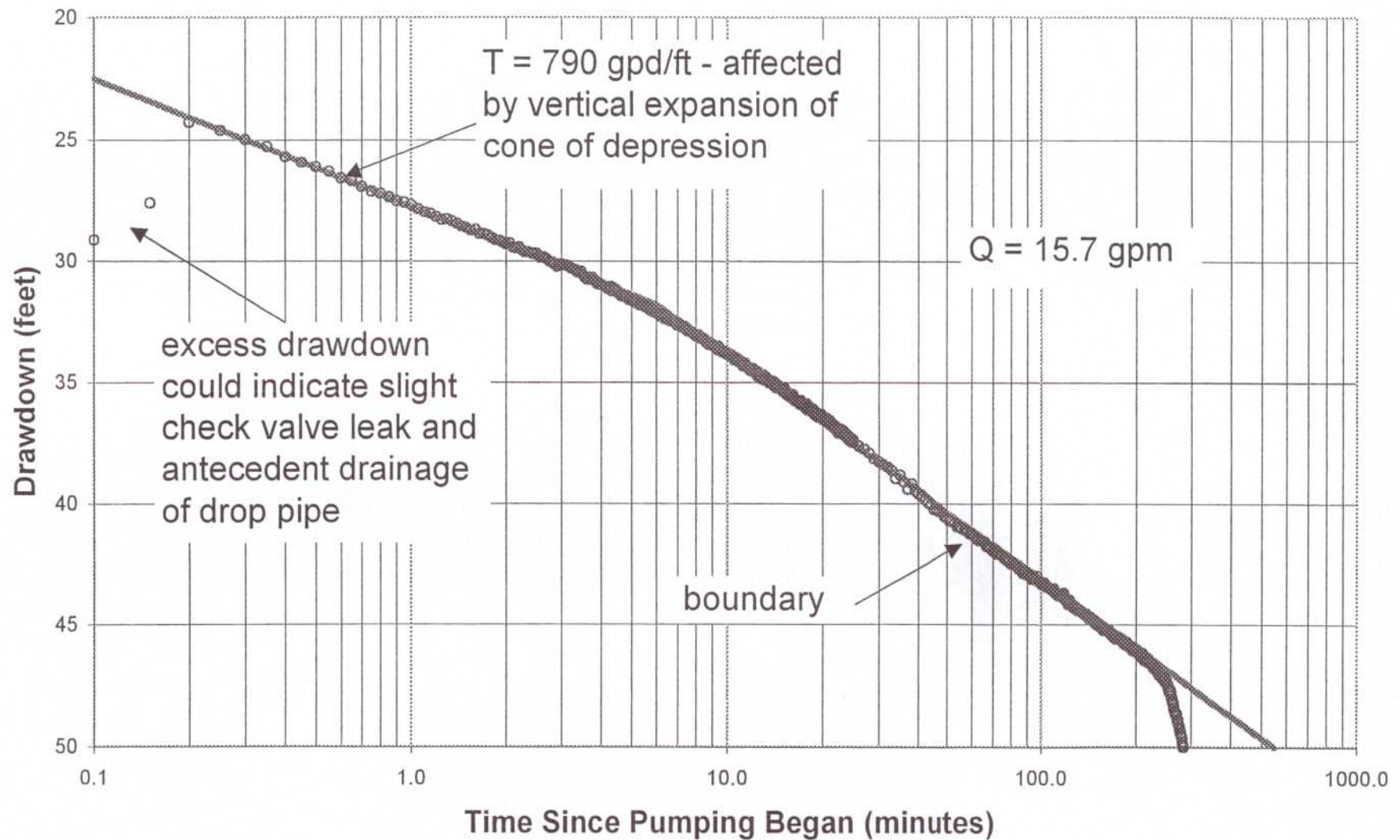


Figure 12. Well R-26 Screen 1 Pumping  
Hantush Solution For Anisotropy of 1.0

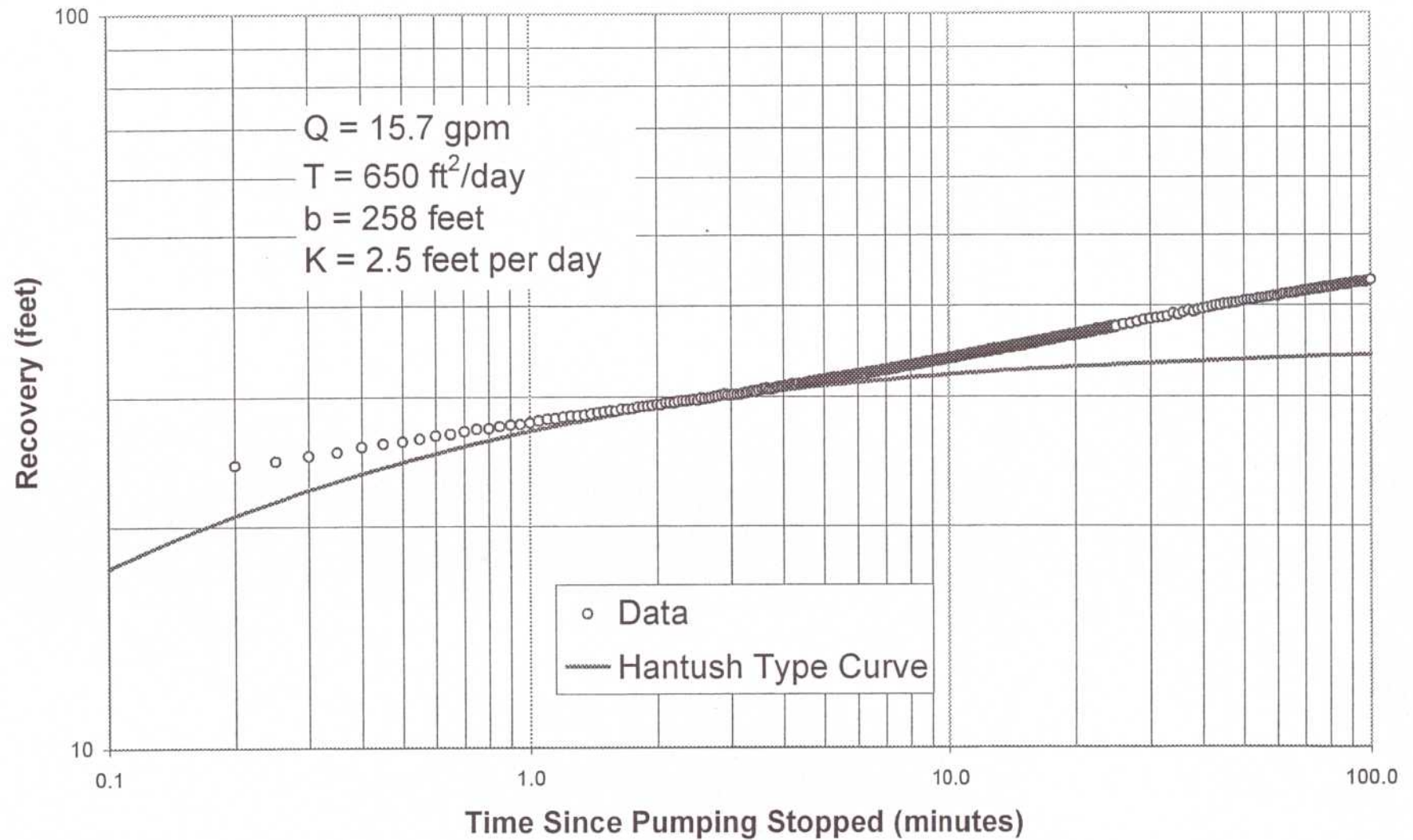


Figure 13. Well R-26 Screen 1 Pumping  
Hantush Solution For Anisotropy of 0.1

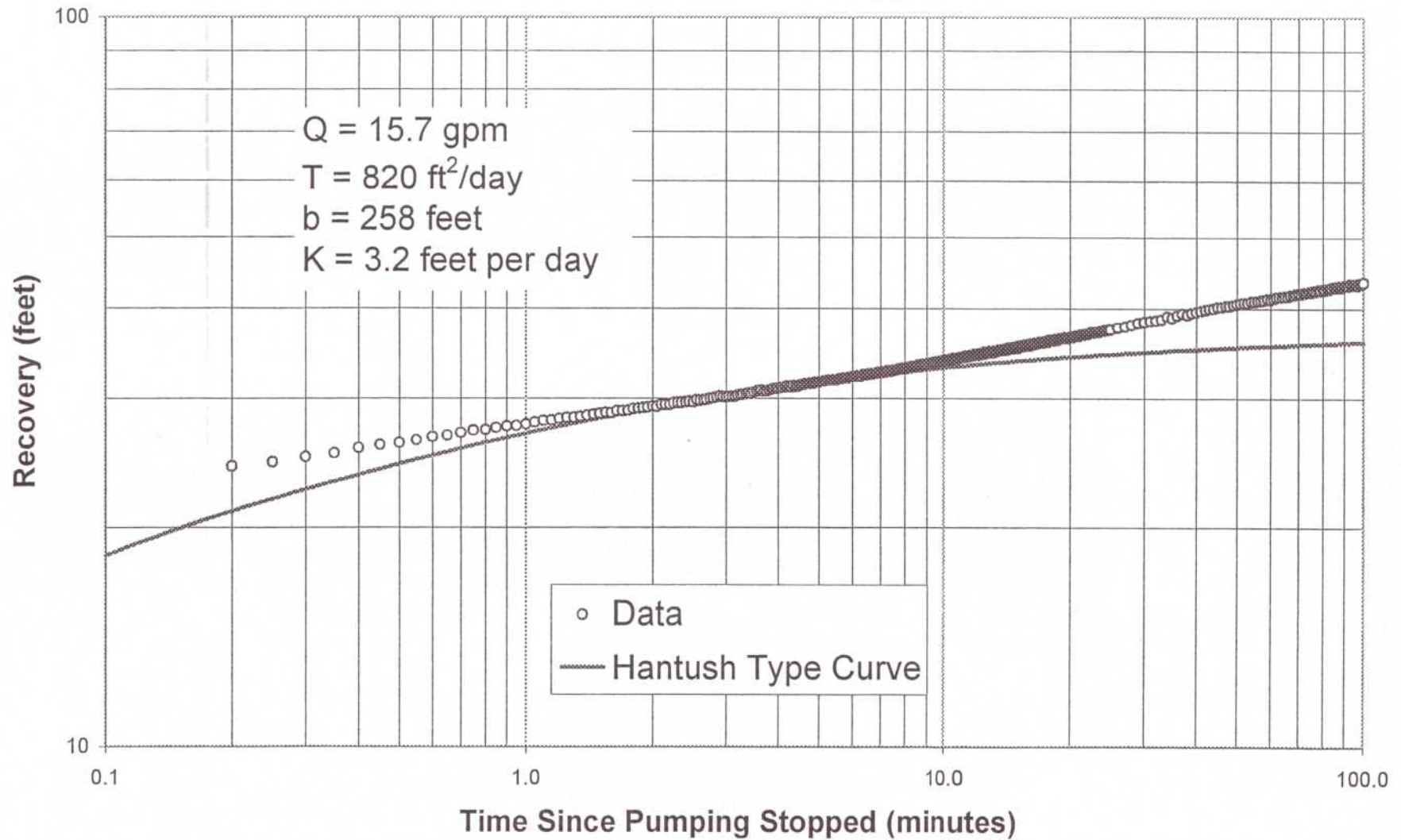


Figure 14. Well R-26 Screen 1 Pumping  
Hantush Solution For Anisotropy of 0.01

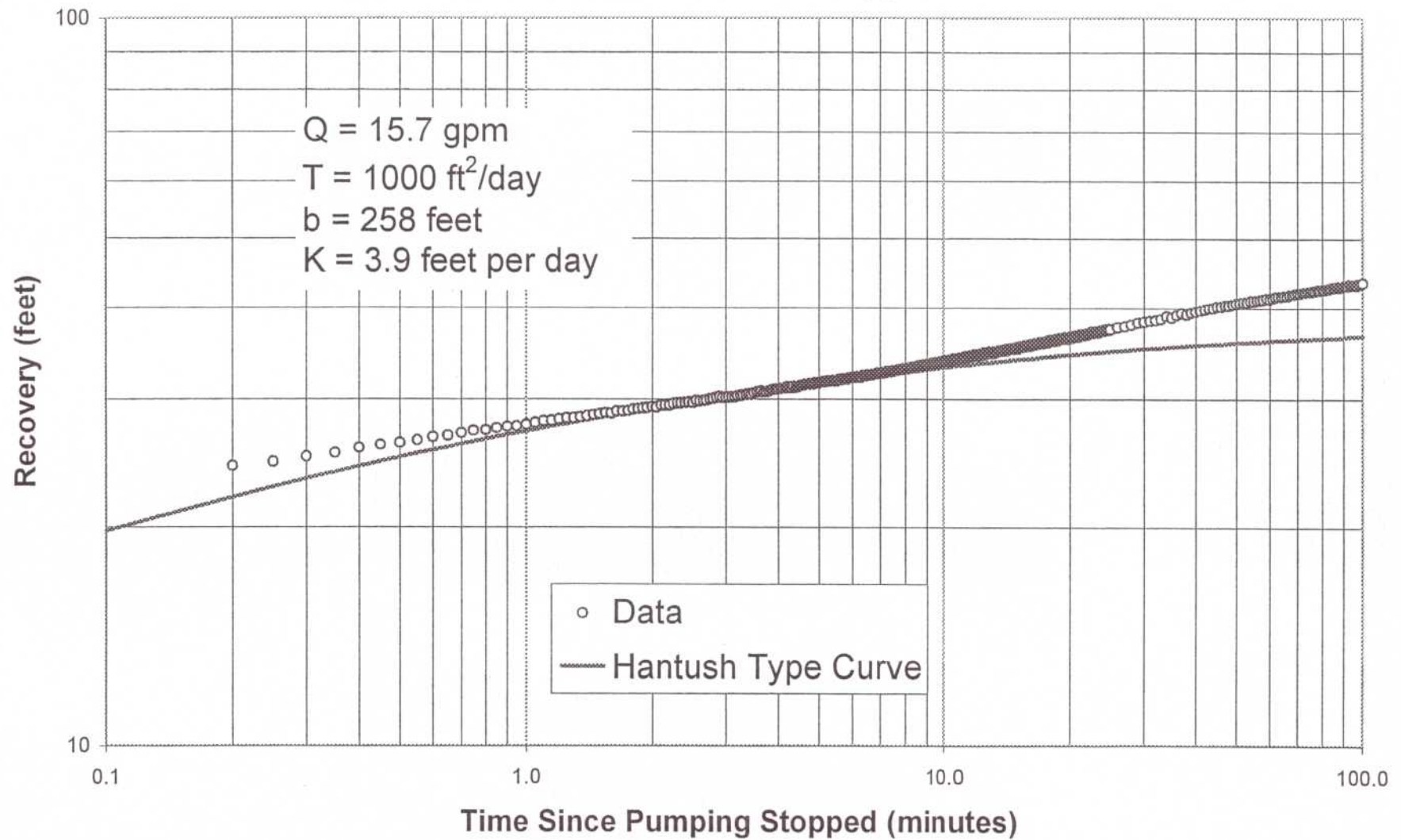


Figure 15. Well 26 Screen 1 Drawdown After Restart

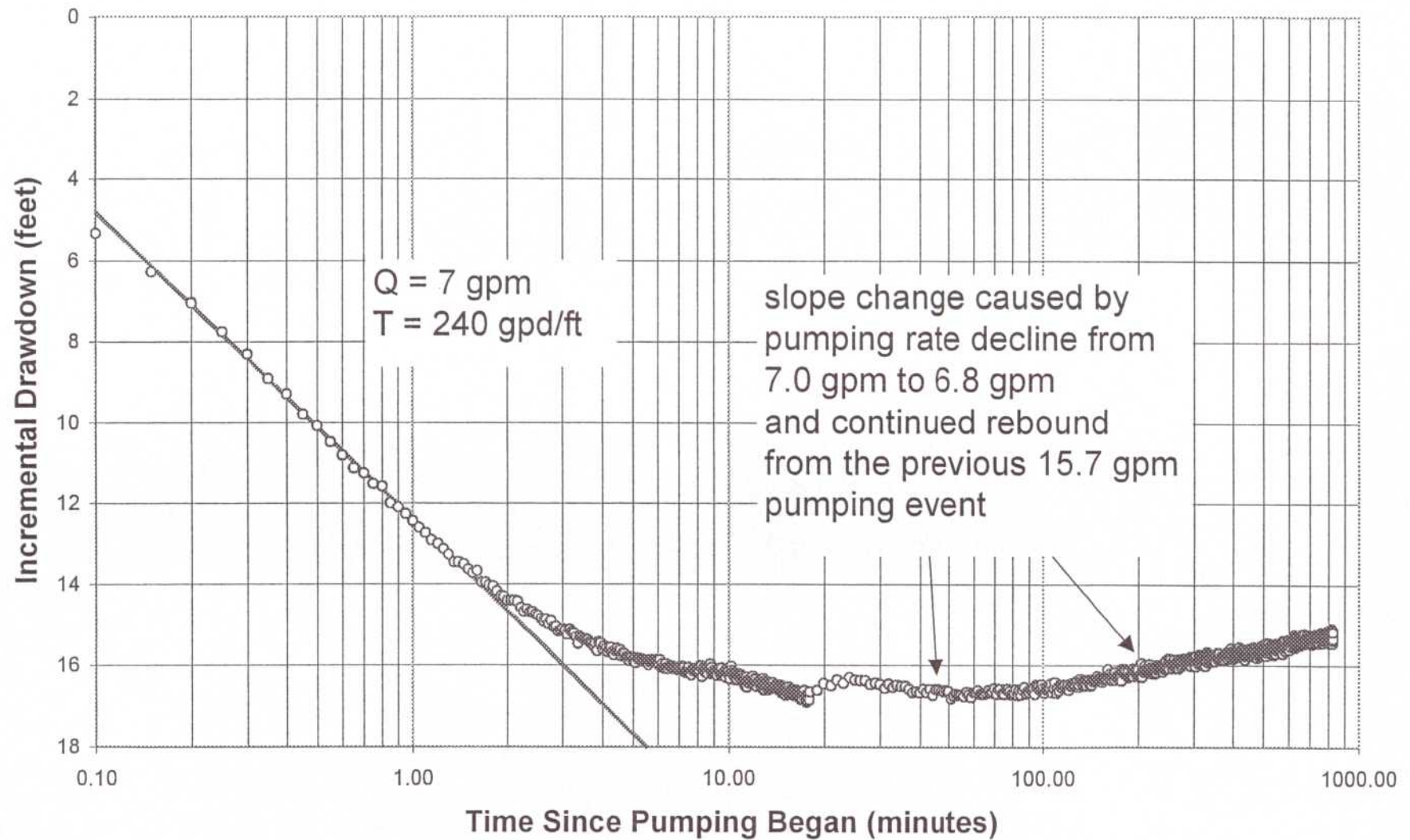


Figure 16. Well R-26 Screen 1 Restart  
Hantush Solution For Anisotropy of 1.0

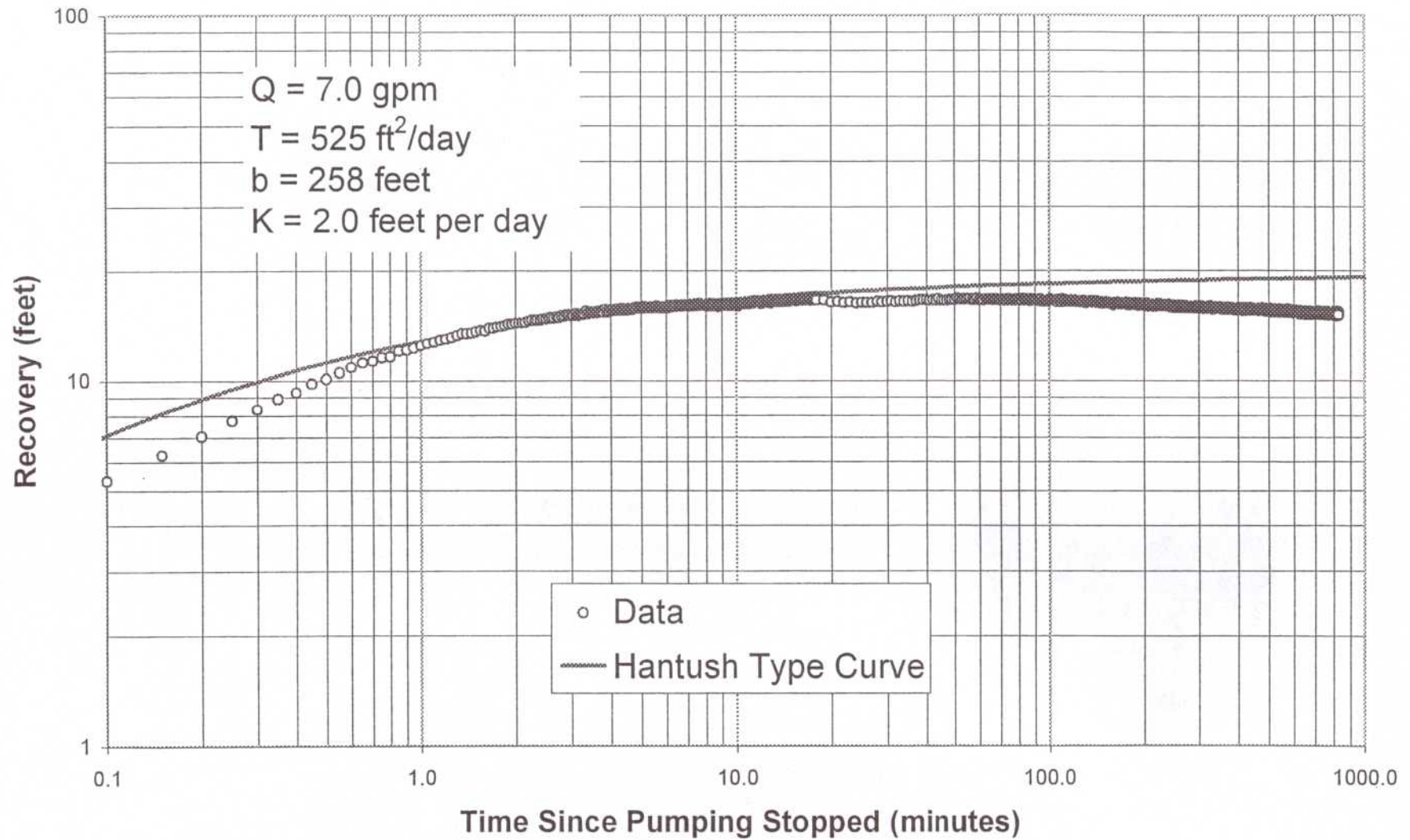


Figure 17. Well R-26 Screen 1 Restart  
Hantush Solution For Anisotropy of 0.1

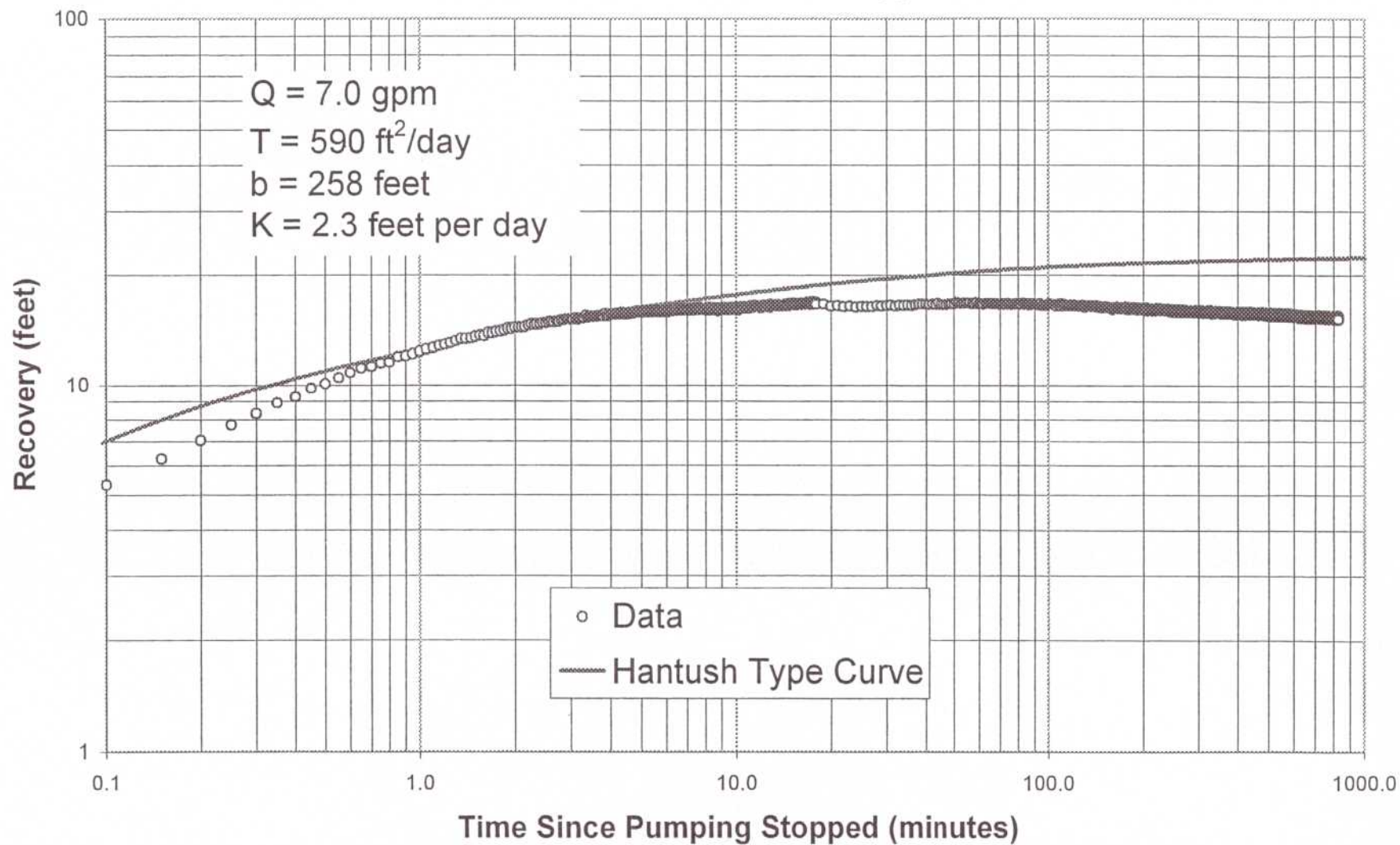


Figure 18. Well R-26 Screen 1 Restart  
Hantush Solution For Anisotropy of 0.01

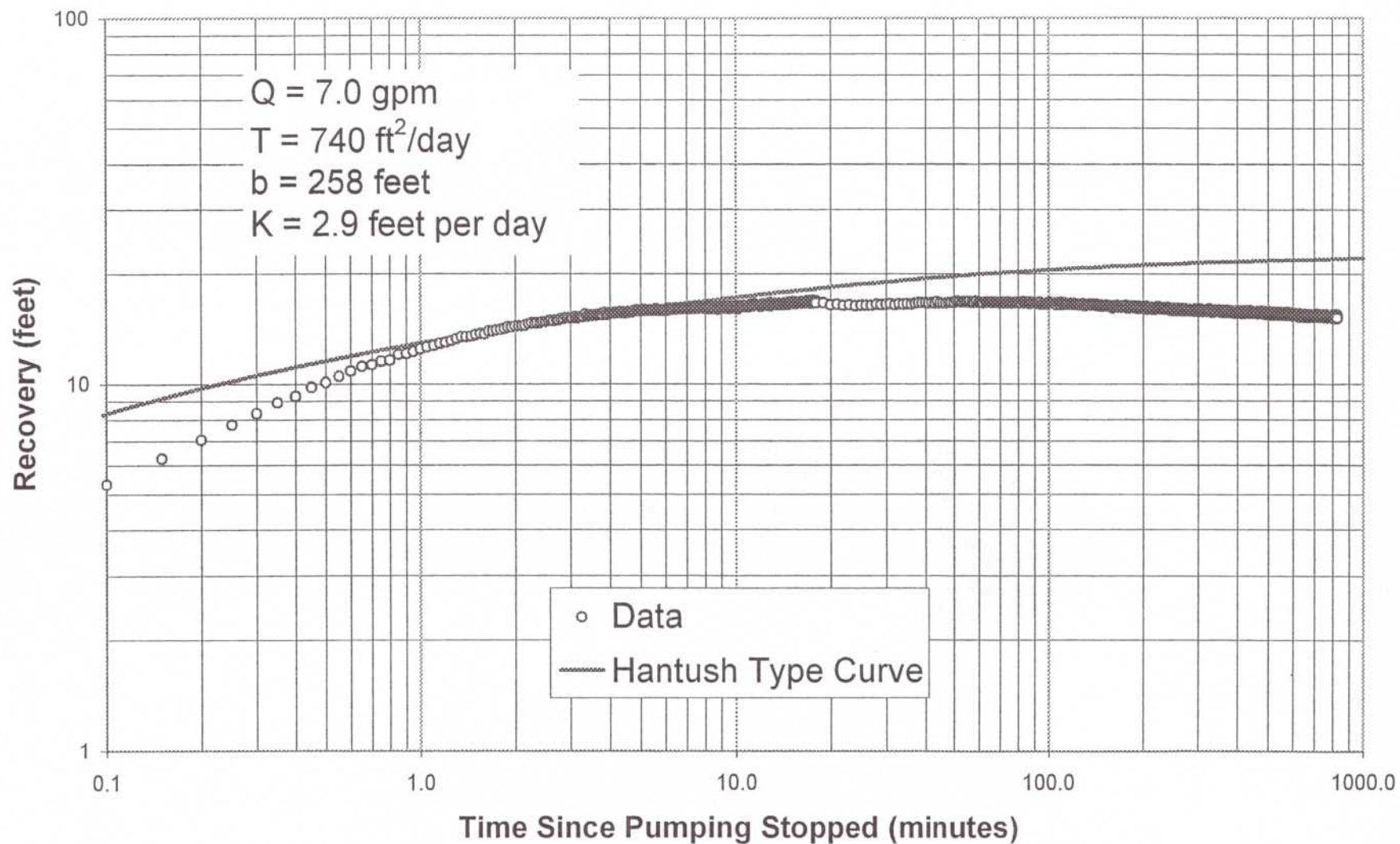


Figure 19. Well R-26 Screen 1 Recovery

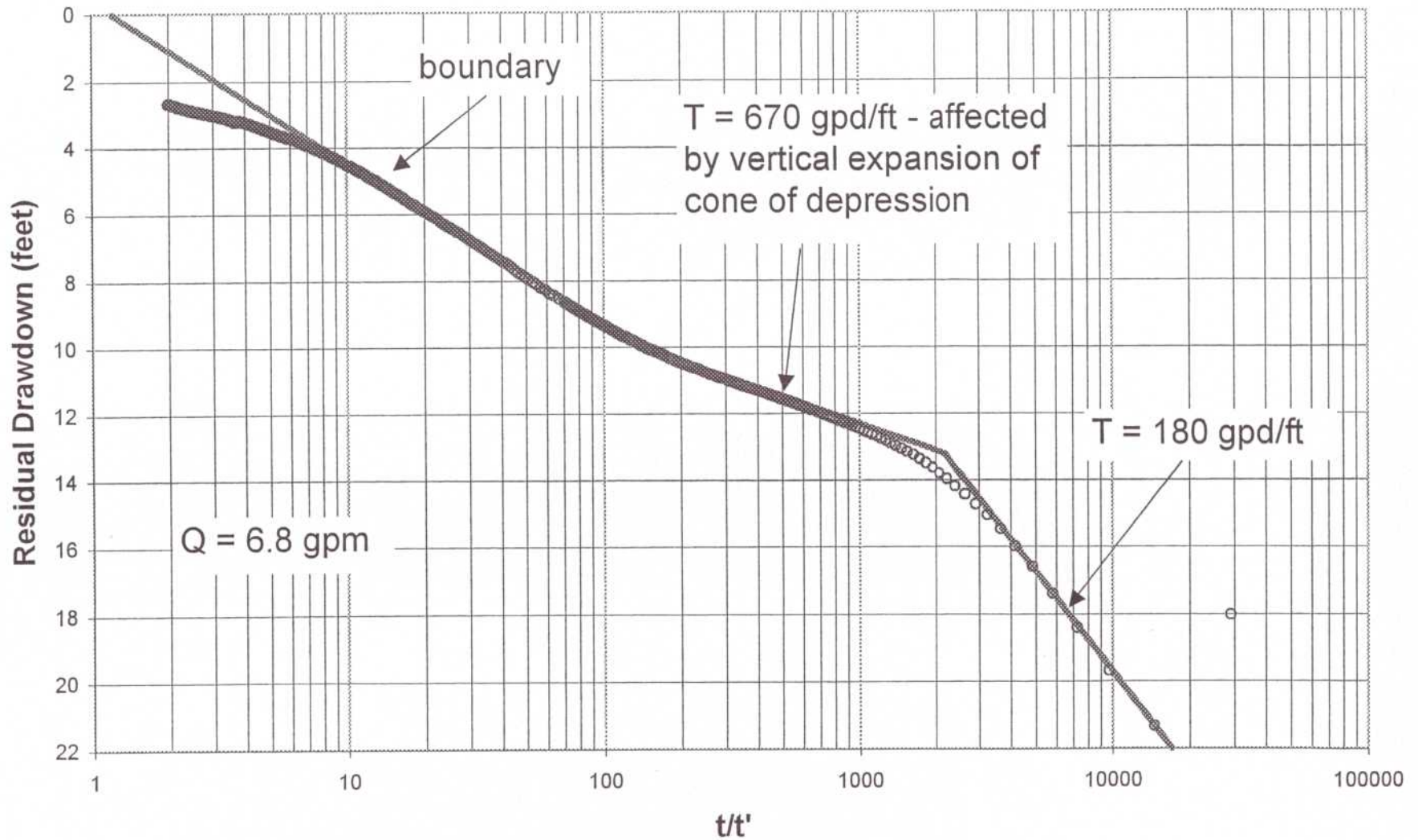


Figure 20. Well R-26 Screen 1 Recovery  
Hantush Solution For Anisotropy of 1.0

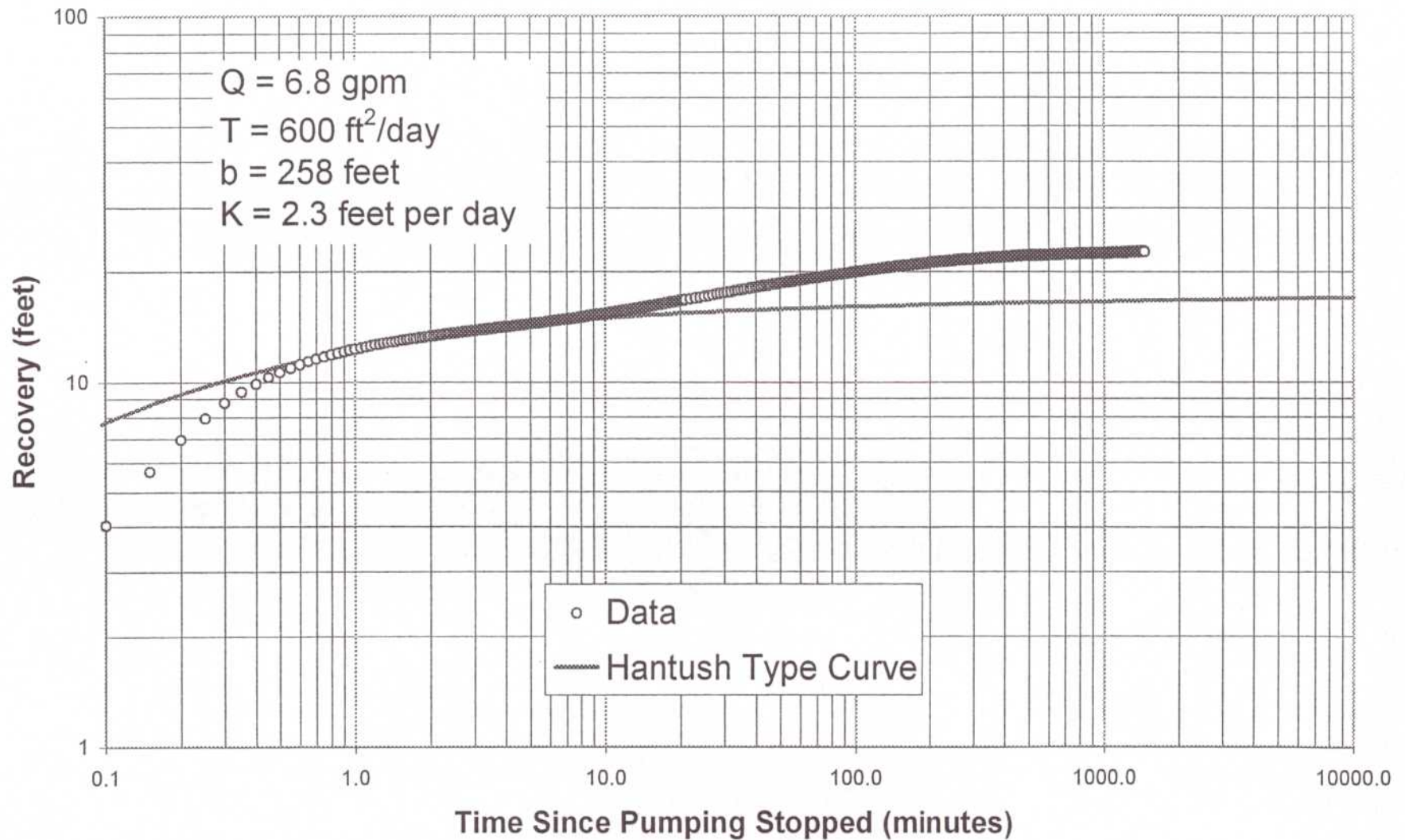


Figure 21. Well R-26 Screen 1 Recovery  
Hantush Solution For Anisotropy of 0.1

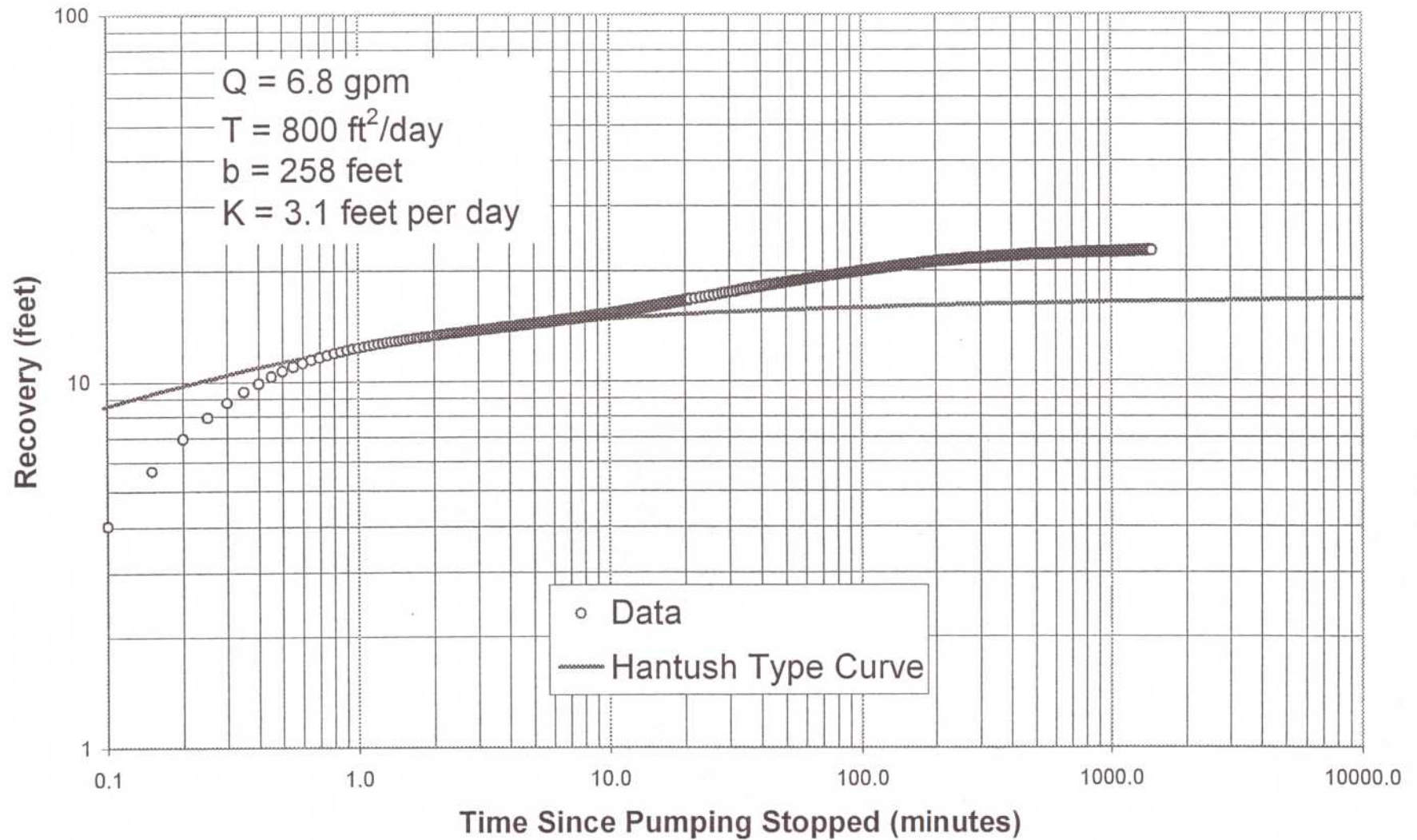


Figure 22. Well R-26 Screen 1 Recovery  
Hantush Solution For Anisotropy of 0.01

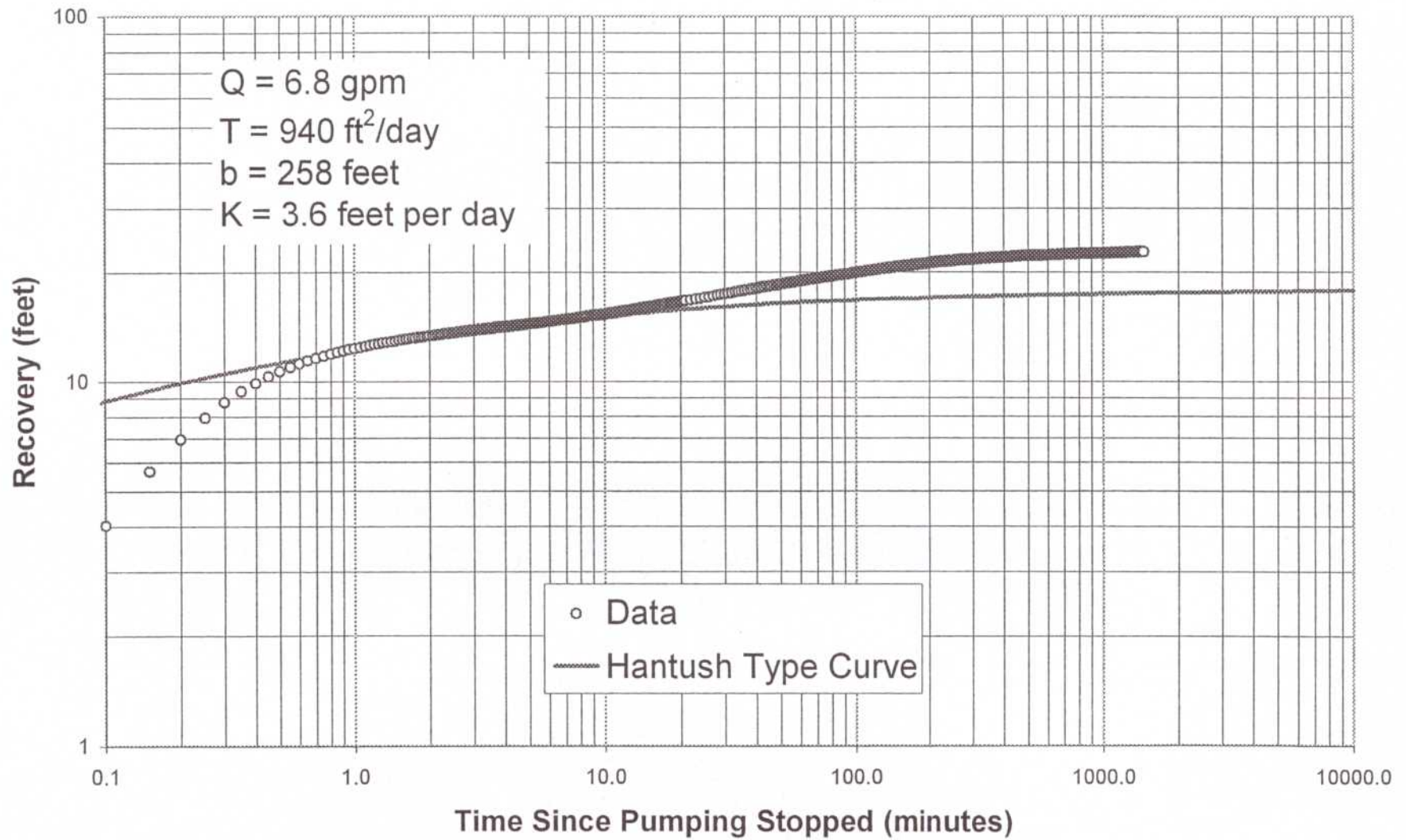


Figure 23. Well R-26 Screen 2 Preliminary Test

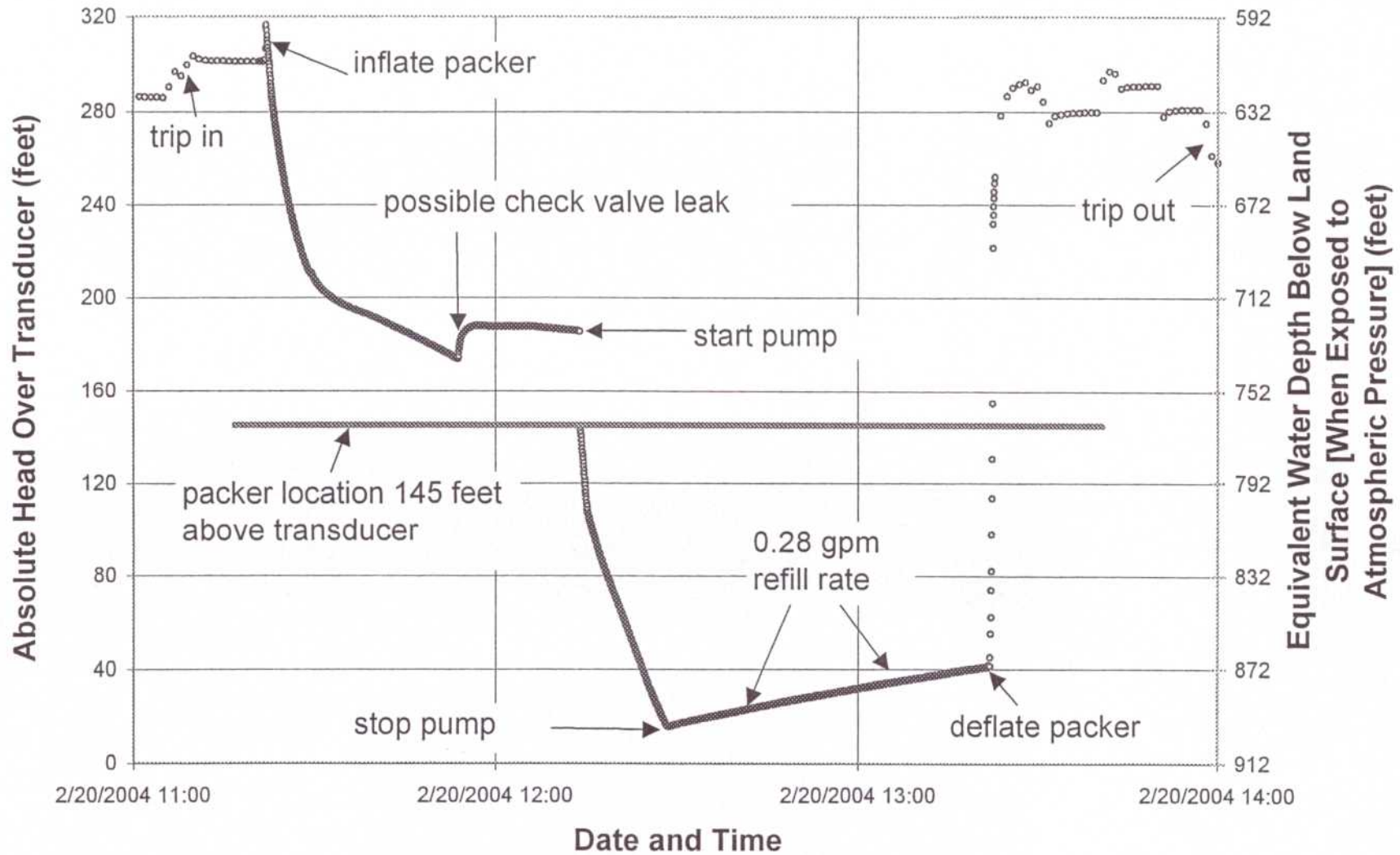


Figure 24. Well R-26 Screen 2 Shut In Recovery Data

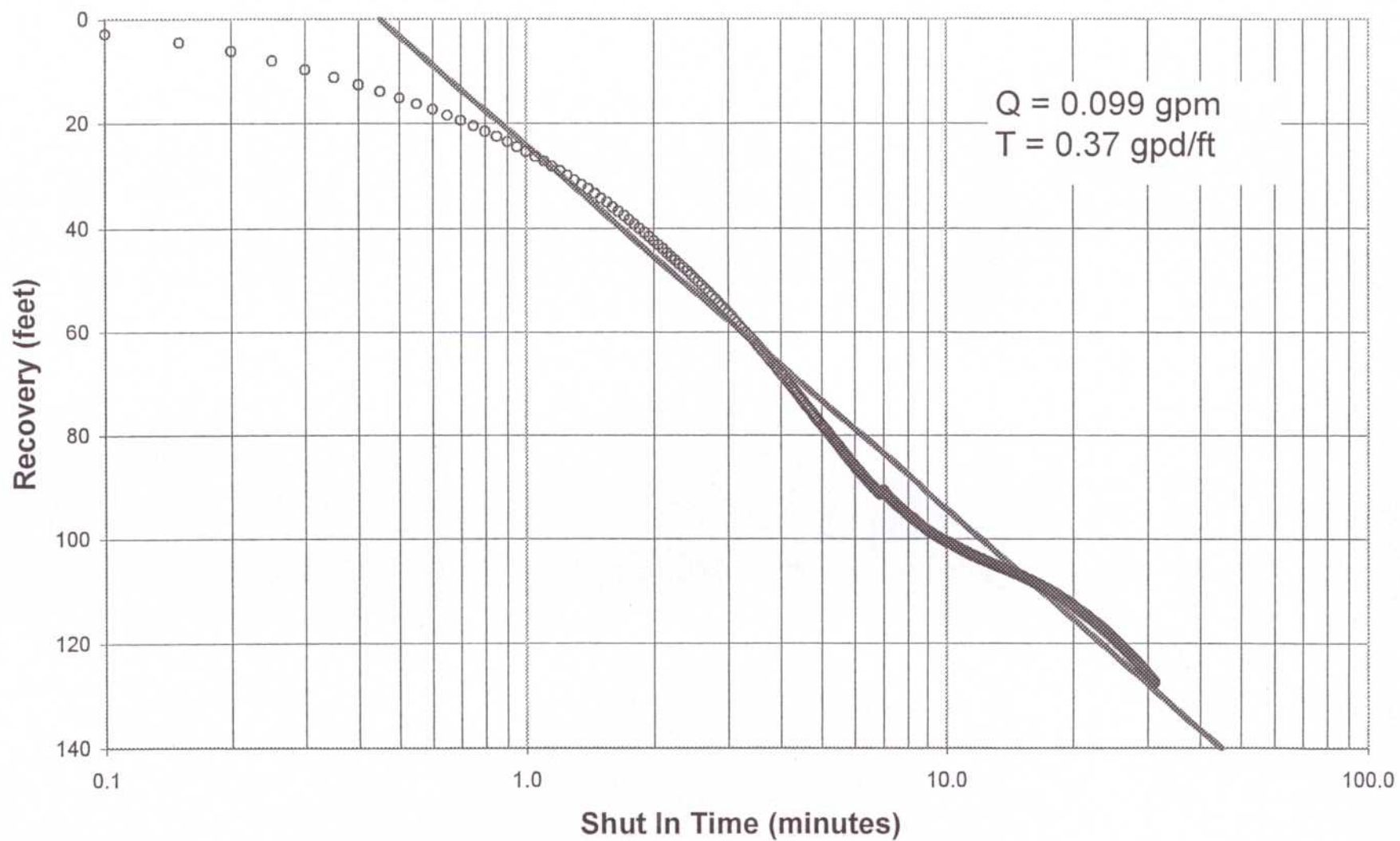


Figure 25. Log-Log Plot of Well R-26 Screen 2 Shut In Data

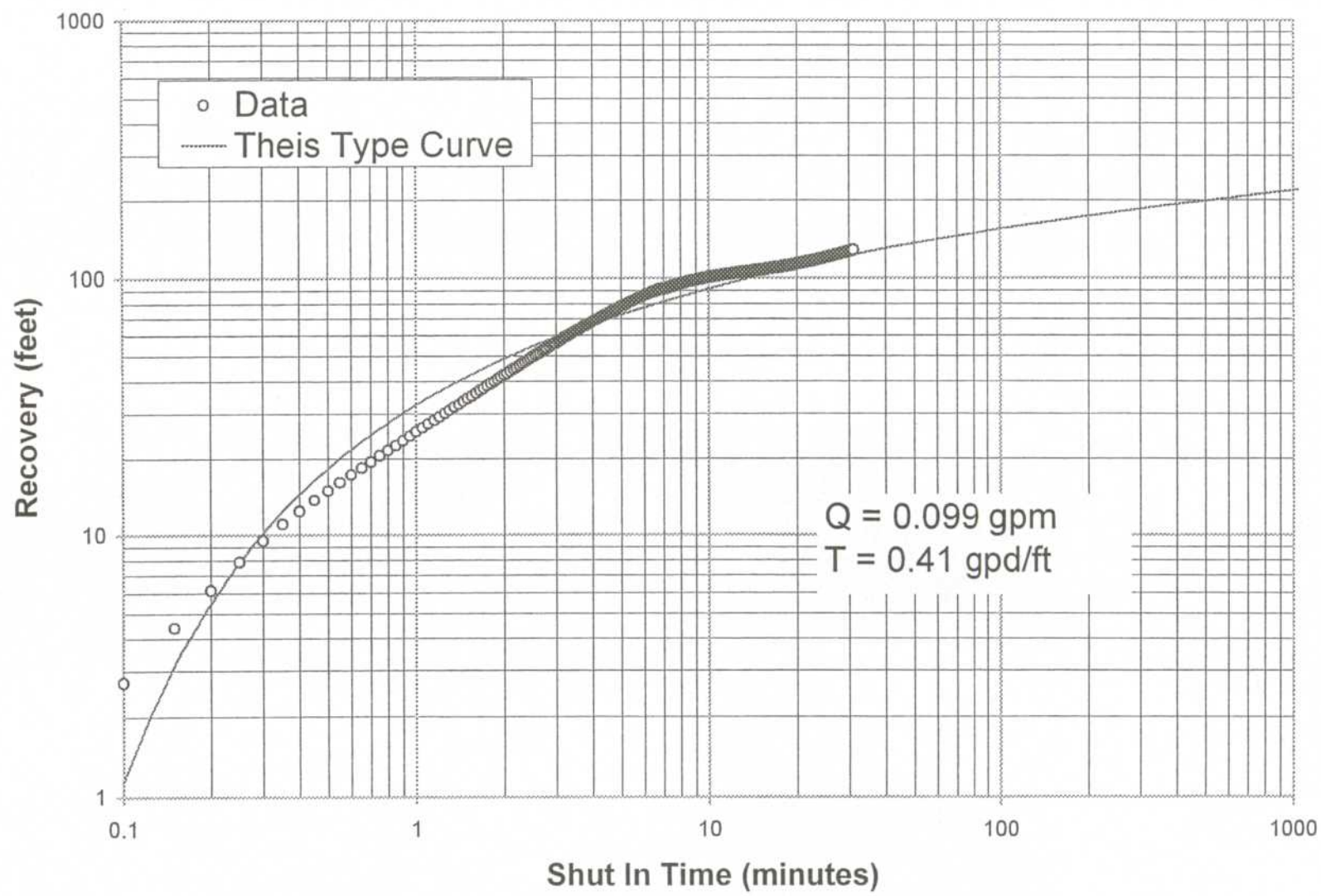


Figure 26. Well R-26 Screen 2 Long Term Test

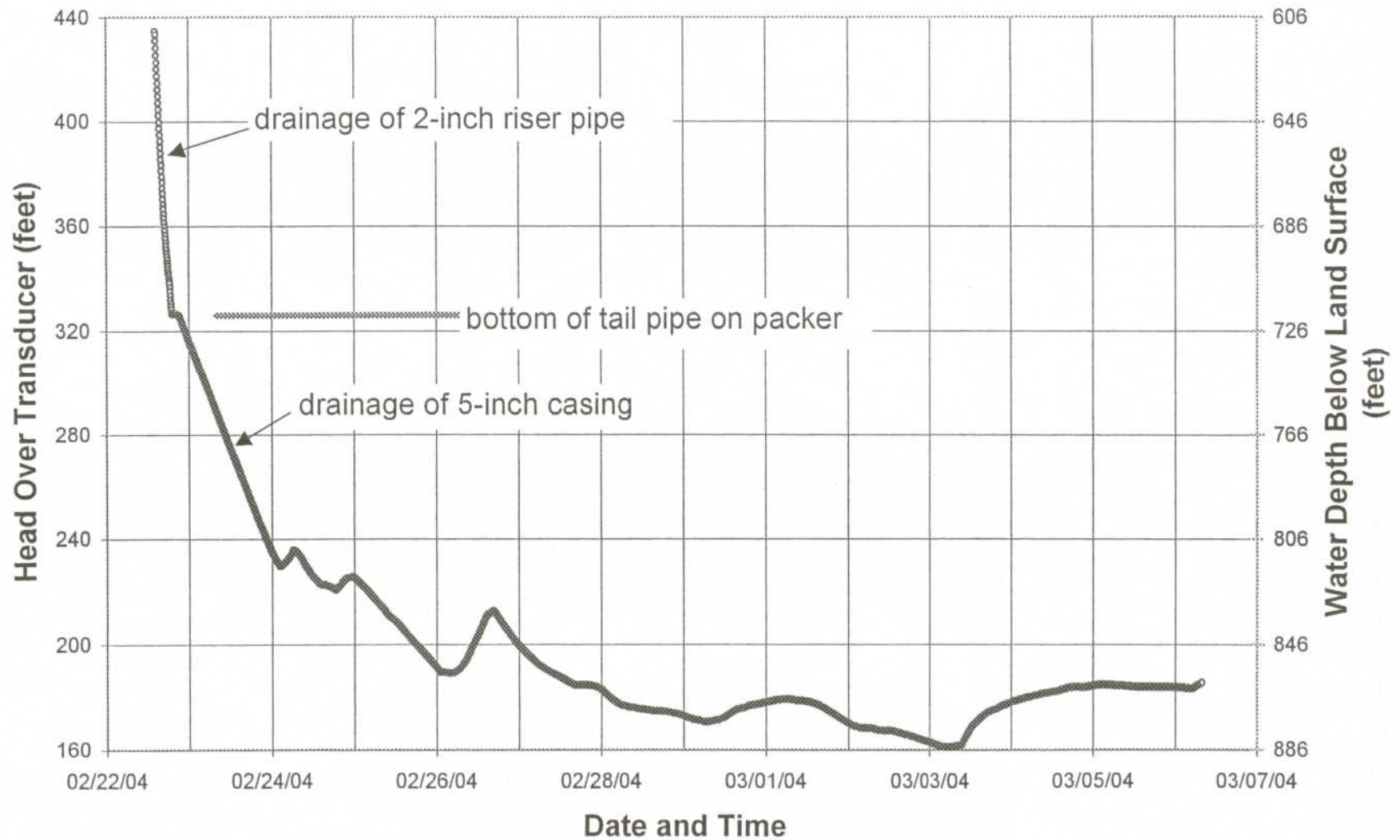


Figure 27. Well R-26 Screen 2 Long Term Test - Expanded Scale 1

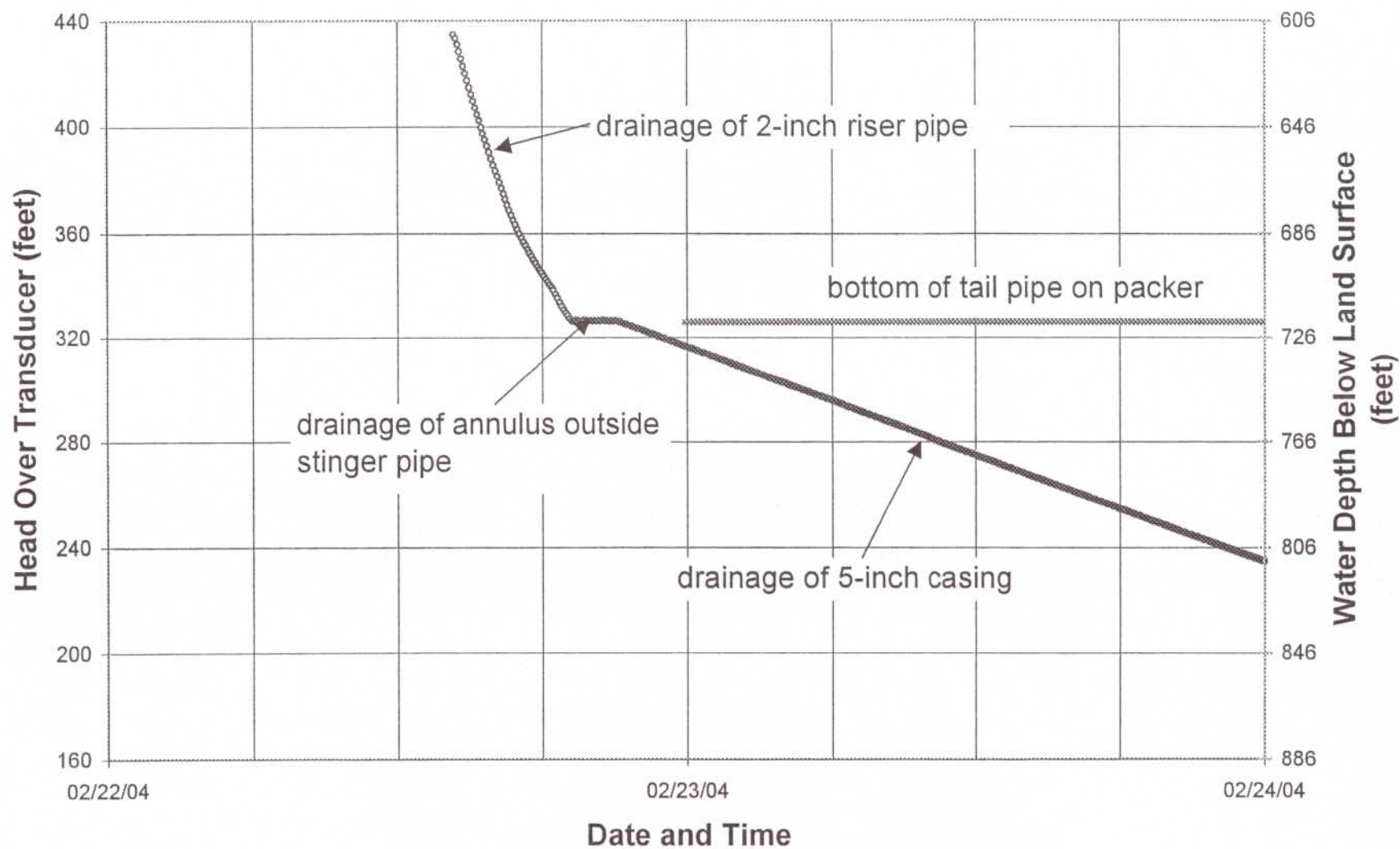


Figure 28. Well R-26 Screen 2 Long Term Test - Expanded Scale 2

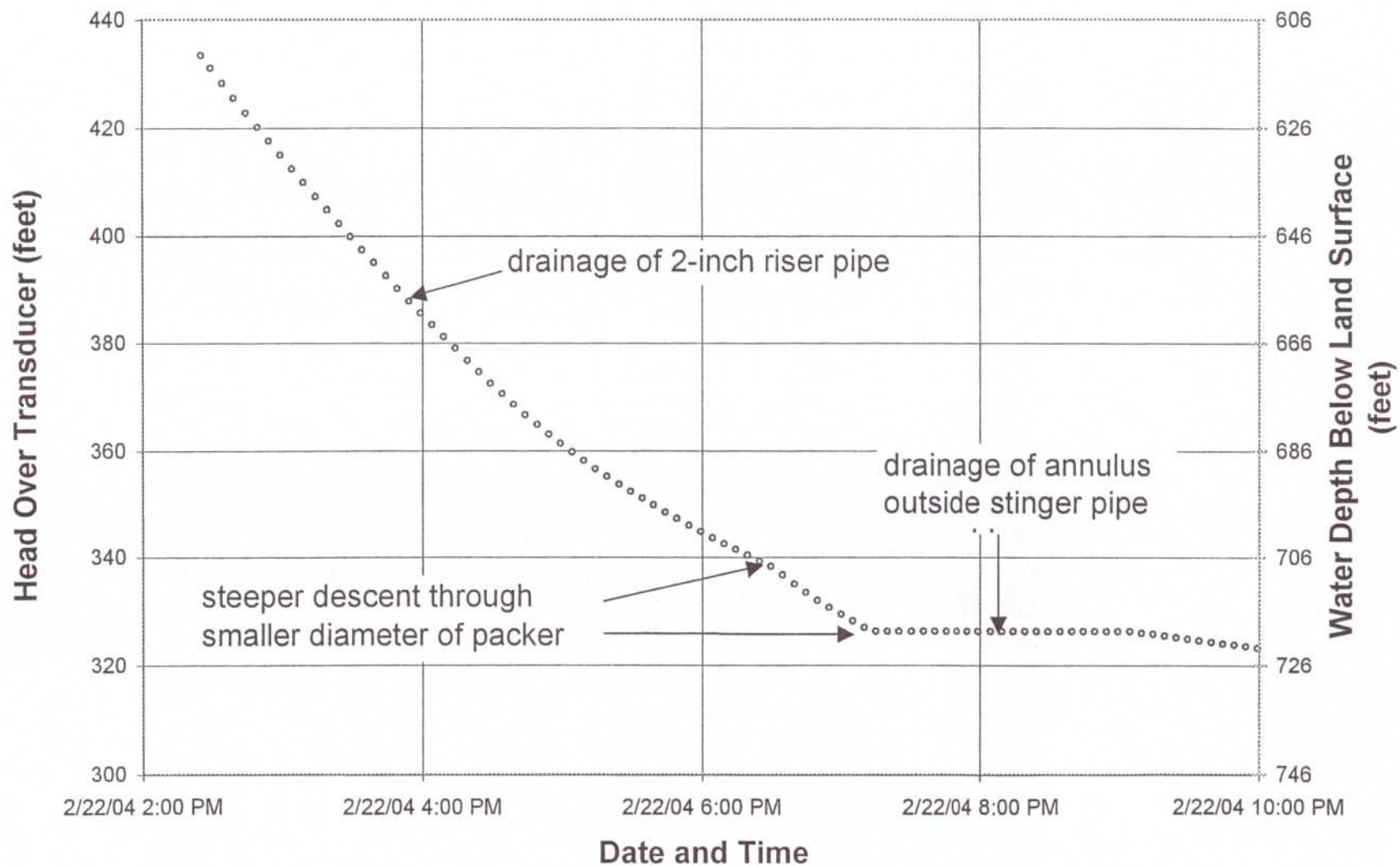


Figure 29. Well R-26 Screen 2 Long Term Test Flux Rates

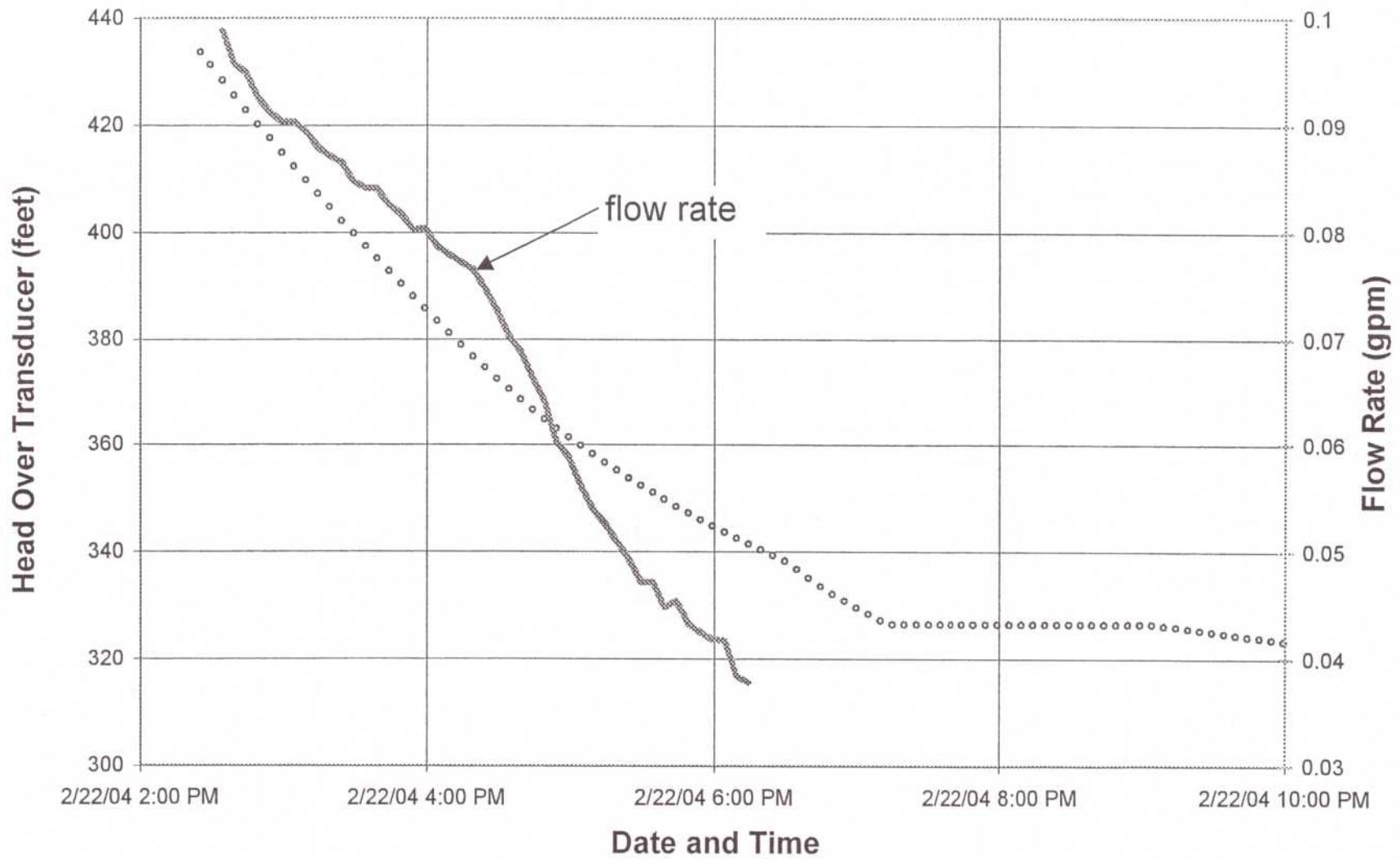
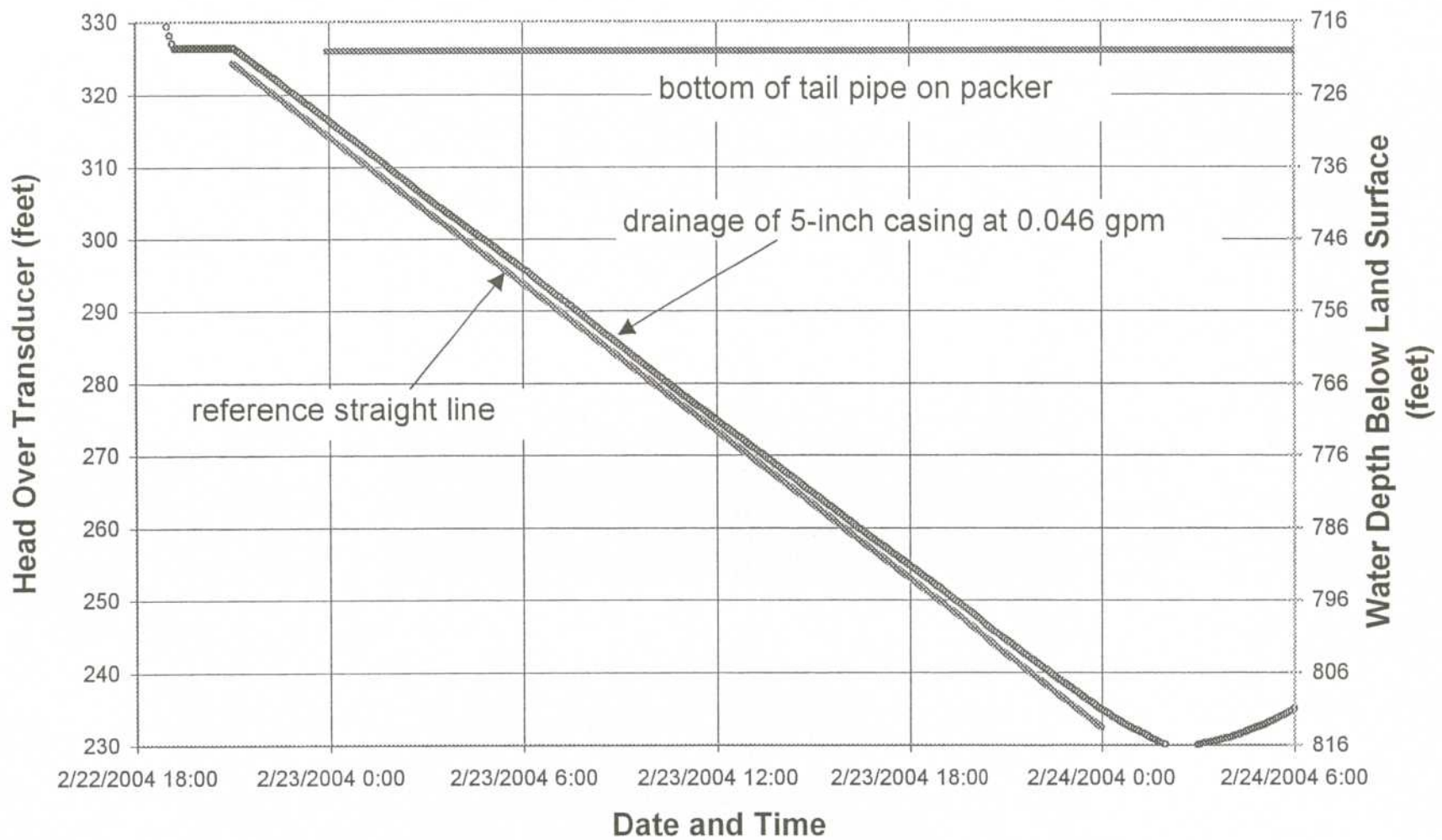


Figure 30. Well R-26 Screen 2 Long Term Test - Drainage of 5-Inch Well Casing



## **Appendix F**

---

*Westbay Installation Report  
(included on CD)*

----- Forwarded message follows -----

From: "Enz, Robert D." <renz@doeal.gov>  
To: "'meverett@kleinfelder.com'" <meverett@kleinfelder.com>,  
      "'bbockisch@kleinfelder.com'" <bbockisch@kleinfelder.com>  
Date sent: Thu, 12 Feb 2004 14:11:34 -0700  
Subject: FW: Land Application of Drilling and  
Development Water From R-26

-----Original Message-----

From: Curt Frischkorn [mailto:curt\_frischkorn@nmenv.state.nm.us]  
Sent: Wednesday, January 14, 2004 4:38 PM  
To: Enz, Robert D.; John Young@nmenv.state.nm.us  
Cc: mjohanson@doeal.gov; Whitacre, Thomas; spearson@lanl.gov; bbeers@lanl.gov  
Subject: RE: Land Application of Drilling and Development Water From R-26

Bob:

This email confirms NMED approval for the discharge of drilling and development water from regional well R-26 (described below). The drilling and development water must be discharged as described in the Hydrogeologic Workplan NOI dated July 16, 2002. If you have any questions, please contact me at 505-827-0078.

Curt Frischkorn  
NMED Ground Water Pollution Prevention Section

-----Original Message-----

From: Enz, Robert D. [mailto:renz@doeal.gov]  
Sent: Friday, December 12, 2003 4:35 PM  
To: 'curt\_frischkorn@nmenv.state.nm.us';  
      'John Young@nmenv.state.nm.us'  
Cc: 'mjohanson@doeal.gov'; Whitacre, Thomas;  
      'spearson@lanl.gov'; 'bbeers@lanl.gov'  
Subject: Land Application of Drilling and Development Water From R-26

Dear Curt and John,

I am transmitting the analytical screening data from the sampling of Workplan Well R-26 drilling and development water. Workplan Well R-26 is located at the top of Canyon de Valle in the NW corner of TA-16. Approximately 100,000 gallons of drilling and development water was recently produced during the construction of R-26. The details are as follows.

Pit Water

Approximately 130,000 gallons of drilling and development water are being stored in a lined pit and frac tank at the R-26 drill site. Screening analysis of the pit water produced the following results:

- 1) No PCBs were detected at concentrations greater than Method Detection Limits.
  - 2) No VOAs were detected with the exception of acetone at 2100 ppb and toluene at 13 ppb. It is believed that the acetone detected in the pit water is an artifact of the drilling additive, Quickfoam, that contains isopropyl alcohol.
  - 3) No SVOAs were detected in the sample.
  - 4) Gross alpha activity is 10.7 pCi/L (+/-1.0 pCi/L), below the EPA drinking water MCL of 15 pCi/L.
  - 5) Tritium results were non detect (RL=1200 pCi/L).
  - 6) No perchlorate was detected in the sample (MRL=4.0 ppb). Note: Result was reported as <400 ppb due a 100X dilution performed on the sample.
  - 7) Screening results show that no contaminants exceeded NM WQCC Regulation 3103 ground water standards with the exception of the following:
    - \* Al=7.23 ppm (ground water std=5.0 ppm)
    - \* Fe=1.08 ppm (ground water std=1.0 ppm)
- R-26 is located on the west side of TA-16 near Canon de Valle. It is located upgradient of any PRSs or historic TA-16 outfalls. It will serve as a background well for the southwestern portion of LANL.

DOE proposes to land apply the R-26 drilling and development water, using a water truck, to the dirt sides of the paved road leading from the old fire house at TA-16 to the R-26 location, as well as in the borrow pit located north of R-26 and Canon De Valle. The application will be conducted in accordance with the terms and conditions of the Hydrogeologic Workplan NOI.

Please contact me at 667-7640 or Bob Beers at 667-7969 (office) or 699-2342 (cell) should you have any questions regarding this notification. This notification will be formally transmitted to you via a letter signed by Mat Johansen, DOE Ground Water Compliance Manager.

Bob Enz

----- End of forwarded message -----

KLEINFELDER  
EXPECT MORE

Warning: Information provided via electronic media is not guaranteed against defects including translation and transmission errors.

If the reader is not the intended recipient, you are hereby notified that any dissemination, distribution or copying of this communication is strictly prohibited. If you have received this information in error, please notify the sender immediately.

## **Appendix H**

---

*Activities Planned for Well R-26  
Compared with Work Performed*

## Appendix H

## Activities Planned for Well R-26 Compared with Work Performed

Activity	"Hydrogeologic Workplan" (LANL 1998, 59599)	R-26 SAP (LANL 2003)	R-26 Actual Work
Planned Depth	100 to 500 ft into the regional aquifer	1414 ft TD of approximately 100 ft through regional water table. Regional water table expected at ~1314 ft.	Total drill depth 1485' ft bgs
Drilling Method	Methods may include, but are not limited to HSA, air-rotary/Odex/Stratex, air-rotary/Barber rig, and mud-rotary drilling	Fluid-assisted, open-hole, air-rotary drilling	Fluid-assisted, open-hole, air-rotary, air-rotary casing hammer and mud rotary drilling
Amount of Core	10% of the borehole	In R-26, the core target depth is 250 ft.	Total core depth 250 ft bgs, through 60 ft of alluvium and 190 ft into the Tshirege Member of the Bandelier Tuff
Lithologic Log	Log to be prepared from core, cuttings and drilling performance	Log to be prepared from core, cuttings, geophysical logs and drilling performance	Same as SAP. Note that the log was prepared from core samples to a depth of 105 ft bgs.
Number of Water Samples Collected for Contaminant Analysis	A water sample may be collected from each saturated zone, five zones assumed. The number of sampling events after well completion is not specified.	If perched water is encountered within the unsaturated zone, one groundwater sample will be collected within up to three perched zones. Groundwater samples will be collected within the regional aquifer at the regional water table and at the borehole TD, if feasible.	One water samples was obtained from the shallow perched zone at 240 ft bgs in the core hole. Two samples were collected from the water zone at 604 ft bgs in the deep borehole.
Water Sample Analysis	Initial sampling: radiochemistry I, II, and III, $^3\text{H}$ , general inorganics, stable isotopes, VOCs, and metals. Saturated zones: radionuclides (tritium, strontium-90, cesium-137, americium-241, plutonium isotopes, uranium isotopes, gamma spectrometry, and gross alpha, gross beta, and gross gamma), stable isotopes (hydrogen, oxygen, and in special cases nitrogen), major ions (cations and anions), trace metals, and trace elements.	Groundwater will be analyzed for perchlorate, low-detection tritium, gamma spectroscopy, americium-241; plutonium-238; plutonium-239, 240, strontium-90; technetium-99; uranium-234; uranium-235; uranium-238; bromide, chloride, fluoride, nitrate, nitrite, oxalate, phosphate, sulfate, uranium, target analyte list metals, and stable isotopes of hydrogen, oxygen, and nitrogen.	Same as SAP
Water Sample Field Measurements	Alkalinity, pH, specific conductance, temperature, turbidity	Carbonate alkalinity, pH, specific conductance, temperature, turbidity	pH, specific conductance, temperature, turbidity
Number of Core/Cuttings Samples Collected for Contaminant Analysis	Twenty samples of core or cuttings to be analyzed for potential contaminant identification in each borehole.	A minimum of two samples will be collected from each saturated zone encountered during drilling, if possible.	Samples core/cuttings were submitted for analysis from Thirteen intervals.
Cuttings/Core Sample Analytes	Uppermost sample to be analyzed for a full range of compounds: deeper samples will be analyzed for the presence of radiochemistry I, II, and III analytes, tritium (low and high detection levels), and metals. Four samples to be analyzed for VOCs.	Bromine, chlorine, fluorine, iodine, nitrate, nitrite, oxalate, phosphate, sulfate, perchlorate, arsenic, strontium, uranium, aluminum, calcium, iron, magnesium, manganese, sodium, potassium $^{18}\text{O}/^{16}\text{O}$ $^2\text{H}/^1\text{H}$ nitrogen, isotopes tritium americium-241 plutonium-238 plutonium-239,240 strontium-90 technetium-99 uranium-234 uranium-235	Same as SAP

## Appendix H

## Activities Planned for Well R-26 Compared with Work Performed

Activity	"Hydrogeologic Workplan" (LANL 1998, 59599)	R-26 SAP (LANL 2003)	R-26 Actual Work
		uranium-238 gamma spectroscopy	
Laboratory Hydraulic-Property Tests	Physical properties analyses will be conducted on 5 core samples and will typically include: moisture content, porosity, particle density, bulk density, saturated hydraulic conductivity, and water retention characteristics.	Up to 8 samples to be selected for laboratory hydraulic testing. In addition, core will be sampled for anions, moisture content and stable isotopes at 13 depths, from 10 to 250 ft bgs, to estimate recharge rates.	Same as SAP
Geology	Ten samples of core or cuttings will be collected for petrographic, X-ray fluorescence (XRF) and X-ray diffraction (XRD) analyses	The geology task leader will determine the number of samples for characterization of mineralogy, petrography, and geochemistry based on geologic and hydrologic conditions encountered during drilling.	Seven samples characterized for mineralogy, petrography, and rock chemistry
Geophysics	In general, open-hole geophysics includes caliper, electromagnetic induction, natural gamma, magnetic susceptibility, borehole color videotape (axial and sidescan), fluid temperature (saturated), single-point resistivity (saturated), and spontaneous potential (saturated). In general, cased-hole geophysics includes: gamma-gamma density, natural gamma, and thermal neutron.	Typical wireline logging service as planned: open-hole geophysics includes array induction imager, triple lithodensity, combinable magnetic resonance tool, natural gamma, natural gamma ray spectrometry, epithermal compensated neutron log, caliper, full-bore formation microimager, elemental capture spectrometer and borehole video.  In general, cased-hole geophysics includes triple lithodensity, natural gamma, natural gamma spectrometry, epithermal compensated neutron log, elemental capture spectrometer.	Compensated Neutron Tool: Cased 500 – 1005 ft bgs Open 70 – 985 ft bgs, 1005 – 1481 ft bgs Triple Litho-Density: Cased 500 – 1005 ft bgs Open 70 – 985 ft bgs, 1005 – 1481 ft bgs Array Induction Tool: Cased 500 – 1005 ft bgs Open 70 – 979 ft bgs, 1005 – 1476 ft bgs Elemental Capture Spectroscopy: Cased 500 – 1005 ft bgs Open 70 – 981 ft bgs, 1005 – 1477 ft bgs Natural Gamma Spectroscopy: Cased 500 – 1005 ft bgs Open 70 – 979 ft bgs, 1005 – 1460 ft bgs Combinable Magnetic Resonance: Open 100 – 967 ft bgs, 1050 – 1464 ft bgs Full-bore Formation Micro Imager: Open 450 – 985 ft bgs, 1005 – 1483 ft bgs
Water-Level Measurements	Procedures and methods not specified in "Hydrogeologic Workplan"	Water levels will be determined for each saturated zone by water-level meter or by pressure transducer.	Water level meter (sounder) used to measure zones of perched saturation and the regional water table
Field Hydraulic-Property Tests	Not specified in hydrogeologic work plan	Slug or pumping tests may be conducted in saturated intervals once the well is completed.	Pending
Shallow Piezometers	Not specified in hydrogeologic work plan	Not specified in SAP	Two piezometers were installed in the core borehole at depths of 250 and 180 ft bgs.
Surface Casing	Approximately 20-in. outer diameter (O.D.) extends from land surface to 10-ft depth in underlying competent layer and grouted in place.	18-in. OD schedule 40, low carbon steel casing will be installed as deep as possible below ground level (nominally 35-40 ft bgs) and will extend approx 3 ft above the ground surface and cemented into place.	13 ¾-in. OD steel casing set at 70' and 9 ¾-in. OD steel casing set from 0 to 1005 ft bgs, removed during well construction
Minimum Well Casing Size	6.625-in. O.D.	5-in. O.D. x 4.5-in. ID	5-in. OD (4.46-in. ID) stainless steel casing with external couplings
Well Screen	Machine-slotted (0.01-in) stainless-steel screens with flush-jointed	Well screen shall be constructed with multiple sections of 5.56-in. O.D. pipe	5.27-in. OD, rod-based stainless-steel screen with a 0.020-in. slot size on

## Appendix H

## Activities Planned for Well R-26 Compared with Work Performed

Activity	"Hydrogeologic Workplan" (LANL 1998, 59599)	R-26 SAP (LANL 2003)	R-26 Actual Work
	threads; number and length of screens to be determined on a site-specific basis and proposed to NMED	based stainless-steel screen, with a 0.02-in. slot size	the lower screen and 0.010-in. slot size on the upper screen.
Sump	Stainless-steel casing with an end cap	5-in-diameter stainless steel casing, 30 ft long.	5-in. OD stainless-steel casing, 34 ft long, with end cap.
Backfill	Uncontaminated drill cuttings below sump and bentonite above sump	A bentonite chip and sand mix will be used to fill the annulus to within 75 ft of ground surface. The mix will be hydrated in place every 100 ft. Cement with 2% bentonite will be used to fill the remaining annulus.	A 75:25 mix of 10/20 sand and bentonite chips placed from TD to 5 ft below bottom of the lower screen (1450 ft bgs) and from 1012 ft bgs to 10 ft below bottom of upper screen (672 ft bgs)
Filter Material	>90% silica sand, properly sized for the 0.010-in. slot size of the well screen; extends 2 ft above and below the well screen	A bentonite seal will be placed below each screened interval and allowed to hydrate for 1 hr to prevent mixing. A two-foot interval of fine-grained (30/70) transition sand will be placed above and below each primary filter pack. The primary filter pack (20/40 sand) will extend from 5 ft below each screened interval to 5 ft above.	For Screen #2, primary filter pack constructed of 10/20 silica sand placed 5 ft below and 11 ft above the screen. For Screen #1, primary filter pack constructed of 10/20 silica sand placed 2 ft below and 32 ft above the screen.  Secondary filter pack constructed of 20/40 silica sand placed to 3-ft above primary filter pack of lower screen (1408 ft bgs) and to 2-ft (618 ft bgs) above primary filter pack of upper screen.
Transition Seal	N/A*	N/A	A 67% to 33% mixture of 10/20 silica sand and 3/4 in. bentonite chips from 1408 ft bgs to 1111 ft bgs
Bentonite Seal	N/A	N/A	3/4-in. bentonite chips placed from 1479 ft bgs to 1450 ft bgs (5 ft below Screen #2) 3/4-in. bentonite chips placed from 1012 ft bgs to 672 ft bgs between screens (2 ft below Screen #1) 3/4-in. bentonite chips placed from 618 ft bgs to 70 ft bgs
Concrete Backfill	N/A	N/A	2,500 psi concrete with 4% bentonite from 70 ft bgs to near surface

\* N/A – Not specified in the two referenced documents.

## TARGET PAGE

This target page represents media that was not scanned. The original media can be obtained through the Records Processing Facility.

ER ID # 092033

RECORD TYPE:

CD

DATE:

9-15-03

SYMBOL:

N-A

SUBJECT:

Well - R-26 Completion

Report Appendix B

Borehole Video